[**CAVEOLIN-1:** A CRITICAL REGULATOR OF INFLAMMATION AND FIBROSIS**]**

by

[**Xiao Mei Wang**]

[Bachelor of Medicine, Shanghai Medical University, 1999]

[Master of Science, Fudan University, 2002]

Submitted to the Graduate Faculty of

[School of Medicine] in partial fulfillment

of the requirements for the degree of

[Doctor of Philosophy]

University of Pittsburgh

[2006]

UNIVERSITY OF PITTSBURGH

[SCHOOL OF MEDICINE]

This [thesis/dissertation] was presented

by Xiao Mei Wang

It was defended on

[November 1, 2006]

and approved by

Bruce R. Pitt, Ph.D., Professor and Chairman of Environmental and Occupational Health

Tim D. Oury, M.D. Ph.D., Associate Professor, Department of Pathology

Xiao-Ming Yin, M.D., Ph.D., Associate Professor, Department of Pathology

Thesis Director/Dissertation Advisor: Augustine M.K. Choi, M.D., Professor, Department of Medicine

Thesis Committee Chair: Robert P. Bowser, Ph.D., Associate Professor, Department of Pathology

CAVEOLIN-1: A CRITICAL REGULATOR OF INFLAMMATION AND FIBROSIS

Xiao Mei Wang, M.S.

University of Pittsburgh, [2006]

Caveolin-1 (cav-1) has been reported to regulate apoptosis, lipid metabolism and endocytosis. In the present study, we demonstrate that cav-1 can act as a potent immunomodulatory molecule in murine macrophages and play an important role in the development of fibrosis.

In murine alveolar and peritoneal macrophages, loss of function experiments using siRNA showed that down-regulating cav-1 expression increased lipopolysaccharide (LPS)-induced proinflammatory cytokine tumor necrosis factor-alpha (TNF-α) and interleukin-6 (IL-6) production but decreased anti-inflammatory cytokine interleukin-10 (IL-10) production. Gain of function experiments demonstrated that overexpression of cav-1 in RAW264.7 decreased LPS-induced TNF-α and IL-6 production and augmented IL-10 production. Cav-1 interacted with TLR4 as revealed by co-immunoprecipitation in peritoneal macrophages. Overexpressing cav-1 in RAW264.7 disrupted Toll like receptor 4 (TLR4) MyD88 and TRIF complex formation; regulated mitogen-activated protein kinase (MAPK) phosphorylation; and inhibited NF-κB activation. Furthermore, the anti-inflammatory modulation by cav-1 involved p38, since the administration of SB203580 significantly abrogated the effects of cav-1, and peritoneal macrophages isolated from MKK3 null mice did not demonstrate any modulation of cav-1. Interestingly, HO-1 translocated into caveolae after LPS stimulation. Carbon monoxide (CO), the gaseous byproduct of HO activity responsible for the anti-inflammatory effects of HO-1, did not regulate cytokines production in cav-1 null macrophages.

We observed marked reduction of cav-1 expression in lung tissues and in primary pulmonary fibroblasts from IPF patients, compared to controls. Transforming growth factor-β_1 (TGF-β_1), the well-known pro-fibrotic cytokine, decreased cav-1 expression in human pulmonary fibroblasts. Cav-1 was able to suppress TGF-β_1-induced extracellular matrix (ECM) production in cultured fibroblasts through the regulation of the c-Jun N-terminal kinase (JNK) pathway. Interestingly, highly activated JNK was detected in IPF and bleomycin (BLM)-instilled lung

tissue samples, which was dramatically suppressed by adenovirus cav-1 infection. Moreover, JNK1 null fibroblasts showed reduced Smads cascades signaling, mimicking the effects of cav-1. We also demonstrated that cav-1 markedly ameliorated BLM-induced pulmonary fibrosis as evidenced by histological analysis, hydroxyproline content and immunoblot analysis.

In summary, our data suggest that cav-1 acts as a potent immunomodulatory and anti-fibrotic effector molecule. Cav-1 may mediate the anti-inflammatory effects of HO-1/CO in immune cells involving the MKK3/p38 MAPK pathway. Cav-1 also plays a pivotal role in ECM regulation and the development of fibrosis, possibly through the MAPK and Smads pathway. This study suggests cav-1 as a novel therapeutic target for patients with fibrosis and inflammation.

TABLE OF CONTENTS

LIST OF FIGURES

PREFACE

It is with great pleasure that I offer my acknowledgement to a number of people for their help in completing this degree. First, I would like to thank all my dissertation committee members for inspiring and excellent guidance throughout my entire studies. A very special thank you goes to my advisor, Dr. Augustine Choi. He endured numerous emails and meetings to provide the ceaseless guidance and support that saw me through this project. His high expectation reinforced my enthusiasm of my dissertation. I am indebted to the faculty and staff in Dr. Choi's lab - Hong Pyo Kim PhD, Danielle Morse MD, Ruiping Song MD, PhD, Zhihong Zhou MD, Stefan Ryter PhD, Yingze Zhang PhD, Emeka Ifedigbo MS, and Fang Liu, BS, whose support and involvement made this study possible.

I would like to acknowledge the Interdisciplinary Biomedical Program, the Cellular and Molecular Pathology Program, and the Division of Pulmonary, Allergy and Critical Care Medicine, School of Medicine, University of Pittsburgh. I would also like to acknowledge the American Heart Association for partial financial support during my study.

I am thankful to my friends here at the University of Pittsburgh for their unwavering support and interest in my study.

My immeasurable gratitude goes to my parents and my brother for standing by me and giving me a way to work out my project by taking care of my lovely daughter Karen. My unconditional love goes to my daughter Karen for giving me a reason to smile. Finally, my thanks go to my husband Xiaohui for the encouragement when I felt weary and for all the understanding and support during my life.

1.0 INTRODUCTION

1.1 CAVEOLAE &CAVEOLIN-1

1.1.1 Caveolae & Caveolin-1 (Cav-1)

First described in the 1950s, caveolae are nonclathrin-coated plasma membrane microdomains rich in glycosphigolipids, sphingomyelin, and cholesterol (1-4). They are membrane vesicles with a diameter of 50 to 100 nm (5), which exist in single or cluster forms, with an appearance of flask-shaped membrane invaginations or flat pits, depending on the different stages of the invagination (6, 7). The actin cytoskeleton anchors caveolae (8-10). Caveolae are found in terminally differentiated cells, including endothelial cells, pneumocytes, fibroblasts, adipocytes and muscle cells (11).

Originally, caveolae described vesicles performing clathrin-independent endocytosis (12, 13). Many other functions are proposed for caveolae, including vesicular transportation (transcytosis of molecules across the cells, potocytosis and polonized protein trafficking, cholesterol transportation, calcium metabolism) (14-16), and most strikingly, the regulation of signal transduction (17-19). Caveolae are regarded as signalosome (11). Various receptors, intracellular signaling molecules, and proteins were reported to localize in caveolae (Figure 1) (20-22). Depending on different cell types and physiological status, caveolae exhibits multifunctional biological roles (15, 17, 23, 24).

Caveolins are the major components of caveolae (11). Three caveolins have been identified to date in mammalian cells: cav-1, -2 and -3 (11). The human cav-1 and cav-2 genes are localized in the 7q31.1 region (25). The cav-1 gene contains three exons while the cav-2 gene contains two exons (26). Cav-1 and cav-2 are independent transcriptional units with an analogous last exon (27). Human cav-3 gene is on chromosome 3p25 with two exons (28, 29). Cav-1 is the structural component and marker of caveolar microdomains (5). It has two isoforms

cav-1α (178 residues; 24 kDa) and β (147 residues; 21 kDa) (30–32). Whether the two isoforms arise from the same mRNA with different initiation or different mRNAs is still unclear (30, 33). Caveolae formed by different cav-1 isoforms have different molecular composition (30).

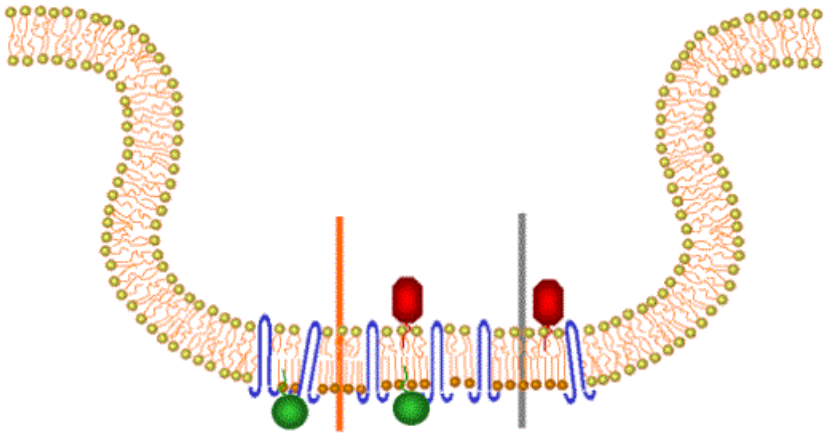

Figure 1 Diagram of the composition of caveolae. Orange: Glycosphingolipids; Yellow: normal lipids; Blue: Caveolin; Red: GPI linked enzymes and receptors; Green: palmitolated, Src-like kinases trans-membrane receptors; grey and orange: caveolae associated signaling receptors. [Cell. 1992, 68:673-682, reference (34)]

Cav-1 has three distinct domains: the hydrophilic cytosolic N-terminal (1-101 residues), C-terminal (135-178 residues) and the hydrophobic central stretch (102-134 residues) (11). These characteristics make cav-1 form a hairpin-like structure with N and C termini orienting towards the cytoplasm (11). The cav scaffolding domain (82-101 residues) is essential for the formation of cav oligomers and interaction with other proteins (35, 36). The N-terminal membrane attachment domain (82-101 residues) and C-terminal membrane attachment domain (135-150 residues) are required for cav membrane attachment (37, 38). The C-terminal domain is also involved in protein-protein interactions (39). Cav-1 exists as an oligomeric complex of 14 to 16 monomers (with a high molecular mass of 350-450 kDa.) through oligomerization domain (61-101 residues) (36). Cav-1 and cav-2 often co-express and associate (with a molecular weight of about 200-600 kDa) in endothelial cells, pneumocytes, fibroblasts and adipocytes (40). Cav-3 expression is limited to muscle cells (28). Cav-1 is critical for the formation of caveolae. Transfection of cav-1 into cells lacking caveolae (lymphocytes, Caco-2 cells) induced caveolae

formation (41). Cav-2 null mice show no defects in caveolae formation (42). There are two kinds of post-translational modifications of cav-1: phosporylation of tyrosine 14 (43) and palmitoylation of cysteine 133, 143 and 156 (44). Phosporylation modifications are related to protein-protein interaction (45). Palmitoylation modifications are involved in cholesterol binding (38, 46). Conserved sequences of aromatic residues (ΦXΦXXXXΦ and ΦXXXXΦXXΦ, with Φ being Trp, Phe or Tyr) can be recognized by cav, and are called cav binding motifs (11, 47).

Caveolae perform their signal transduction functions through compartmentalization of many signaling molecules and interaction with cav-1 (11). A wide variety of signaling proteins are reported to localize in caveolae and interact with cav-1 including: receptor tyrosine kinases and their downstream targets (EGFR, PDGFR, H-Ras, Raf-1, ERK, PI3K) (48-54); non-receptor tyrosine kinases (Src family, Fak) (53, 55); receptor serine/threonine kinases (TGFβ receptor type I) (56, 57); G-protein coupled receptors and the downstream molecules (G-protein alpha subunits, adenylyl cyclase, PKA, PKC isoforms) (47, 58-62); steroid hormone receptors (AR and ER) (63-65); eNOS etc. (66-68). Generally, the binding of the signaling molecules to cav-1 results in their inactivation. For example, cav-1 is regarded as a tumor suppressor gene, since cav-1 interacts with growth factor receptors. Cav-1 binds EGFR via the cav binding motif within the kinase domain (DVWSYGUTUWEL), which inhibits autophosphorylation and activation of the receptor (48). Cav-1 binds to and inhibits MEK or ERK activation in a PDGF stimulation model (52).

1.1.2 Cav-1 and inflammation

The expression of cav-1 in immune cells was debated for a long time. Initially, caveolins were reported to be absent in macrophages (69). However, recently, with more specific elaborate detection methods, it is more convincing that caveolae and cav-1 exist in immune cells including mouse macrophages (5, 44, 50, 70, 71), human and bovine dendritic cells (72), human mast cells, and human lymphocytes etc. (42, 73). For mouse peritoneal macrophages (PM), evidences from immunoblot, RT-PCR, electron microscopy and immunofluorescence supported the existence of caveolae and cav-1 in the plasma membrane (69, 74, 75). Cav-1 expression is primarily on the plasma membrane, while cav-2 is located in the Golgi apparatus (74). Overexpression of cav-1 in non cav-1 expressing cells J774 led to the translocation of cav-2 to the plasma membrane (74). By immunoflurescence microscopy, cav-1 was detected in mouse bone marrow macrophages

(76). Rat resident peritoneal macrophages were also found to express cav-1 (77). The identification of cav-1 expression in macrophage like cell lines was controversial. By immunoblot and RT-PCR, THP-1 cells expressed cav-1 (78). Cav-1 mRNA was detected by RT-PCR in RAW264.7 cells and J774 cells (74, 75). However they failed to detect cav-1 protein expression by immunoblot and immunoflurescence microscopy, though one previous reported described cav-1 expression in RAW264.7 cells (74, 75). Usually activation of macrophages led to increased cav-1 expression (74). For example, lipopolysaccharide increased cav-1 levels in peritoneal macrophages of C3HeB/FeJ mice (75). Upon elicitation by Freund's adjuvant, the expression of cav-1 was increased in rat peritoneal macrophages and associated with an increased number of morphologically distinguishable caveolar invaginations as shown by electron microscopy (77). In THP-1 cells the expression level of cav-1 increased 50 fold upon differentiation into macrophages (78). However, one exception was that mouse resident and thioglycollate elicited peritoneal macrophages expressed cav-1 quantitatively similar to the level of 45% and 15% of that in NIH3T3 fibroblasts (74). The protein levels corresponded well with the mRNA levels as determined by ribonuclease protection assays (74).

Macrophages exist in different functional subtypes according to environmental conditions (79). Alveolar macrophages (AM) are bone marrow-derived resident macrophages and play pivotal roles in pulmonary phagocytosis and inflammation (80, 81). Although Kasper et al. found cav-1 staining in rat alveolar macrophages by immunohistochemistry, they hypothesized that this was the result of phagocytosis of other cell type debris (82). Thus, studies of cav-1 in alveolar macrophages are absent and little is known about the expression and function of cav-1 in this cell type. In this study, we used two independent methods to detect cav-1 expression in mouse alveolar macrophages.

The biological significance of cav-1 in macrophages is not clear. Cav-1 has been shown to play a role in apoptosis in macrophages (83, 84). When treated with various unrelated apoptotic agents, including simvastatin, camptothecin and glucose deprivation, in glycolate-elicited mouse peritoneal macrophages, cav-1 expression was specifically and markedly increased, while cav-2 levels remained unaffected (83, 84). Cav-1 was shown to play a pivotal role in endocytosis and lipid metabolism in macrophages and play an active role in the pathophysiology of atherosclerosis (76, 85). Cav-1 can directly bind to cholesterol and lipid acids (76, 85, 86). CD36 and SR-BI, class B scavenger receptors, which bind HDL and

selectively transfer core cholesteryl-ester to the cells, localized in caveolae (70, 87). Transfection of cav-1 into J774 and RAW264.7 cells inhibited HDL-mediated cholesteryl-ester uptake (87). Increased cav-1 expression in THP-1 cells was associated with increased HDL cholesteryl-ester uptake and increased cholesterol efflux (88). Cav-1 was also found to be secreted, which might play a role in lipid removal and cholesterol retro-endocytosis (89).

The relationship between cav-1 and inflammation is mainly focused on uptake of antigen by antigen presenting cells (72), internalization of bacteria (90) and regulation of eNOS activity (91). Caveolae are known to be involved in non-clathrin coated endocytosis and may regulate the internalization of particles such as viruses and bacteria (90, 92-94). When treated with the caveolae inhibitor filipin, the speed of both fluid-phase and receptor-mediated endocytosis was decreased (95). In macrophages and mast cells, FimH mediated internalization of bacteria was dependent on caveolae-like vesicles (73, 90). The compounds that disrupt caveolae formation can effectively block bacterial uptake (73, 90). Stuart et al. reported that filipin and nystatin, drugs that specifically disrupt caveolae microdomains by cholesterol chelation, impaired the entry of *C trachomatis serovar K.* into J774A.1 cells (96). Cav-1 also suppresses inflammation via its interaction with and inhibition of eNOS activity (91, 97). Santizo et al. showed that downregulation of cav-1 combined with upregulation of eNOS decreased leukocyte adhesion in pial venules of ovariectomized female rats (97). Bucci et al. used the scaffolding domain of cav-1 to inhibit edema formation and vascular leakage to the same extent as glucocorticoid in rats (91). In the present study, cav-1 was shown to have a direct effect on cytokine production in the LPS-induced inflammation model in mouse macrophages.

1.1.3 Cav-1 and fibrosis

Interstitial pulmonary fibrosis (IPF) is a progressive chronic interstitial lung disease with a high mortality (median survival of newly diagnosed patients is about 3 years) and a uniformly poor prognosis (98). The biochemical mechanism in the pathogenesis of IPF is still poorly understood (99). Current medical therapeutic drugs, such as corticosteroids, cytotoxic drugs and interferon-γ (IFN-γ) have been based on suppression of the inflammation and fibrosis process, but thus far have offered little benefit against the progression of the disease (100). Although there is no known etiologic stimulus that initiates IPF, many investigators believe that endogenous and exogenous stimuli injure the alveolar epithelium, followed by an abnormal

repair process (101). Among these processes, various cytokines and growth factors are critical (102). TGF-β_1 has been implicated to be one of the important cytokines and chemokines in the initiation and progression of fibrosis (102).

Recently, cav-1 has been reported to associate with TGF-β receptors by several investigators (56, 103). Schwartz et al. found that TGF-β receptor I (TGF-βRI) and TGF-βRII localize in cav-1 enriched fractions by density gradient fractionation in human endothelial cells (103). Furthermore, immunoprecipitation showed that cav-1 interacted with TGF-β receptors and regulated eNOS activation (103). Razani et al. reported that cav-1 interacted with TGF-βRI via the scaffolding domain of cav-1, inhibited the phosphorylation of Smad-2, disrupted its interaction with Smad-4 and prevented Smad-2 complex nuclear translocation in mouse fibroblasts (56). Moreover, many studies demonstrated that cav-1 expression is abnormal in experimental lung fibrosis (104-106). Tourkina et al. found that cav-1 expression is low in bleomycin-induced lung fibrosis tissue and scleroderma lung fibroblasts (104). Kasper et al. reported that cav-1 expression decreased with the treatment of $CdCl_2$ and TGF-β_1 in rat lung slices in vitro (106). They also reported loss of cav-1 expression in type I pneumocytes of rats and mini pigs in an irradiation-induced lung injury model, suggesting that low cav-1 expression might be an early indicator of subcellular alterations during lung fibrogenesis (105). Taken together with the studies of cav-1 knock out mice (107), which develop severe lung fibrosis, we hypothesize in the present studies that cav-1 might play a role in the pathogenesis of lung fibrosis by regulating ECM production.

1.2 HO-1& CO

1.2.1 Heme oxygenase-1 (HO-1)

HO, first identified in 1960s as a highly conserved enzyme, catabolizes the degradation of heme to generate biliverdin, iron and carbon monoxide (CO) (108, 109). Biliverdin is rapidly converted to bilirubin by biliverdin reductase (110). Iron binds to ferritin (110) (Figure 2). There are three isoforms of HO identified so far (111). HO-1 is highly inducible by a variety of stimuli, including hydrogen peroxide (H_2O_2), ultraviolet-A (320–380 nm) radiation, sodium m-arsenite ($NaAsO_2$), heme, proinflammatory cytokines, bacterial endotoxins, growth factors, and tumor promoters (108). Furthermore, HO-1 responds to cellular stress related to oxygen tension such as hyperoxia and hypoxia (108). HO-2 and HO-3 are constitutively expressed (108). HO-1, also known as the stress protein HSP32, has a molecular weight of ~30–33 kDa; HO-2 has a molecular weight of ~36 kDa (108). Also, HO-1 and HO-2 differ in gene organization, structure and in chromosomal localization (108). HO-1 and HO-2, also known as Hmox1 and Hmox2, are the products of distinct genes (107). There are five exons and four introns in the human, mouse and rat HO-1 gene (107). According to fluorescence in situ hybridization, HO-1 and HO-2 genes localize to different chromatin regions. HO-1 lies in 22q12; while HO-2 lies in 16p13.3 (112).

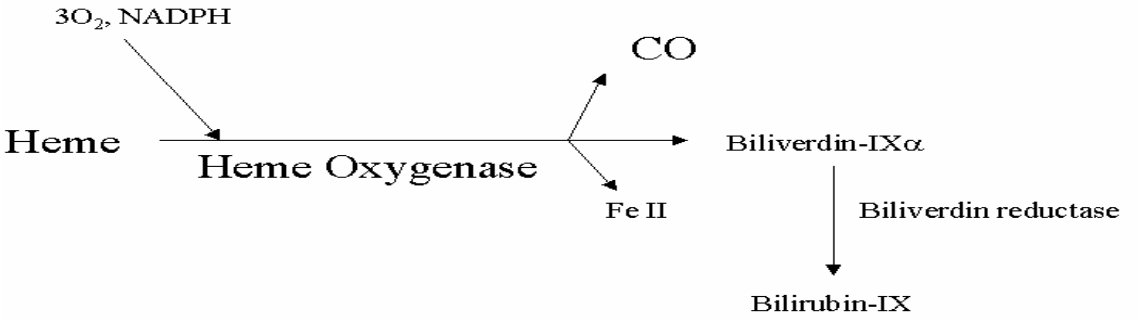

Figure 2 Diagram of heme metabolism. Heme oxygenase oxidizes heme to biliverdin-IXα. The reaction requires 3 mol of molecular oxygen and NADPH:cytochrome *P*-450 reductase as a source of electrons. The cleavage of the heme ring releases the coordinated iron, as well as carbon monoxide (CO). The principal HO reaction product, biliverdin-IXα, is further metabolized to bilirubin-IXα by biliverdin reductase.

HO-1 is most abundant in tissues and cells involved in the uptake and degradation of plasma heme, including spleen, liver parenchyma, hematopoietic stem cells in bone marrow, kidney and macrophages (113). In other tissues or cells not directly involved in hemoglobin metabolism, the expression of HO-1 typically is low under basal conditions. However, HO-1 levels increase dramatically in response to diverse cellular stress stimuli (113).

Traditionally, HO-1 had been characterized as endoplasmic reticulum (ER) associated proteins, for two reasons: its activity was detected to be rich in microsomal (104,000*g*) fractions; the C-terminal hydrophobic domain of HO-1 indicates a typical membrane compartmentalization (114). This was confirmed by tranfection experiments. Shibahara et al. transfected rat HO-1 cDNA into monkey kidney cells and found that HO-1 was highly expressed in the ER (115). Recently, HO-1 was found to localize in caveolae in pulmonary endothelial cells and in nucleus of primary astroglial cell (116, 117).

HO-1 is highly inducible upon many stimuli, which cause oxidative stress (108). And the regulation of HO-1 is primarily at the transcriptional level. Although there is report saying that in rat, message stability regulated by heat shock nuclear factor is one of the mechanisms in HO-1 regulation (118). The mouse HO-1 gene contains one proximal and two distal enhancers (4kb and 10 kb upstream from the transcription initiation site) (118). LPS requires the distal enhancers to induce HO-1, while hypoxia does not (118). Promoter studies reveal the existence of the stress response element (StRE) in the enhancer regions of HO-1 gene (118). The mouse StRE contains AP-1 transcription factor bindig site. Mutation of the AP-1 binding site abolishes the HO-1 upregulation by heavy metals, hydrogen peroxide, arsenate and LPS in vitro (119). AP-1 activation was also shown to mediate hyperoxia-induced HO-1 gene transcription in lung in accordance with STAT (120). AP-1 family includes Jun, Fos, NF-E2, Nrf1 and Nrf2. There are evidences that Nrf2 is of particular importance in regulation of HO-1 expression (108).

It was also published that induction of HO-1 by hemorrhagic shock and resuscitation is primarily regulated by AP-1 ina ROS-dependent manner (121). Hypoxia-inducible factor-1 (HIF-1) is also an important transcriptional activator, which binds to hypoxia response elements in mouse HO-1 gene. Mutation, which abolishes the HIF-1 binding site, also abolishes hypoxia-induced HO-1 induction (122). IL-6 response element has been identified to involve in IL-1 induction of HO-1 gene (123).

HO-1 serves as a protective gene by virtue of its anti-inflammatory, anti-apoptotic and anti-proliferative actions, manifested in a variety of cell types (116). In the present study, we will focus on the anti-inflammatory properties. All three byproducts of HO-1 were reported to mediate the protective function of HO-1 (116). CO has been shown to mimick the highly protective action of HO-1 in several rodent disease models (113). HO-1 expression or CO administration mediate the potent anti-inflammatory effects in monocytes and macrophages (124). Biliverdin and bilirubin are thought to contribute the protective effect largely because of their anti-oxidant properties (125, 126). Fe^{2+} induces ferritin expression, which is a multimeric iron-chelating protein, and it binds to free Fe^{2+} that would otherwise promote the generation of reactive oxygen species (ROS) and free radical (127).

HO-1 demonstrated the anti-inflammatory properties in a lot of studies (116). HO-1 null mice had a chronic inflammation which progress with the age (128). And human reported to be deficient in HO-1 died from the inflammatory syndrome (129). The anti-inflammatory effects of HO-1 was also shown in many animal models including hypoxia (130), ischemic-reperfusion injury (131), endotoxin induced damage (132), atherosclerosis (52, 84), hypertension (133), allograft and xenograft transplantation (134) etc. Intratracheal adenoviral mediated HO-1 cDNA transfer into rat lung protected against the development of pulmonary damage during hyperoxia, as determined by pleural effusion volume and histological analysis. There were significant reductions of edema, hemorrhage, inflammation and apoptosis. The survivability against hyperoxia also markedly increased in adenovirus HO-1 infected rats compared with the control-infected rats (130). In an ischemic-reperfusion injury model in rat kidney, HO-1 induced by hemin reversed the impaired renal function after reperfusion, while SnPP, the chemical inhibitor of HO-1 activity, significantly inhibited the intercellular adhesion molecule ICAM-1 expression, activated caspase-3 expression and infiltration of macrophages (131), Another study in an acute lung injury model found that adenovirus HO-1 administration and hemin can both attenuate neutrophilic inflammation of the lung after aerosolized lipopolysaccharide (LPS) exposure. Interestingly, HO-1 gene was transferred to alveolar macrophages (AMs) besides the airway epithelium as revealed by immunohistochemical analysis. Moreover, overexpression of exogenous HO-1 in the macrophages had a high level of endogenous IL-10 production. Additionally, the increased production of IL-10 in the macrophages was critical for the resolution of neutrophilic migration in the lung after LPS exposure as evident from experiments using IL-

10 knockout mice (132). In various other models, HO-1 significantly reduced edema, leukocyte adhesion and migration, inflammatory cytokines production, and death (135). Many reports indicate that CO can mediate the anti-inflammatory of HO-1 (136, 137). Many studies suggested that other by-products of HO activity also confer the cyto-protective effects.

As mentioned before, biliverdin and bilirubin perform the cyto-protective effects probably through their anti-oxidant properties (125, 126, 138, 139). Bilirubin was shown to efficiently scavenge peroxyl radicals at micromolar concentrations in vitro. The anti-oxidant activity of bilirubin increased as the concentration of oxygen in the system is decreased from 20 percent (normal air concentration) to 2% (physiological concentration). The anti-oxidant activity of bilirubin was even higher compared with that of alpha-tocopherol, which is thought to be the best suppressor of lipid peroxidation (138). In another model of heart ischemia-reperfusion injury model, exogenous bilirubin administration at the concentration of 100 namomolar efficiently restored myocardial function and suppressed infarct size and mitochondrial damage, mimicking the effects of overexpressing HO-1 by hemin. And HO-1 overexpressing was associated with increased bilirubin concentration in tissue and the perfusion buffer (139).

HO-1 releases Fe^{2+} from the heme molecule. Free iron induces the expression of iron-sequestering protein ferritin. It also activates the ATPase pump, which removes intracellular iron out of the cell. Extracellular iron chelator binds to iron, like desferoxamine mysylate (127). Ferritin appears to confer for HO-1 cyto-protective functions sometimes. In endothelial cells, the expression of ferritin was the pathway by which HO-1 had oxidantive stress resistance (140). Heme administration markedly aggravated cytotoxicity with increased polymorphonuclear leukocyte oxidants and hydrogen peroxide. However, if the cells are briefly pulsed with heme and incubate for 16 hours, the cells become highly resistant to oxidant- mediated injury. An induction of both HO-1 and ferritin were observed. Apoferritin, when added to the cultures, was taken up in a dose-responsive manner. And it protected endothelial cells from the oxidant-mediated injury. The mutant ferritin, which lacks the iron binding capacity and ferroxidase activity, has no cytoprotective effects (140). In a hyperoxic lung injury model, ferritin was suggested to mediate the cyto-protective effects against hyperoxia instead of HO enzyme activity (127). However, in an endotoxin induced injury model, hemoglobin suppressed LPS-induced hepatic and renal functions, TNF alpha production, and neutrophil alveolitis. But pre-treatment

of iron binding protein desferoxamine and apoferritin failed to protect against the damage, suggesting that the cyto-protection provided by HO-1 is independent of ferritin (141).

The present study will mainly focus on HO-1 / CO functions.

1.2.2 Carbon monoxide (CO)

Carbon monoxide was first discovered in the late 18th century and labeled as a toxic gaseous molecule. It is a colorless and odorless gase molecule, and one of the major pollutants from the incomplete combustion and oxidation of organic matter, like tobacco, wood and coal, etc. (113). Because of its higher affinity to hemoglobin (245 times that of oxygen), CO can displace oxygen from hemoglobin, shift the oxygen dissociation curve to the left, and lead to tissue hypoxia (113). Symptoms of CO toxicity include headache, dizziness and shortness of breath. And it happens when CO-Hb level reaches 20%. 50% - 80% CO-Hb will result in death. US environmental protection agency recommends the allowable exposure levels - 9ppm for 8 hours or 35 ppm for 1 hour (142).

In 1969, CO was discovered to be produced endogenous - generated form the heme degradation, which is thought to account for more than 75% CO production in the body (143). In healthy nonsmokers, basal levels of CO-Hb range from 1% to 3% and exhalation of CO ranges between 0 to 6 ppm. In smokers, CO-Hb range from 10% to 15%, and exhalation reaches 7 to 70 ppm (144). Although it seems that increased CO content would be deleterious at first, recently, with more studies carried on, CO has been proposed to act as a signaling molecule rather than just a simply waste product (145). There are good evidences suggest that CO involves in the membrane potential gradients along and across the GI muscle layers. Along with the facts that CO is water soluable, it is not stored, and it diffuses quickly, CO seems to be a great cadidate for neurotransmitter. This hypothesis was confirmed by the report that genetic deficient of HO-2 results in reduced size of inhibitory junctions, which can be restored by exogenous CO treatment (146). CO serves as a protective gaseous molecule by virtue of its anti-apoptotic effects. Exposure to exogenous CO suppressed TNF-α-induced apoptosis in mouse fibroblasts (124) and endothelial cells (147), similar to HO-1 over expression (124). In endothelial cells, p38 MAPK was demonstrated to be critical, as administration of SB203580, the selective chemical inhibitor

of p38, abolished the anti-apoptotic effects of CO (147). Furthermore, HO-1 or CO requires the activation of NF-κB pathway to protect against TNF-α-mediated endothelial cell apoptosis (148).

CO exerts an anti-proliferative effect in a variety of cell types, including cancer cells, T cells, and smooth muscle cells (148, 149). In VSMC, exogenous CO application lead to G_0 / G_1 arrest, which involving the sGC pathway, p21 and p38 pathways (148, 149). In contrast, CO induced proliferation in endothelial cells (150).

In many cellular and animal models, exogenously administrated of CO at low concentration (250 ppm) can modulate inflammatory responses (130, 136, 151, 152). As the severity of the inflammation increased (for example bacterial infection, asthma and diabetes), CO levels increased as evidenced by the increased CO exhalation in patients, as well as HO activity up-regulation (145, 153-155). CO inhibited LPS induced tumor necrosis factor-α (TNF-α) production and increased interleukin-10 (IL-10) production in RAW264.7 cells and mice (124). Unlike NO, the effects are guanylate cyclase /cyclic GMP independent and involve the MAP kinase pathway, particularly MKK3/p38 MAP kinase pathway (124). CO was reported to be anti-inflammatory in the xenograft in the model of heart and lung. CO can inhibit platelet function and monocyte activation, which is thought to contribute to the suppression of the graft rejection (134, 156, 157). Also, CO was found to block eosinophil influx and inhibit interleukin-5 (IL-5) production in allergen-challenged mice, suggesting that CO has anti-inflammatory effects in allergen-induced inflammation (134).

The mechanisms underlying the effects of CO are far from completely understood. Soluble guanylyl cyclase (sGC) is one of the pathways. CO binds to the heme moiety of sGC, which activates cGMP. However, the capacity of NO-induced cGMP activation is 30-100 times higher compared with that of CO, despite the fact that the affinity of CO to sGC is equivalent to NO. Evidence suggests that NO is able to induce HO-1 and increae generation of CO, which in return inhibiting NOS activity, indicating HO-1 / CO as the feedback regulator of NO functions. NO is a vasorelaxant and also a potential free radical. HO might function to suppress NO free radical production while maintaining the vasodilatory properties by means of CO-induced cGMP production (142). In the last twenty years, CO is the second gas discovered to originate inside the body and have salutary effects besides NO. Certain findings indicate that HO-1 / CO and NOS / NO are functionally interrelated in mediating their protective effects (158, 159). CO induces the

expression of NOS in certain situations, while in others, inhibits expression of NOS / NO (160). In a TNF-α and D-galactosamine-induced hepatitis mouse model, the protective action of CO was dependent on the activation of NF-κB, which triggers transcription of NOS with production of NO, and subsequently on the upregulation of HO-1 (161). It is well known that eNOS localizes in caveolae and that cav-1 regulates eNOS activity (86, 162). Here we are interested in the localization of HO-1 and its relationship to cav-1.

MAPK signaling pathways have also been described as one of the mechamisms of CO-mediated cyto-protection (142). Three MAPK pathways have been discovered – ERK, JNK and p38. All of them are reported to involve in CO-mediated effects depending on different experimental conditions and cell types. For example, CO inhibits T cell proliferation and IL-2 production via ERK pathway (142). CO inhibits TNF-alpha, IL-1 beta and macrophage inflammatory protein-1 production via p38 pathway (142). CO decreases portal venous resistance and preserve hepatic function in an ischemia-reperfusion rat model via p38 pathway. Additionally, CO decreased IL-6 production through JNK pathway in response to LPS (142).

CO has been decribed to activate K^+ channels in a variety of tissues (142). Endogenously produced CO, by HO-2 in the arteries, inhibited vascular sensitivity to phenylephrine via the tetraethylammonium sensitive K^+ channel (142). In human intestinal smooth muscle cells, CO activated a delayed K^+ current resulting in membrane hyperpolarization. The current was blocked by quinidine. Ecogenous cGMP was able to restore the function. In rabbit corneal epithelial cells, exogenous CO activated a non-Ca^{2+}-activated large conductance K^+ channel with increased intracellular cGMP levels. CO also direct activated large conductance Ca^{2+}-activated K^+ channels through an interaction with histidine residues on the α subunit, which was different from the mechanism of NO (through the ß subunit) (142).

Other mechamisms might involves the binding of CO to ferrous heme containing proteins, including cytochrome c oxidase, cytochrome p450, NOS and some heme containing transcription factors (142). Some of these proteins seem to mediate the functions of CO. For example, CO binds to heme containing transcription factor NPAS2 and regulates circadian gene expression (163). CO binds to cytochrome p450 and inhibits its activity (164).

2.0 THE ANTI-INFLAMMATORY EFFECTS OF CAV-1

In the present study, we directly detect the expression of cav-1 in mouse alveolar macrophages and demonstrate its regulation of LPS-induced cytokine production in a variety of mouse macrophages.

2.1 CAV-1 EXPRESSION IN ALVEOLAR MACROPHAGES

We first examined cav-1 expression in mouse alveolar macrophages by immunoblot analysis. As shown in Figure 3A, the levels of cav-1 expressed in alveolar macrophages and peritoneal macrophages are similar, with increased levels observed in NIH3T3 mouse fibroblasts. To better characterize the expression of cav-1 in murine alveolar macrophages, we performed co-localization studies using antibodies specific for the mouse macrophage-specific marker Mac-3 (165) and cav-1. Mac-3 immunostaining established that approximately 94% of cells derived from bronchoalveolar lavage (BAL) cells were macrophages. As shown in Figure 3B, double immunofluorescence staining of BAL macrophages with Mac-3 and cav-1 demonstrated cav-1 expression in alveolar macrophages. Cav-1 staining is mainly present on the surface and perinuclear compartments (Figure 3B) and extensively co-localizes with the Mac-3 antigen (Figure 3B), a known macrophage plasma membrane marker.

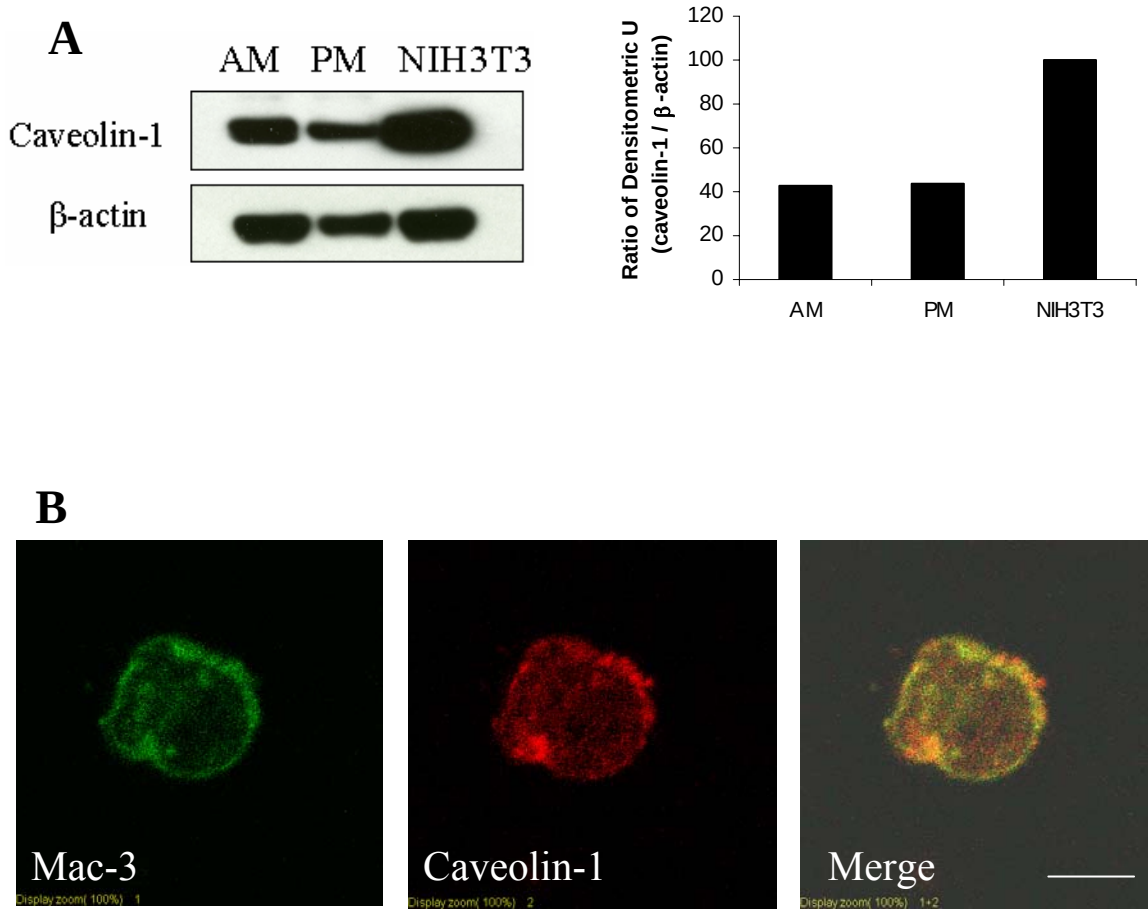

Figure 3 Cav-1 expression in mouse alveolar macrophages. Mouse alveolar macrophages were isolated and cultured. (A) Cav-1 and β-actin expressions were determined by Western blot analysis in murine peritoneal macrophages and NIH3T3 fibroblasts. (B) Immunofluorescence staining of cav-1 and Mac-3 were performed in murine alveolar macrophages. To investigate the quality of the alveolar macrophages, we stained them with the murine macrophage specific marker Mac-3. Isolated cells were subjected to immunofluorescence microscopy. 5×100 cells were counted and the green staining cells were regarded as macrophages. The percentage of positive staining cell was 94±2%. Scale bar: 7 μm.

2.2 THE ANTI-INFLAMMATORY EFFECTS OF CAV-1

2.2.1 Cav-1 regulates LPS-induced cytokines production

To assess the function of cav-1 in macrophages, we isolated murine alveolar macrophages and investigated the modulation of cytokines production in response to LPS. We transfected siRNA targeting specific cav-1 mRNA sequences into these macrophages. At 24 hours post-transfection, cav-1 protein levels were significantly decreased compared with that of the control, as evaluated by Western blot analysis (Figure 4A). Alveolar macrophages subjected to cav-1 knockdown exhibited significant and selective augmentation of proinflammatory cytokines TNF-α and IL-6 production and significant suppression of the anti-inflammatory cytokine IL-10 production after LPS stimulation (Figure 4B-D).

To further confirm whether cav-1 can modulate LPS-induced cytokine production, we used a cav-1 overexpressing RAW264.7 macrophage cell line. Overexpression of cav-1 caused marked attenuation of LPS-induced proinflammatory cytokines TNF-α and IL-6 and augmentation of anti-inflammatory cytokine Il-10 (Figure 5).

A

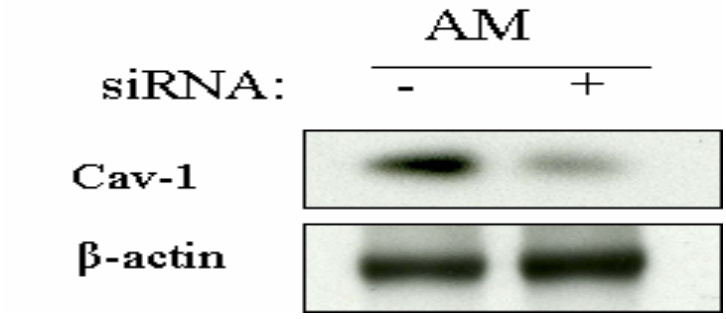

B

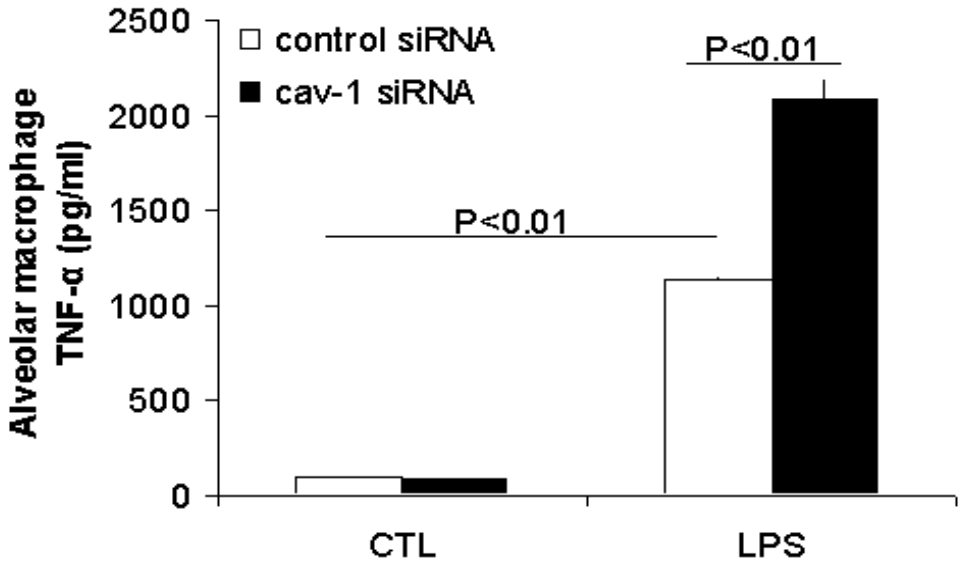
Alveolar macrophage TNF-α (pg/ml)
2500
2000
1500
1000
500
0
control siRNA
cav-1 siRNA
P<0.01
P<0.01
CTL
LPS

C

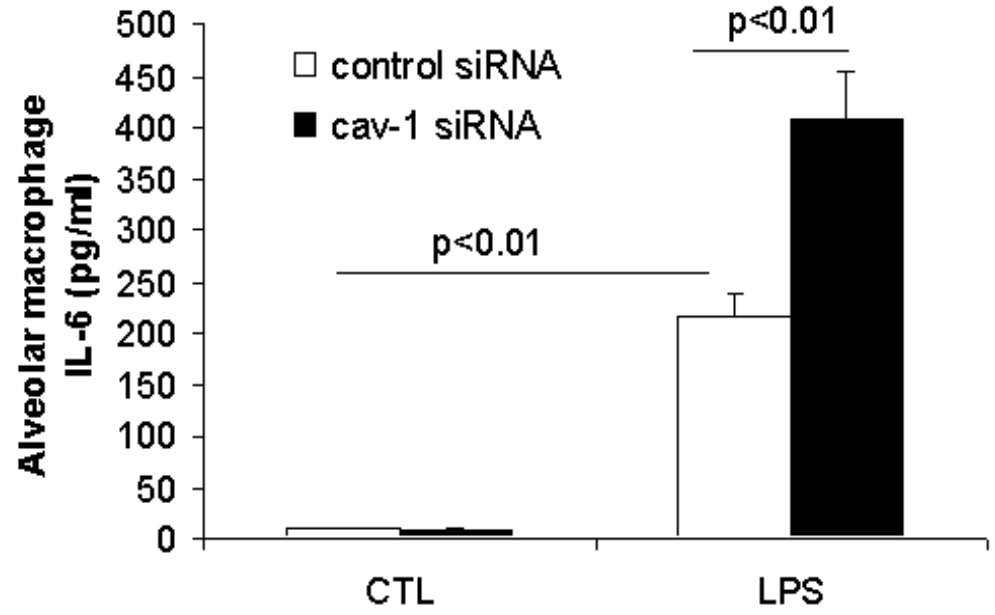
Alveolar macrophage IL-6 (pg/ml)
500
450
400
350
300
250
200
150
100
50
0
control siRNA
cav-1 siRNA
p<0.01
p<0.01
CTL
LPS

D

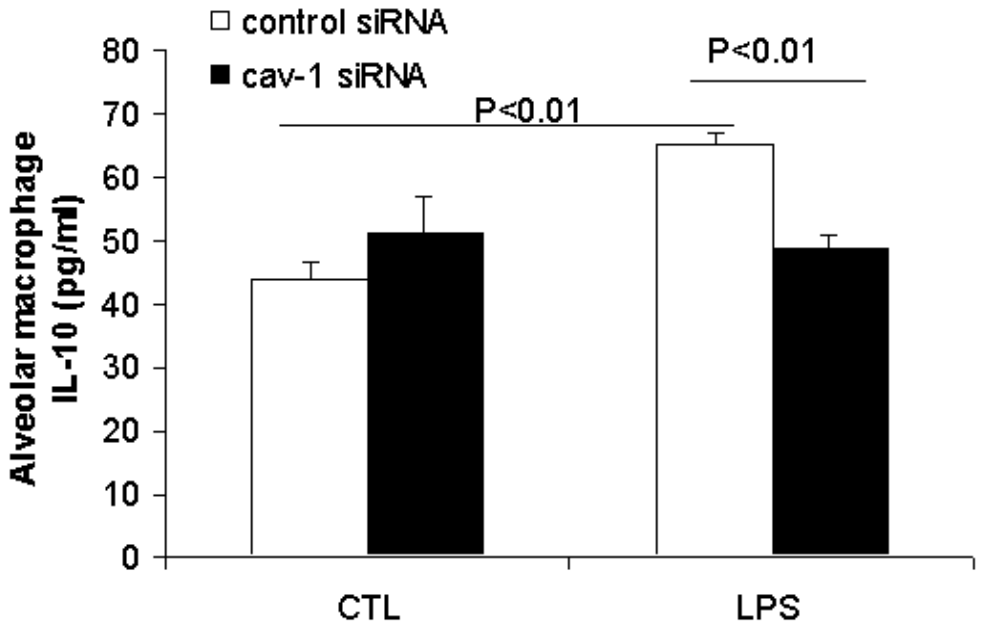

Figure 4 Modulation of LPS-induced cytokine production by down-regulating cav-1 expression in murine alveolar macrophages. Mouse alveolar macrophages were isolated and cultured. (A) The cells were transfected with siRNA of cav-1 and control siRNA for 24 hours. Cav-1 and β-actin expressions were determined by Western blot analysis. After 24 hours post-transfection, the culture medium of transfected peritoneal macrophages was harvested with or without LPS treatment for 4 hours. TNF-α (B), IL-6 (C) and IL-10 (D) cytokine production was determined by ELISA. Values were mean ± S.E., n = 3.

2.2.2 Cav-1 interacts with TLR4 and regulates TLR4 signaling

We next attempted to delineate the possible downstream mechanism by which cav-1 exerts its anti-inflammatory effects. It has been previously demonstrated that the effects of LPS on macrophages require recruitment of an LPS receptor complex (TLR4 and MD-2) to lipid rafts containing CD14 (166). Walton et al. reported that LPS induced membrane translocation of TLR4 and MD-2 to caveolar fractions of human aortic endothelial cells, by cell fractionation and immunofluorescence analyses (89, 167). Cav-1 has been reported to regulate membrane receptor signaling either by direct binding or through interaction with the downstream signaling molecules (22).

A

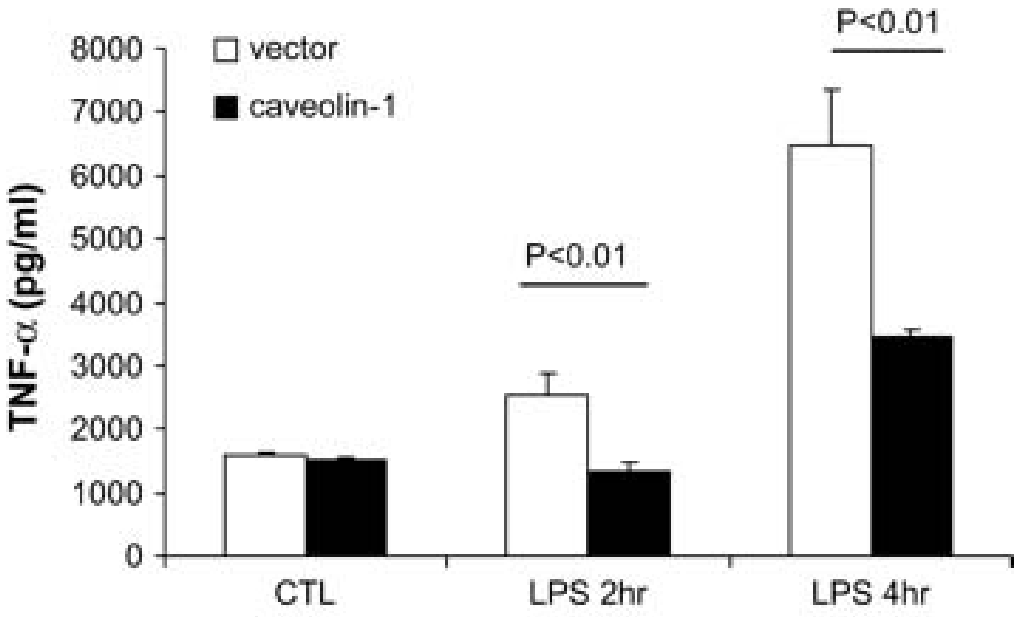
vector
caveolin-1
TNF-α (pg/ml)
8000
7000
6000
5000
4000
3000
2000
1000
0
P<0.01
P<0.01
CTL
LPS 2hr
LPS 4hr

B

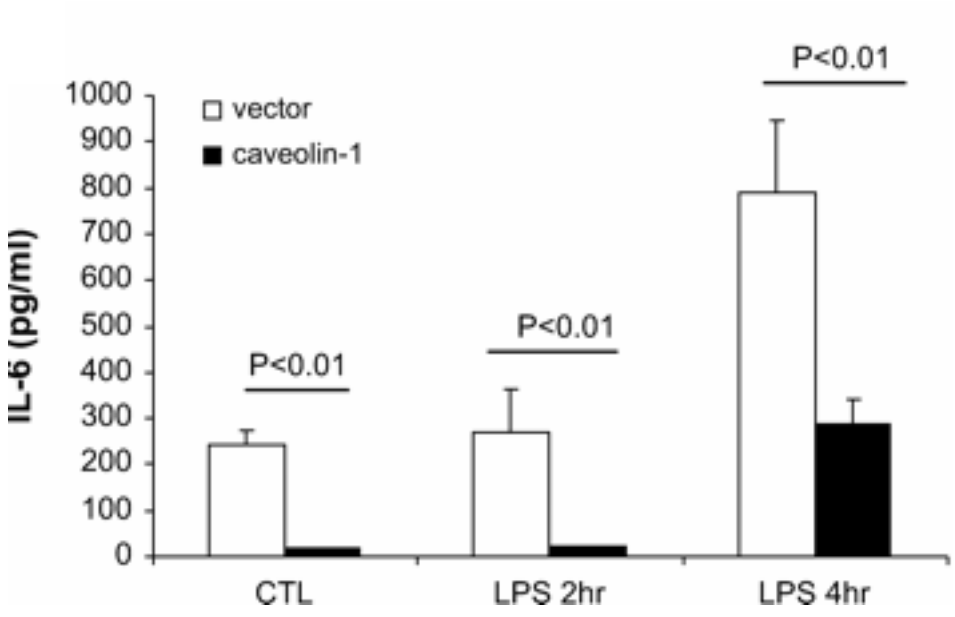
vector
caveolin-1
IL-6 (pg/ml)
1000
900
800
700
600
500
400
300
200
100
0
P<0.01
P<0.01
P<0.01
CTL
LPS 2hr
LPS 4hr

C

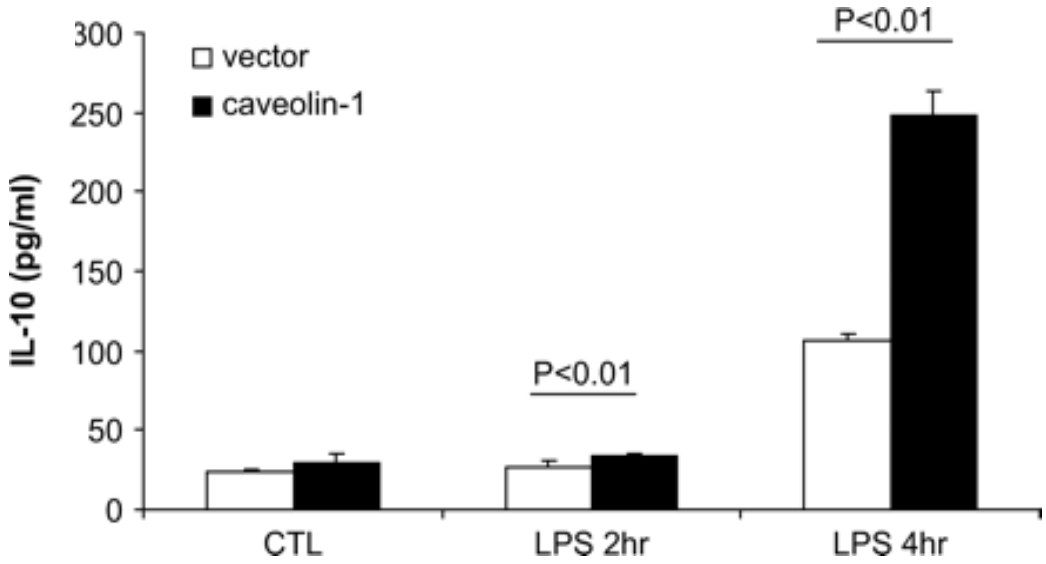

Figure 5 Over-expressing cav-1 in RAW264.7 modulates LPS-induced cytokines production. RAW264.7 cells stably transfected with cav-1, were serum starved for 24 hours and administrated LPS for 2 and 4 hours. The culture medium was harvested. (A) TNF-α (B) IL-6 and (C) IL-10 were determined by ELISA. Values were mean ± S.E., n = 3.

Interestingly, TLR4 contains a putative cav-1 binding motif (^{739}FIQSRWCIF^{747}) (11). It is possible that cav-1 may interact with the TLR4 complex and regulate its downstream effector functions.

We tested our hypothesis by co-immunoprecipitation. As demonstrated in Figure 6A and B, the antibody against TLR4 can pull down cav-1 protein and the antibody against cav-1 can pull down TLR4 protein. These data supported the interaction of cav-1 and TLR4 in the caveolar fraction of peritoneal macrophages.

Next, we determined the effects of cav-1 on TLR4 signaling. We tested whether cav-1 can affect TLR4 complex formation with MyD88 and TRIF. With cav-1 overexpression, MyD88 and TRIF association with TLR4 was markedly decreased (Figure 6C).

We next tested the hypothesis that cav-1 binds to TLR4 through the putative cav-1 binding motif. We performed PCR-based site-directed mutagenesis to mutate the two aromatic amino acid residues into Ala (Figure 7A) and inserted the construct into a Flag tagged expressing plasmid. We transfected the constructs into RAW264.7 (Figure 7B) and subjected them to co-immunoprecipitation. As shown in Figure 7C, the mutant transfectants did not interacted with TLR4 compared to the wild type, suggesting that cav-1 interacts with TLR4 through the cav-1 binding motif.

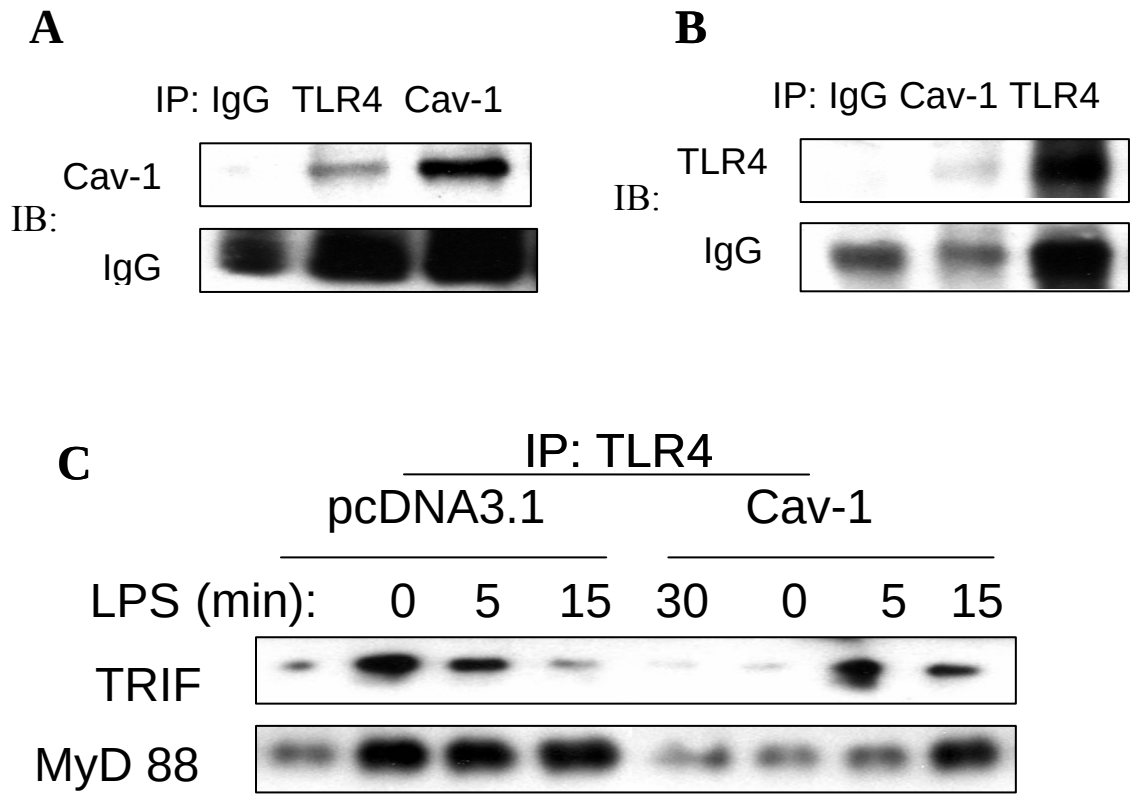

Figure 6 Cav-1 affects TLR4 signaling. (A, B) TLR4 interacts with cav-1. Peritoneal macrophages were isolated. The cells were serum starved for 12 hours. The caveolar fraction was isolated and subjected to immunoprecipitation and Western blot analysis. (C) Cav-1 decreased TLR4 complex formation after LPS stimulation. Cav-1 overexpressing and vector control cells were serum starved for 24 hours and treated with LPS for different time points. The cells were harvested and subjected to immunoprecipitation and Western blot analysis.

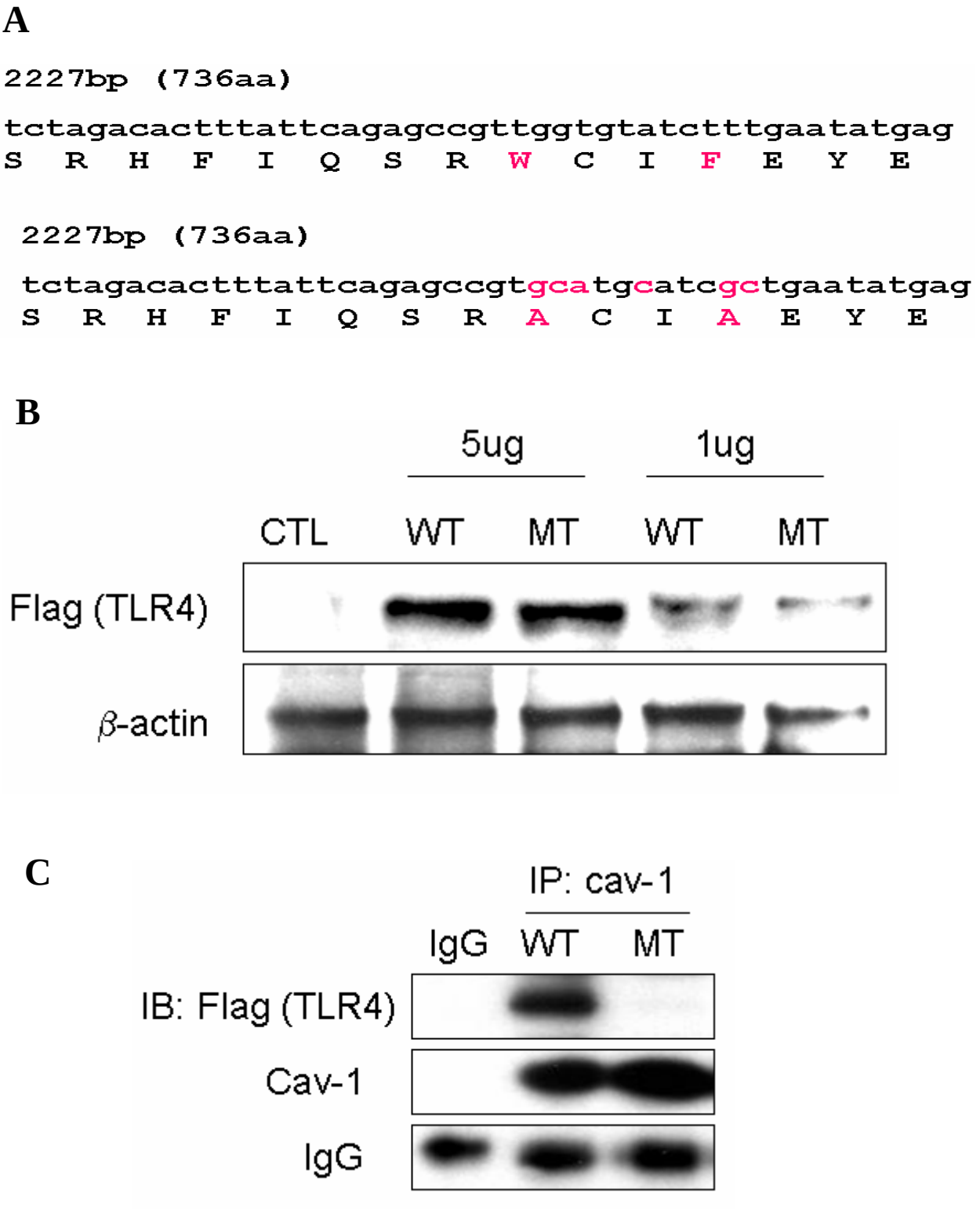

Figure 7 Cav-1 interacts with TLR4 through the cav-1 binding motif. (A) The designed mutation site and sequences of TLR4. (B) The WT and MT constructs were transfected into RAW264.7

cells. The cells were subjected to Western blot analysis. (C) After transfection, the cells were serum starved and subjected to co-immunoprecipitation as indicated. WT: wild type; MT: mutant.

2.2.3 Cav-1 modulates NF-κB signaling

NK-κB is well-known transcription factor that regulate LPS-induced cytokine production (168). We next investigated if cav-1 modulates the transcription factor NF-κB pathway. Cav-1 stably transfected RAW264.7 cells and vector control cells were treated with LPS. Cytosolic protein and nuclear extracts were obtained at different time points. We detected IκBα phosphorylation to indicate IKK activity and NF-κB p65 phosphorylation in the cytosolic fraction by immunoblot analysis. As shown in Figure 7A and B, LPS-induced IκBα and p65 phosphorylation in the cytosol was markedly inhibited in the cav-1 overexpressing cells compared to that of the control cells. Nuclear translocation of NF-κB p65 was significantly reduced as revealed by immunoblot analysis (Figure 8B). By immunofluorescence staining, we observed that p65 nuclear translocation occurred as early as 5 mins, while in control cells the translocation was rare at 5 min (Figure 8C). After 15 min, we observed significant p65 nuclear translocation in cav-1 overexpressing cells (data not shown). We also tested NF-κB activity by electrophoretic mobility shift assay (EMSA). Control cells treated with LPS showed a predicted increase in NF-κB binding activity; whereas cav-1 overexpressing cells treated with LPS showed a marked reduction in NF-κB binding activity (Figure 8D).

A

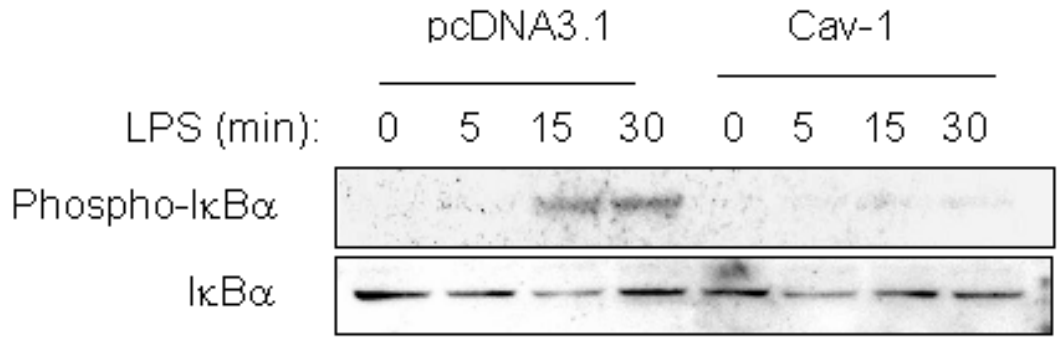

B

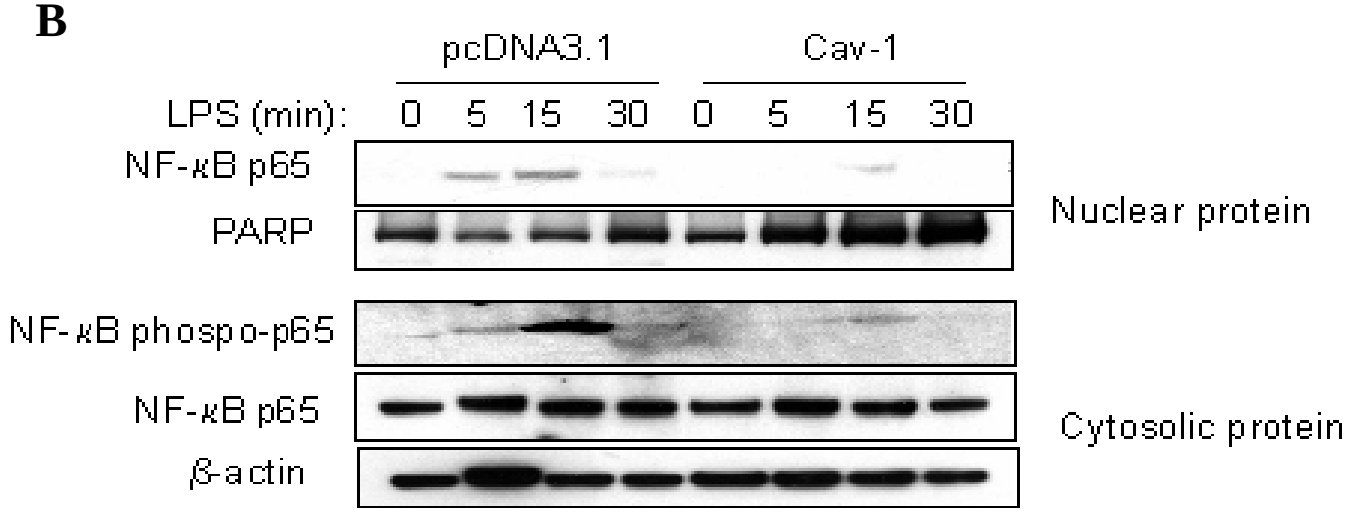
pcDNA3.1
Cav-1
LPS (min):
0 5 15 30 0 5 15 30
NF-κB p65
PARP
Nuclear protein
NF-κB phospo-p65
NF-κB p65
β-actin
Cytosolic protein

C

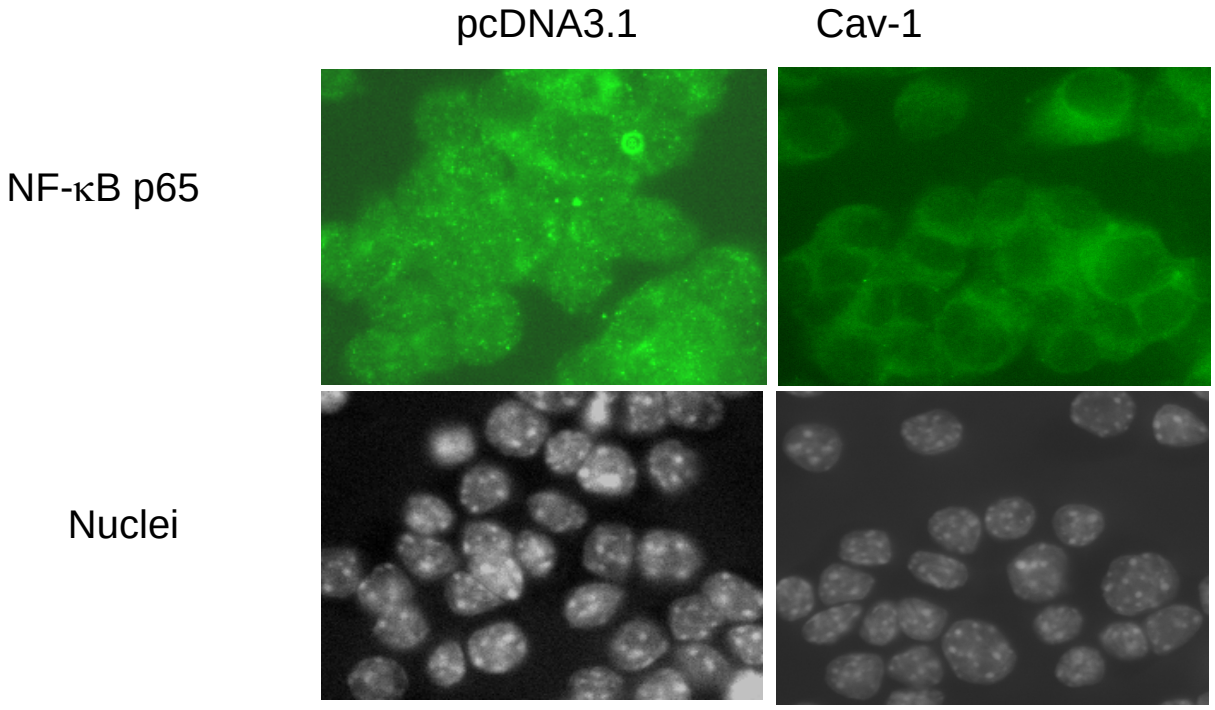
pcDNA3.1
Cav-1
NF-κB p65
Nuclei

D

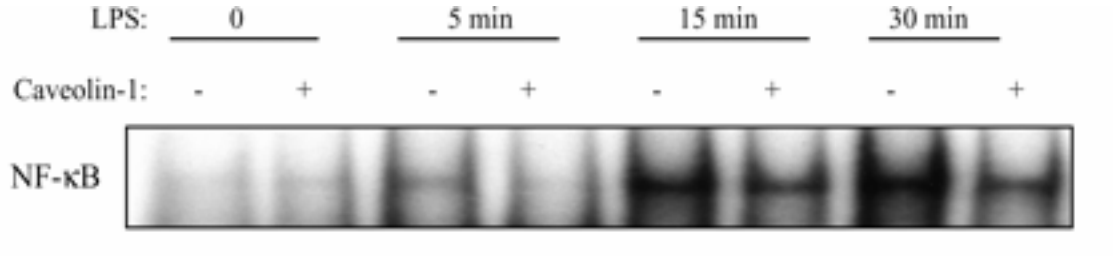

Figure 8 Cav-1 modulates NF-κB signaling. Cav-1 stably transfected RAW264.7 cells and control cells were treated with LPS. (A, B) Cytosolic protein and nuclear extracts were obtained at different time points and subjected to Western blot analysis for phospho-IκBα, IκBα, NF-κB phospho-p65, NF-κB p65. (C) Immunofluorescence staining for NF-κB p65 after 5 min LPS induction in RAW264.7 cells stably transfected with cav-1 and vector. (D) EMSA for NF-κB binding activity at different times of LPS induction.

2.2.4 Cav-1 modulates the MAPK pathway

Given that MAPK (ERK1/2) and PI3K mediate cytokine production and are regulated by cav-1 in fibroblasts and endothelial cells (169, 170), we examined whether MAPK and PI3K are modulated in cav-1 overexpressing RAW264.7 cells. LPS-induced activation of ERK1/2 MAPK, JNK MAPK and PI3K was significantly decreased while p38 MAPK activation was significantly increased in cav-1 overexpressing cells (Figure 9).

Because PI3K and all three MAPK pathways were regulated by cav-1, we tested which pathway attenuation would lead to a loss of cytokine modulation by cav-1. UO126 (the inhibitor of MEK1/2, upstream kinase of ERK) decreased TNF-α and IL-10 production compared with DMSO/LPS treatment (Figure 10). Wortmannin (the inhibitor of PI3K) decreased IL-10 production compared with DMSO/LPS treatment. SB203580 (the inhibitor of p38 MAPK) and

SP600125 (JNK inhibitor) decreased TNF- α, IL-6, and IL-10 cytokine production. We observed significant differences in cytokine production (TNF-α, IL-6, and IL-10) between cav-1 overexpressing and control vector RAW264.7 cells in DMSO/LPS, UO126/LPS, and wortmannin/LPS treatments. These findings suggest that ERK1/2 and PI3K pathways are not involved in the regulation of cytokine production by cav-1. However, SB203580, the inhibitor of p38 MAPK, eliminated the differences of TNF-α, IL-6, and IL-10 production between cav-1 overexpressing RAW264.7 and vector control cells. Administration of JNK inhibitor SP600125 had no effect on the modulation of the cytokine TNF-α and IL-10 production by cav-1, whereas reversed the modulation of cav-1 on IL-6 production. We observed that cav-1 increased p38 phosphorylation (Figure 9) while decreasing other MAPKs and PI3K activation. Chemincal inhibition of p38 activation eliminated the modulation of LPS-induced TNF-α, IL-6, and IL-10 production by cav-1. To explore further the role of p38 MAPK, we isolated mouse PMs from MKK3 (a major upstream kinase of p38) null mice and wild-type littermates and transfected with siRNA of cav-1. Decreasing cav-1 in MKK3 (-/-) macrophages had no effect on LPS-induced TNF- α, IL-6, and IL-10 production compared with the control siRNA transfectants (Figure 11).

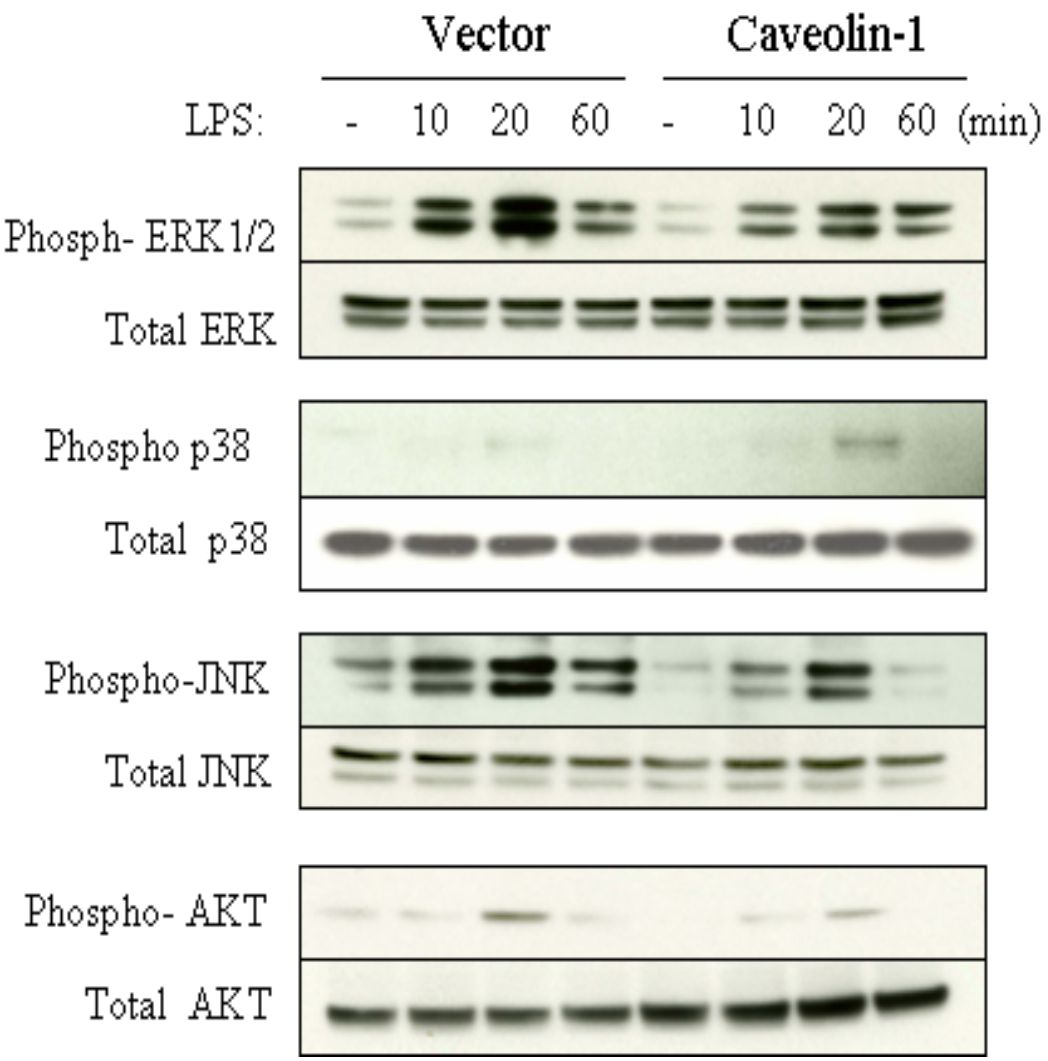

Figure 9 Modulation of MAPK and PI3K pathway by cav-1. After serum starvation for 24 h, RAW264.7 cells stably transfected with cav-1 gene and with control vector were treated with or without LPS for 10 min, 20 min, and 60 min. The cells were harvested and subjected to Western blot analysis for phosphorylated ERK1/2, JNK, p38, and Akt. The same blots were washed and blotted for total ERK1/2, JNK, p38, and Akt as the loading control.

A

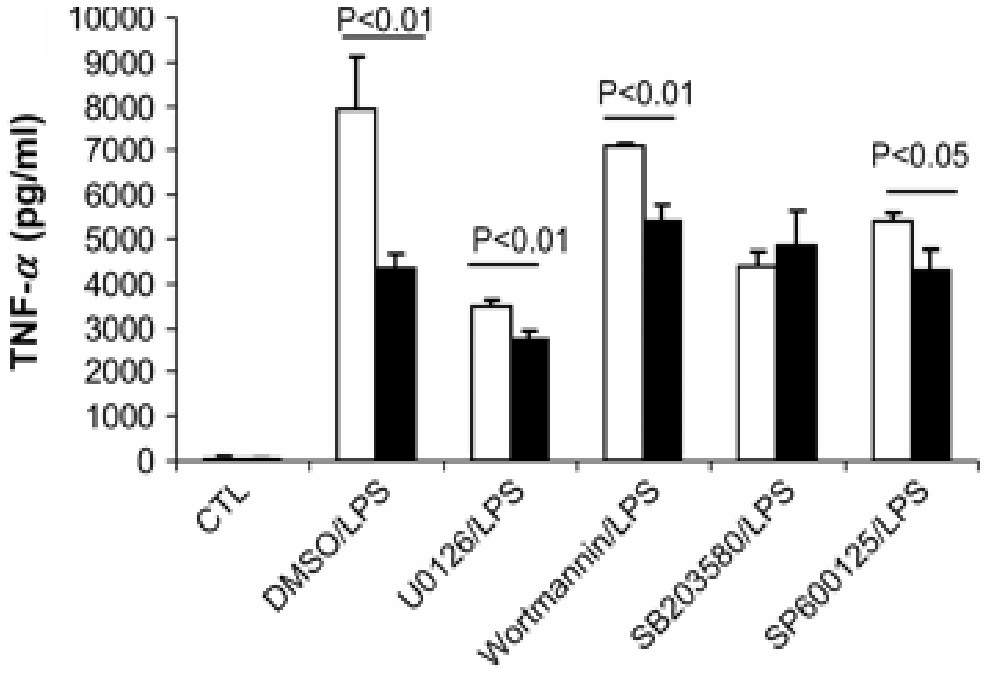
TNF-α (pg/ml)
10000
9000
8000
7000
6000
5000
4000
3000
2000
1000
0
P<0.01
P<0.01
P<0.01
P<0.05
CTL
DMSO/LPS
U0126/LPS
Wortmannin/LPS
SB203580/LPS
SP600125/LPS

B

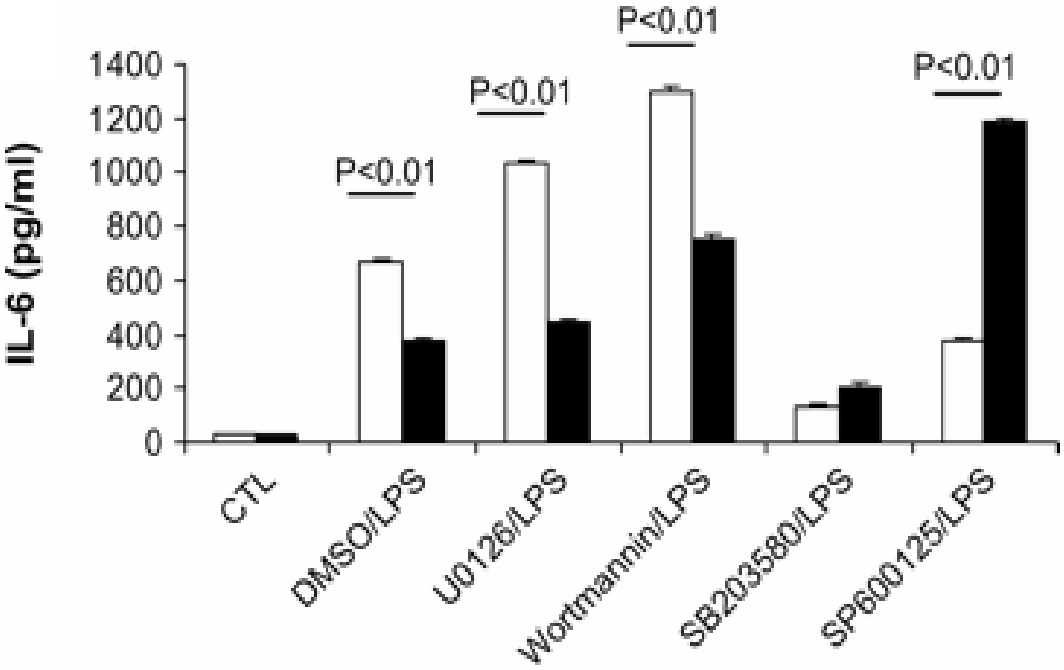
IL-6 (pg/ml)
1400
1200
1000
800
600
400
200
0
P<0.01
P<0.01
P<0.01
P<0.01
CTL
DMSO/LPS
U0126/LPS
Wortmannin/LPS
SB203580/LPS
SP600125/LPS

C

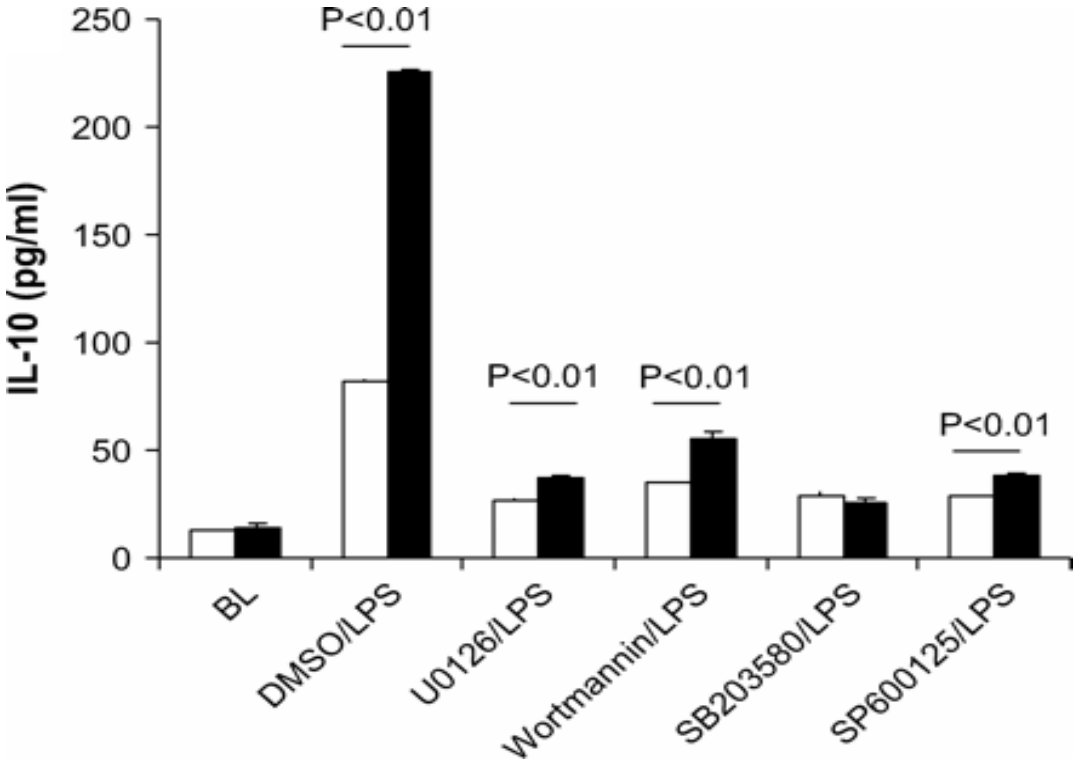

Figure 10 The p38 and JNK pathway are involved in the regulation of cav-1 on cytokines production. RAW264.7 cells stably transfected with cav-1 gene (filled bars) and with control vector (open bars) were serum starved for 24 h. The cells were pretreated for 2 h with DMSO with or without chemicals, including UO126, Wortmannin, SB203580, and SP600125. The treated cells were then administrated LPS for 4 h. The culture media were harvested. Cytokines levels in culture medium (A) TNF-α, (B) IL-6, and (C) IL-10 were determined by ELISA. Values were mean ± S.E., n = 3.

A

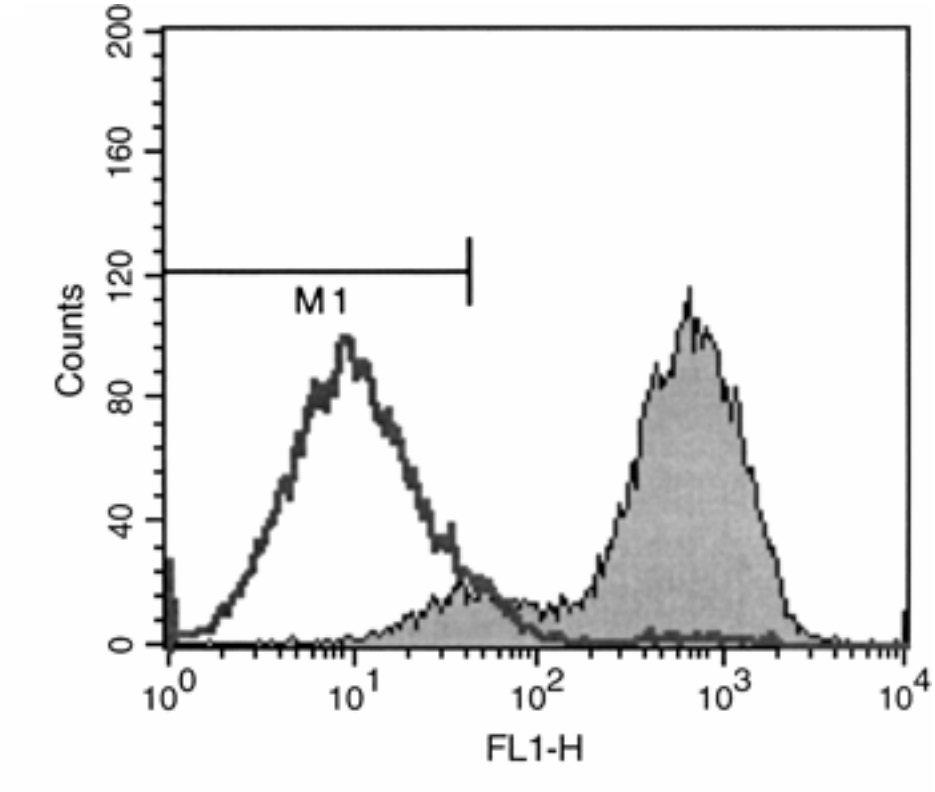
Counts
200
160
120
80
40
0
M1
10^0
10^1
10^2
10^3
10^4
FL1-H

B

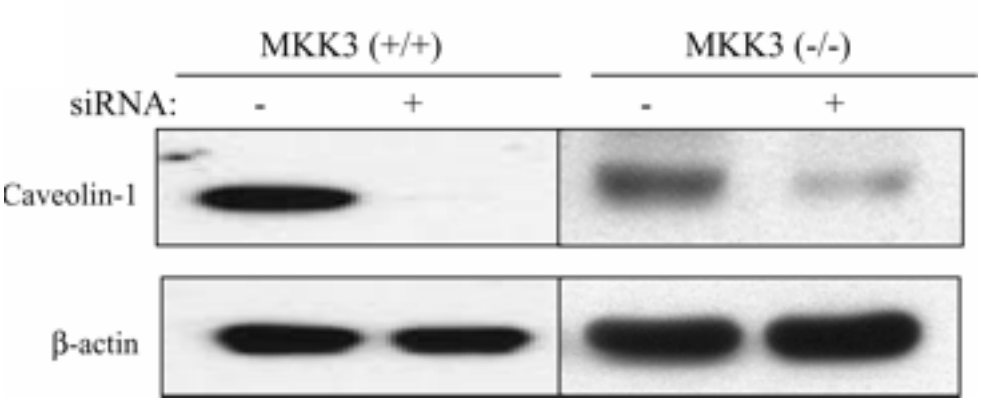
MKK3 (+/+)
MKK3 (-/-)
siRNA:
-
+
-
+
Caveolin-1
β-actin

C

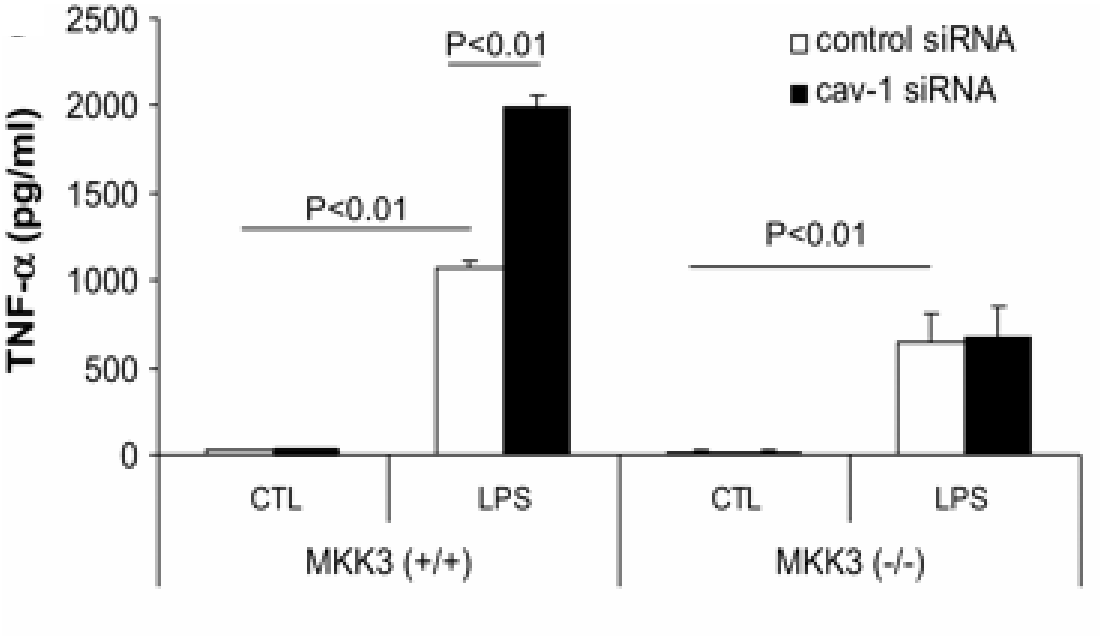

D

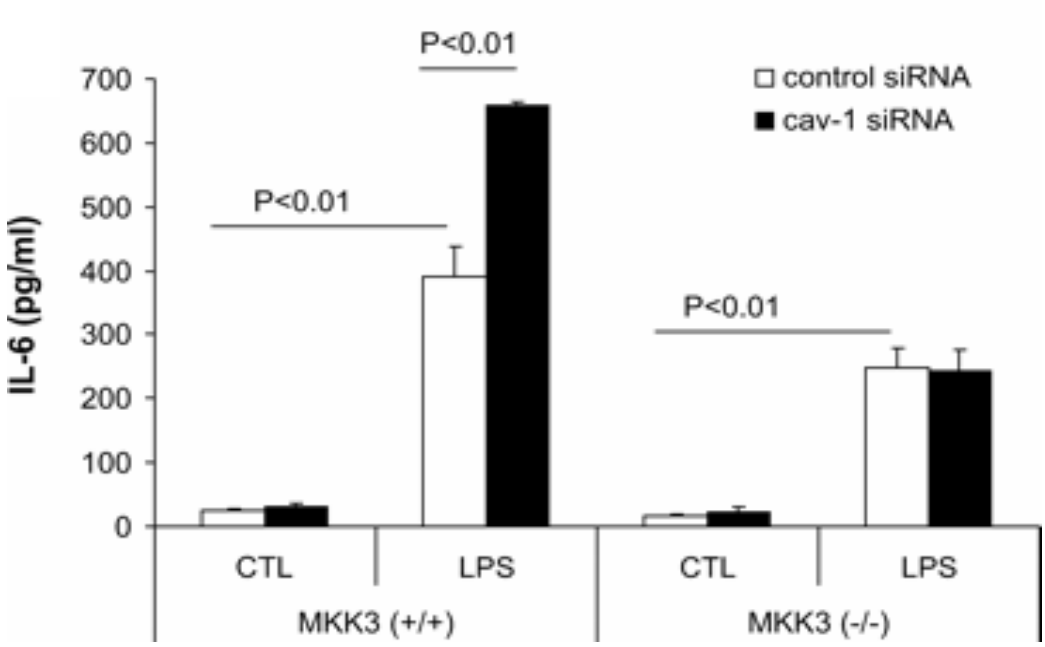

Figure 11 MKK3/p38 mediates the modulation of LPS-induced cytokine production by cav-1. PMs were isolated and cultured from MKK3 (+/+) and MKK3 (-/-) mice. (A) To investigate the quality of the macrophages, we performed murine macrophage–specific marker Mac-3 staining. For PMs, the cells were subjected to flow cytometry. The percentage of positive staining cells

was 95%. The cells were transfected with siRNA for cav-1 and the control siRNA. At 24 h posttransfection, the cells were treated with or without LPS for 4 h. The effects of siRNA transfection were determined by Western blot analysis (B).The culture medium was harvested. Medium cytokine levels TNF-α (C), IL-6 (D), and IL-10 (E) were determined by ELISA. Values were mean ± S.E., n = 3.

2.2.5 Cav-1 modulates AP-1 transcriptional activity

AP-1 is also a well-known transcription factor that regulate LPS-induced cytokine production (168). We hypothesized that cav-1 might also attenuate LPS-induced AP-1 activation. Cells treated with LPS showed a predicted increase in AP-1 binding activities, whereas cav-1 overexpressing cells treated with LPS showed a marked reduction in AP-1 binding activities (Figure 12A).

We next examined whether p38 MAPK was involved in the suppression of transcription factor AP-1 and NF-κB activation by cav-1. SB203580, the inhibitor of p38, was administered to RAW264.7 cells stably transfected with cav-1 gene and vector. Cav-1 attenuated the LPS-induced activation of NF-κB and AP-1. When SB203580 was added, the activation of NF-κB and AP-1 were similarly inhibited in vector-transfected cells as in cav-1 overexpressing cells (Figure 12B). SB203580 eliminated the attenuation of cav-1 on NF-κB and AP-1 activation, suggesting that p38 was involved in the suppression of cav-1 on LPS-induced inflammatory transcription factor activation

A

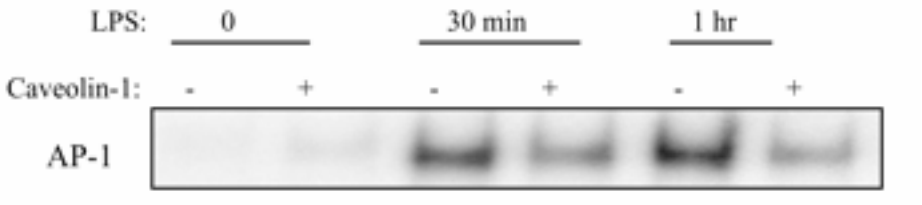

B

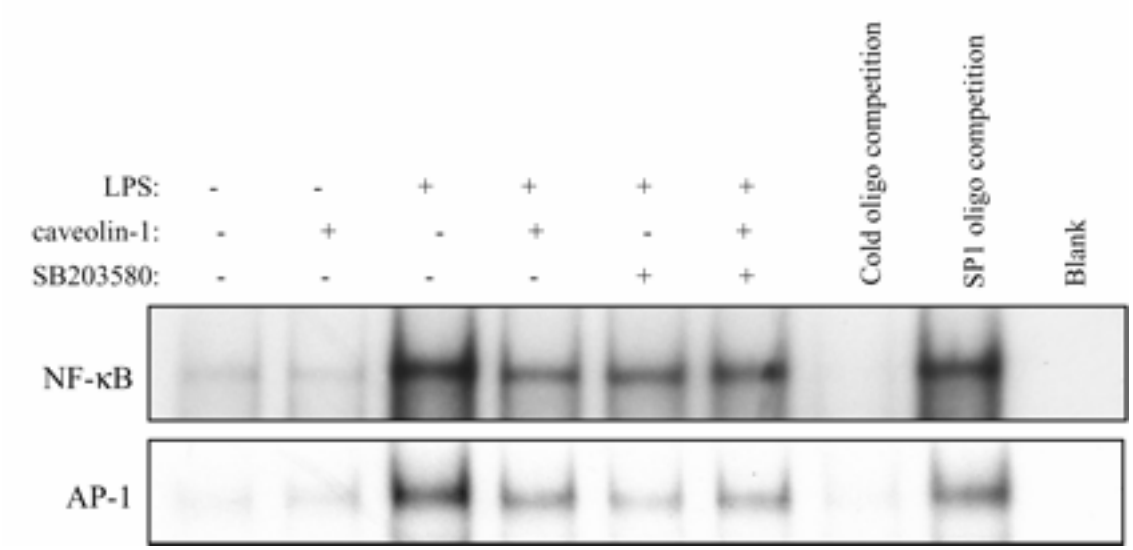

Figure 12 Effects of cav-1 on LPS induced AP-1 activation (A). RAW264.7 cells stably transfected with cav-1 gene and with control vector were serum starved for 24 h. After treatment with LPS for 0 min, 5 min, 15 min, 30 min, and 1 h, the cells were harvested. Nuclear proteins were extracted and subjected to EMSA for AP-1 activation. (B) Effects of SB203580 on LPS induced NF-κB and AP-1 activation. After serum starvation, RAW264.7 cells stably transfected with cav-1 gene or with control vector were pretreated with SB203580 or DMSO for 1 h. The nuclear proteins were extracted and subjected to EMSA for NF-κB and AP-1 activation. Cold oligonucleotides containing the transcription factor-binding site for NF-κB and AP-1 were added as a competition control, and cold oligonucleotides containing SP1 binding site were added as a negative competition control.

2.3 CAV-1 MEDIATES THE ANTI-INFLAMMTORY EFFECTS OF HO-1 & CO

2.3.1 HO-1 localizes in caveolae after LPS stimulation

Given the fact that cav-1 has the similar effects as HO-1 in the regulation of LPS-induced cytokine production and p38 MAPK pathways, we are interested in finding the relationship between these two molecules. We first tested if these two molecules are co-localized in mouse peritoneal macrophages. We observed that in the resident state, cav-1 localized with HO-1 in the high density sucrose fraction, but not in the low density sucrose fraction which is the typical caveolar fraction. After LPS stimulation, a notable potion of HO-1 translocated into the caveolar fraction and co-localized with cav-1 (Figure 13A). Taking advantage of the fact that caveolae are rich in cholesterol and Triton-X 100 insoluble at 4 ^{0}C, we isolated caveolae using ultracentrifugation (171). Consistently, HO-1 was only found in detergent soluble fraction in the resident state, while HO-1 was observed in detergent insoluble fraction after LPS (Figure 13B) and hemin stimulation (data not shown).

A

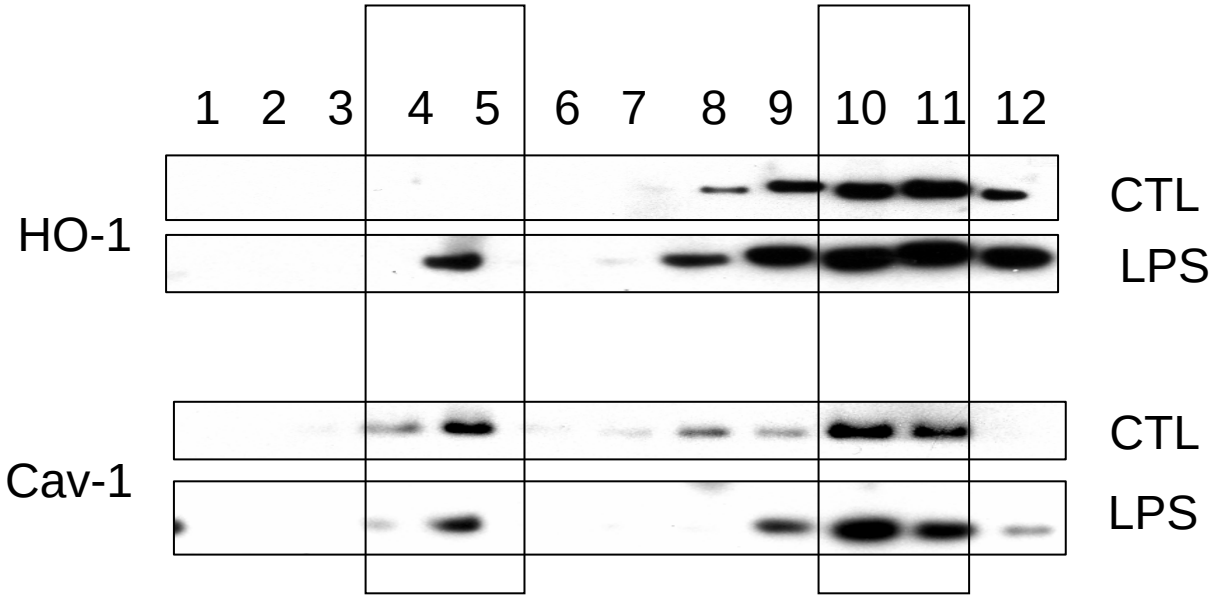

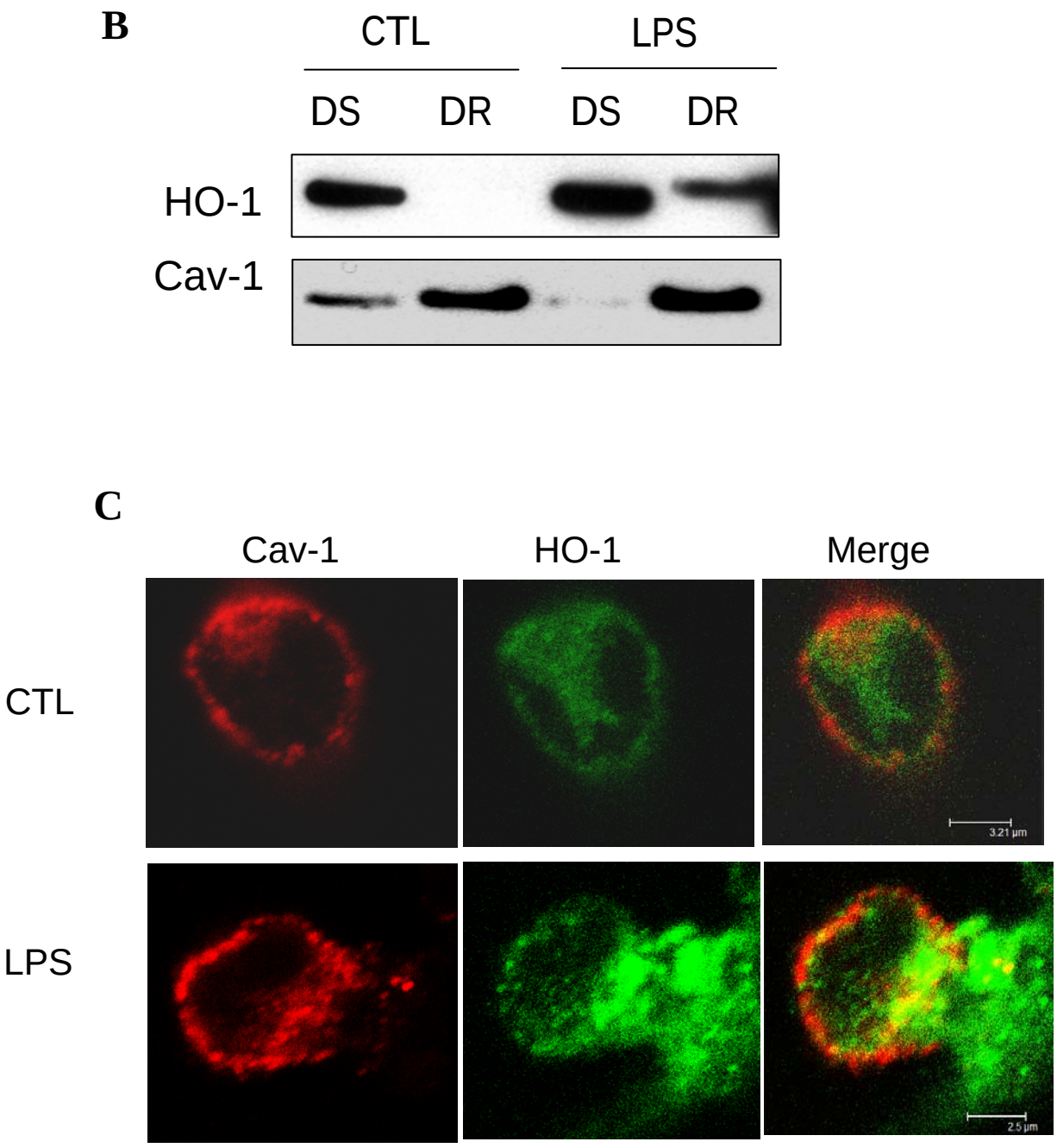

Figure 13 HO-1 translocates into the caveolae after LPS stimulation. Peritoneal macrophages were isolated and subjected to LPS stimulation for 16 hours. (A) The cells were harvested. Sucrose density ultracentrifugation was performed. 12 fractions were subjected to Western blot analysis. (B) 1% Triton-X 100 MBS buffer was used to homogenize the cells prior to ultracentrifugation. The pellets were the detergent resistant fraction: DR. The supernatant was the detergent soluble fraction: DS. (C) Peritoneal macrophages were isolated and cultured. The cells were subjected to immunofluorescence staining for HO-1 and Cav-1. Confocal microscopy was used to identify the co-localization. Arrow indicates yellow color.

Next, we were interested in the question of whether HO-1 translocated into caveolae is functionally active. So we isolated the caveolar fraction of peritoneal macrophages and used the other fractions as the non-caveolar fraction control. As shown in Figure 14, HO activity in caveolar faction is increased after LPS treatment as well as in non-caveolar fractions. The SnPP treated and the non-LPS stimulated samples had low bilirubin content, similar as boiled proteins, indicating that HO-1 activity in caveolae is inducible and specific. We noticed the relative small HO-1 protein content in caveolae. So although it looks that the total HO-1 activity is higher in cytosol on per mg protein basis, actually, HO activity was higher in caveolae than in non-caveolar fraction if standardized with the same HO-1 protein.

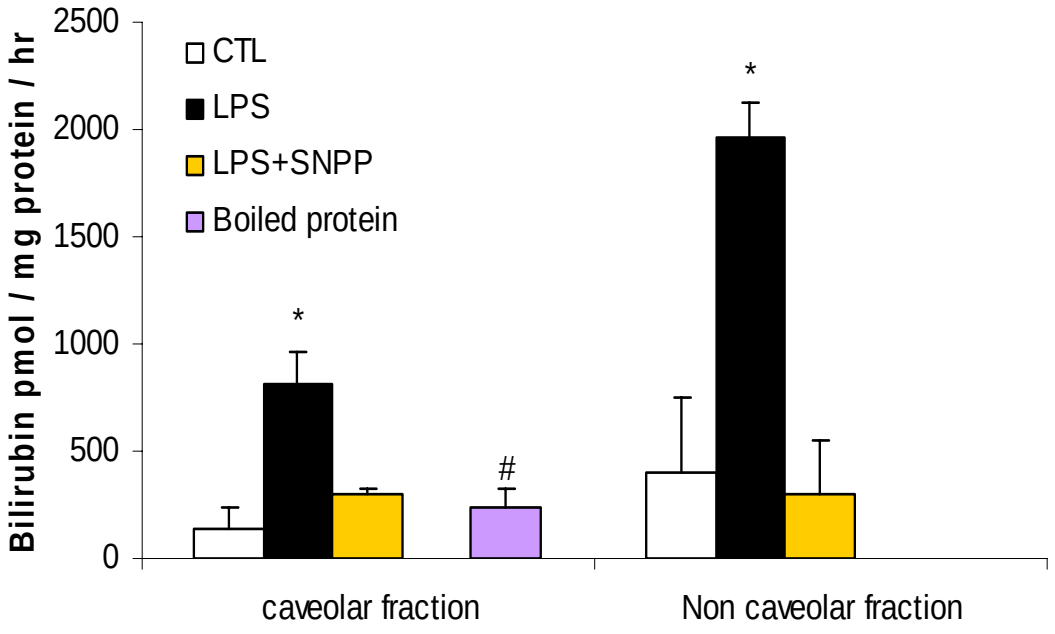

Figure 14 HO activity in caveolae. Peritoneal macrophages were isolated and cultured. The cells were serum starved and stimulated with LPS. The proteins were subjected to caveolar fractionation as indicated in methods. HO activity was determined. * indicated $p<0.05$ as compared to non-LPS stimulation. # indicated $p<0.05$ as compared to LPS induced HO activity in caveolar fraction.

2.3.2 The mechanism of the translocation of HO-1

We were interested in the mechanism of the translocation of HO-1. Previous publications indicate that PKCs were involved in membrane protein trafficking (172). Also, p38 was reported to be critical in the anti-inflammatory effects of HO-1 (145). We chose PKC and p38 as our potential candidates here. We found that inhibition of PKC by GF 109203X did not affect LPS-induced HO-1 translocation. Interestingly, inhibition of p38 by SB203580 markedly suppressed HO-1 translocation (Figure 15A). To further investigate the involvement of p38, we isolated some peritoneal macrophages from MKK3 null mice. As shown in Figure 15B, HO-1 translocated into the caveolar fraction after LPS stimulation in wild type macrophages. In MKK3 null cells, the existence of HO-1 in the caveolar fraction was significantly reduced after LPS compared with wild type cells. As a control, we found that hemin stimulation also induced the HO-1 membrane translocation, which was not affected by MKK3 knockout. These data supported that HO-1 translocation into caveolae is dependent on p38 in particular.

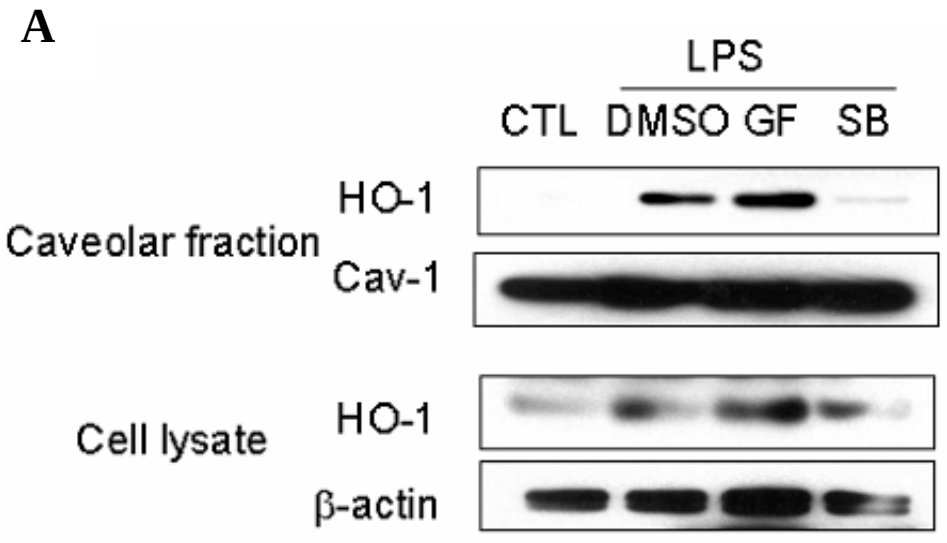

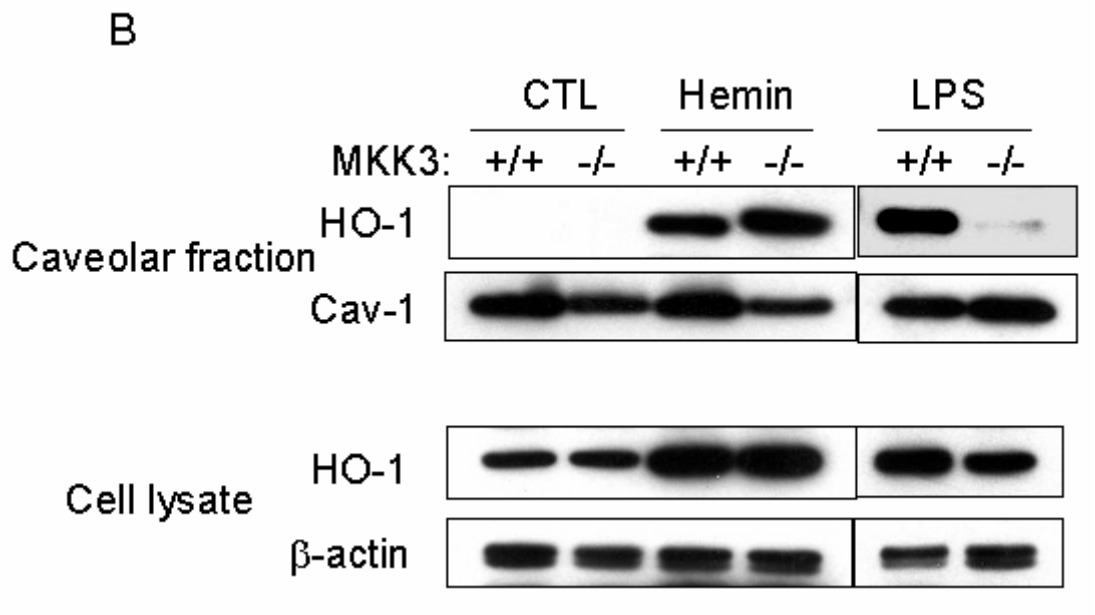

Figure 15 LPS-induced HO-1 translocation into caveolae dependent on MKK3 / p38 pathway. (A) Peritoneal macrophages were isolated from C57BL/6 mice. The cells were treated with GF 109203X or SB 203580 for 1 hour. Then LPS was administrated. The cells were harvested and caveolar fractions or whole cell lysates were isolated and subjected to Western blot analysis for HO-1, cav-1, or β-actin (B) Peritoneal macrophages were isolated from MKK3 null mice and wild type littermates. The cells were treated with hemin or LPS. The cells were then harvested and subjected to caveolar fraction isolation and Western blot analysis for HO-1 and cav-1. The whole cell lysates were also harvested and use as a control.

2.3.3 Cav-1 mediates the anti-inflammatory effects of CO

Cav-1 and HO-1 have similar anti-inflammatory effects in the regulation of LPS-induced cytokines production. TLR4 and HO-1 both localize in caveolae together with cav-1. We hypothesized that cav-1 may mediate the anti-inflammatory effects of HO-1 or that HO-1 mediates the effects of cav-1. We used the peritoneal macrophages isolated from cav-1 null mice to investigate the hypothesis. As demonstrated in Figure 16, 250 ppm CO inhibited LPS-induced TNF-α and IL-6 production. The effects of CO were lost in cav-1 null mice. These data suggested that cav-1 mediates the anti-inflammatory effects of CO.

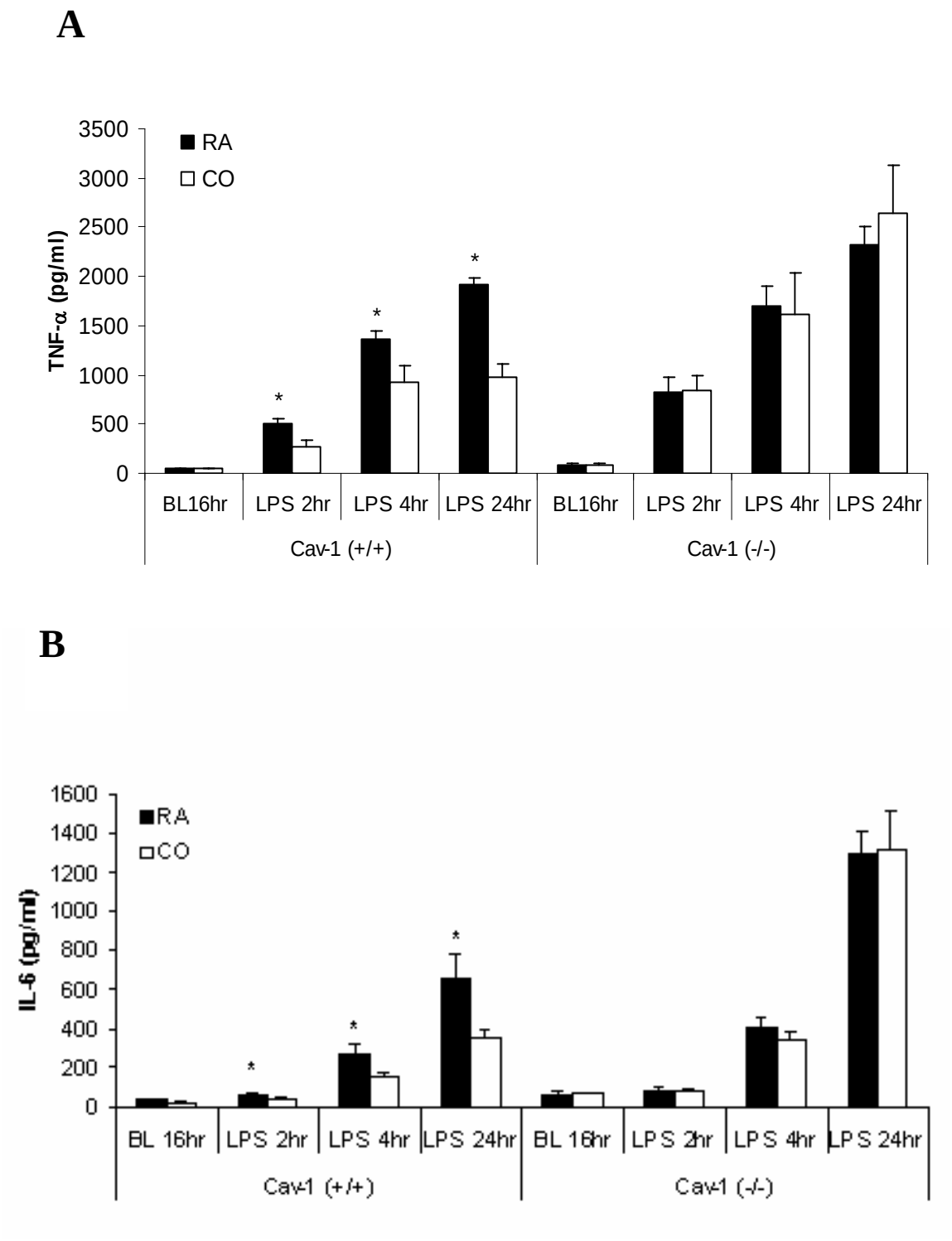

Figure 16 Cav-1 mediates the anti-inflammatory effects of CO. Cav-1 null mice and wild type mice were sacrificed. The peritoneal macrophages were isolated and cultured for 16 hours. The media were harvested after LPS treatment for 2 hours, 4 hours, and 24 hours. Cytokine productions were determined by ELISA. Values were mean ± S.E., n = 3.

2.3.4 Cav-1 regulates LPS-induced cytokines production independent of HO-1

We also tested the possibility that HO-1 mediates the anti-inflammatory effects of cav-1. We used SnPP to inhibit HO activity in RAW264.7 cells overexpressing cav-1 or vector control. As shown in Figure 17, overexpressing cav-1 still inhibited LPS-induced TNF-α and IL-6 production after the administration of SnPP.

A

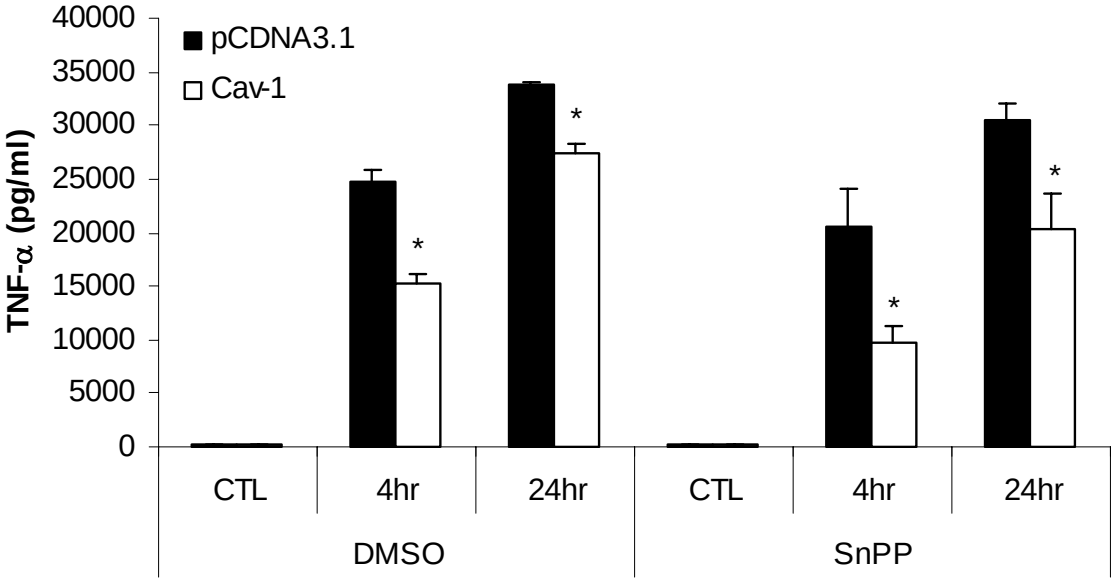

B

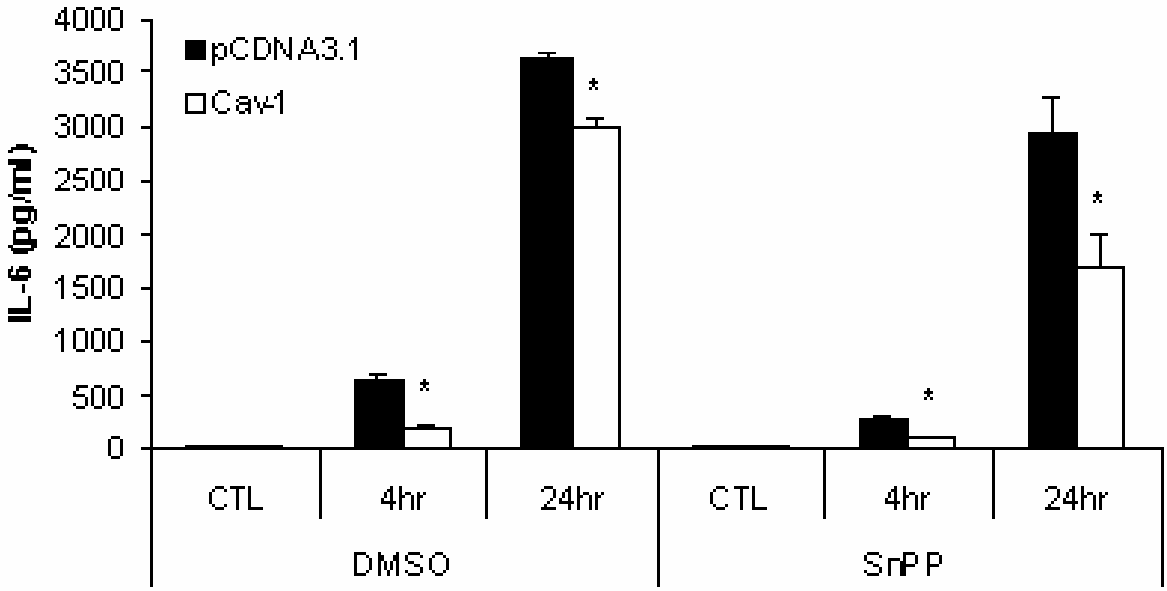

Figure 17 Cav-1 regulates LPS-induced cytokines production independent of HO-1. RAW264.7 cells stably transfected with cav-1 or pcDNA3.1 vector were cultured and serum starved for 24 hours. The cells were treated with different time of LPS. The media were harvested and cytokines productions were determined by ELISA. Values were mean ± S.E., n = 3. * indicated $P<0.05$; CO compared with RA.

2.3.5 CO modulates cav-1 expression and interaction with TLR4

Previously, we showed that cav-1 interacted with TLR4 (Figure 6A). The interaction disrupted TLR4 complex formation (Figure 6B). Together with the data that cav-1mediates CO effects of regulating LPS-induced cytokines production, we next investigated whether CO can

directly modulate cav-1 expression and interaction with TLR4. As shown in Figure 18A, CO treatment (2 hours 250 ppm) induced cav-1 expression markedly in peritoneal macrophages. The induction was increased after 24 hours CO treatment. Administration of hemin, the substrate of HO-1, which induced HO-1 activation, increased TLR4 interaction with cav-1 (Figure 18B). CO treatment mimicked those effects (Figure 18B).

A

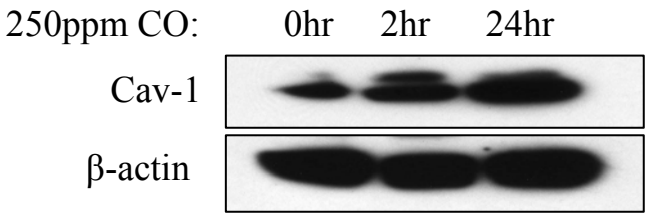

B

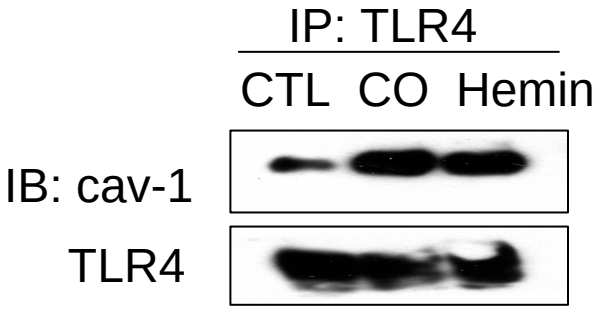

C

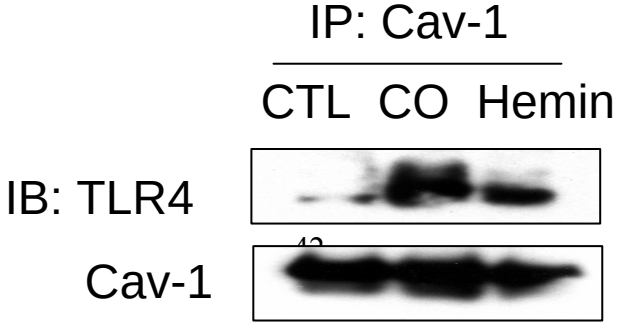

Figure 18 CO modulates cav-1 expression and interaction with TLR4. Peritoneal macrophages were isolated and cultured. (A) The cells were treated with room air or CO for 2 hours and 24 hours. The cells were harvested and subjected to Western blot analysis. (B) The cells were treated with CO or hemin for 16 hours. The cells were harvested and subjected to immunoprecipitaiton and Western blot analysis.

2.3.6 Summary

Cav-1 was demonstrated to have anti-inflammatory effects in macrophages in this chapter. First, cav-1 was shown to exist in mouse alveolar macrophages, mainly localized in plasma membrane and peri-nuclear areas. Down-regulating cav-1 by siRNA increased pro-inflammatory cytokines (IL-6 and TNF-α) production and decreased anti-inflammatory cytokine (IL-10) production in mouse peritoneal and alveolar macrophages. Up-regulation of cav-1 by stable transfection decreased pro-inflammatory (IL-6 and TNF-α) cytokines production and increased anti-inflammatory (IL-10) cytokine production in RAW264.7 macrophage cell line. A cav-1 binding motif was identified within the c-terminal region of TLR4 protein. Co-immunoprecipitation and site-directed mutagenesis further confirmed that cav-1 binds to TLR4 via its binding motif. The association of cav-1 and TLR4 disrupted adaptor molecule MD-2 and TRIF recruitment. Overexpressing cav-1 in RAW264.7 cells marked inhibited NF-κB signaling. IKK activity was reduced. NF-κB p65 phosphorylation and nuclear translocation was inhibited. EMSA showed that cav-1 suppressed AP-1 and NF-kB transcriptional factor activity. MAPK pathway was also affected by cav-1 stable transfection. MKK3 / p38 pathway was shown to involve in the regulation of cytokines production by cav-1.

HO-1, the cyto-protective gene, was shown to translocate into caveolae and co-localize with cav-1 after LPS stimulation. The trafficking of HO-1 was dependent on p38. The caveolar HO-1 had HO activity and CO was generated in sites of caveolae. Exogenous CO administration is able to increase the interaction between TLR4 and cav-1. This LPS-induced HO-1 trafficking loop is appeared to be an important negative regulation mechanism for dampening LPS signal and protection for the cell.

3.0 THE ANTI-FIBROTIC EFFECTS OF CAV-1

In the present studies, we tested our hypothesis that cav-1 might be involved in the pathogenesis of lung fibrosis and regulate ECM production by several independent ways. We extensively investigated cav-1 expression in lung tissue and fibroblasts from IPF patients and control subjects. We report for the first time that cav-1 confers anti-fibrotic effects both in vitro and in vivo. Our data suggest that cav-1 is an important regulator in the pathogenesis of pulmonary fibrosis and indicate an exciting and promising potential role for cav-1 in the therapy for pulmonary fibrosis.

3.1 ALTERED CAV-1 EXPRESSION IN IPF

Cav-1 expression was reported to decrease in experimental animal models of pulmonary fibrosis (173-175). To determine whether expression of cav-1 was altered in patients with IPF, we looked for cav-1 gene expression in an IPF dataset previously described. We observed a 2 fold reduction in cav-1 mRNA in IPF lung tissues ($P = 0.000087$, Figure 19A). We found a similar decrease in another dataset (20) that we recently published (data not shown). The reduction of cav-1 protein expression was confirmed by densitometric analysis of immunoblots (Figure 19B) and by immunohistochemistry staining (Figure 19C). Among the 14 lung tissue samples examined (7 IPF patient and 7 control subject), cav-1 protein expression was decreased by approximately 73% in IPF patients as measured by the ratio of band densitometric units of cav-1 to β-actin compared to the controls ($P = 0.035$, Figure 19B).

Fibroblasts play an active role in ECM production, deposition and chemokine signaling during the process of pulmonary fibrosis (176). We next examined cav-1 expression in human pulmonary fibroblasts (4 IPF and 5 control). We observed marked reduction of cav-1 mRNA

expression in primary pulmonary fibroblasts derived from IPF patients compared to control subjects (P = 0.037, Figure 19D). Similarly, cav-1 protein expression was decreased in primary fibroblasts from IPF patients compared to control subjects (P = 0.014, Figure 19E).

A

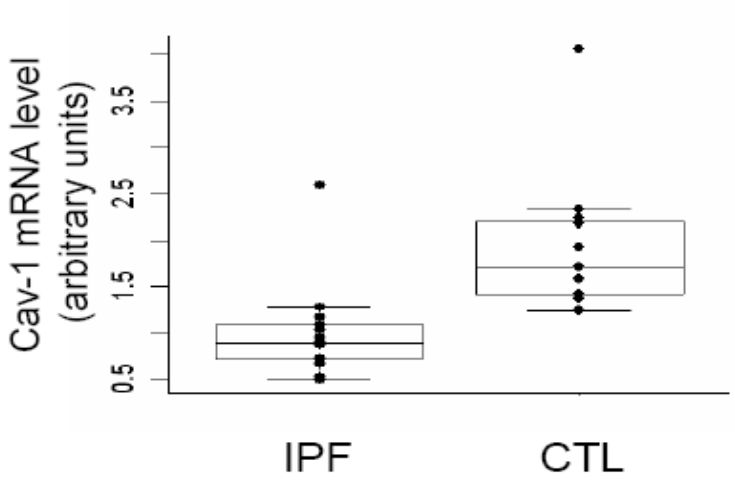

B

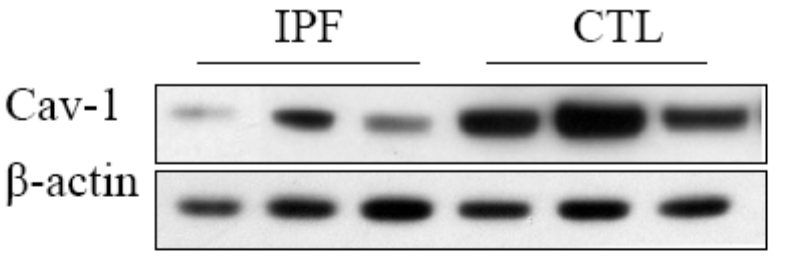

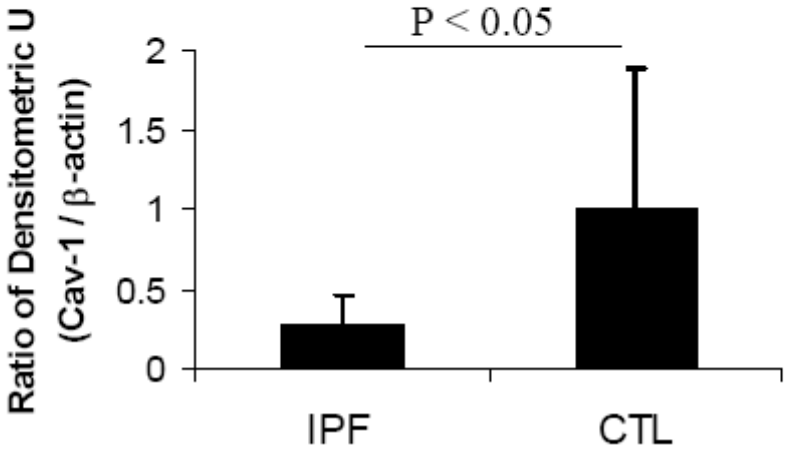

C

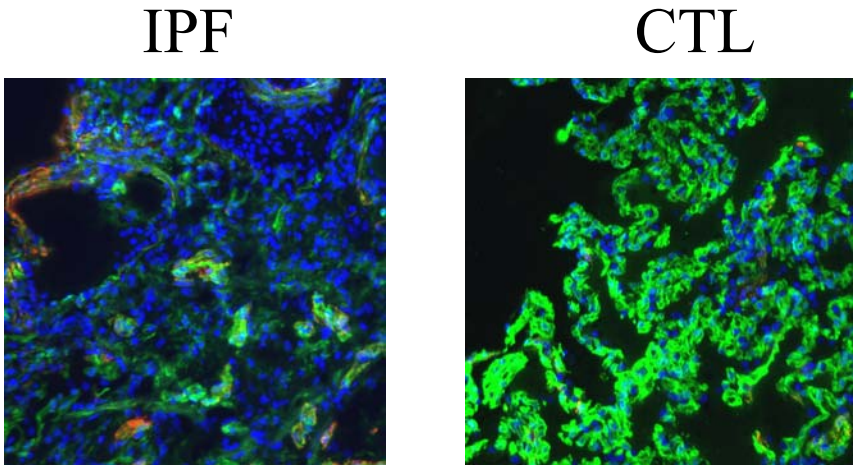

D

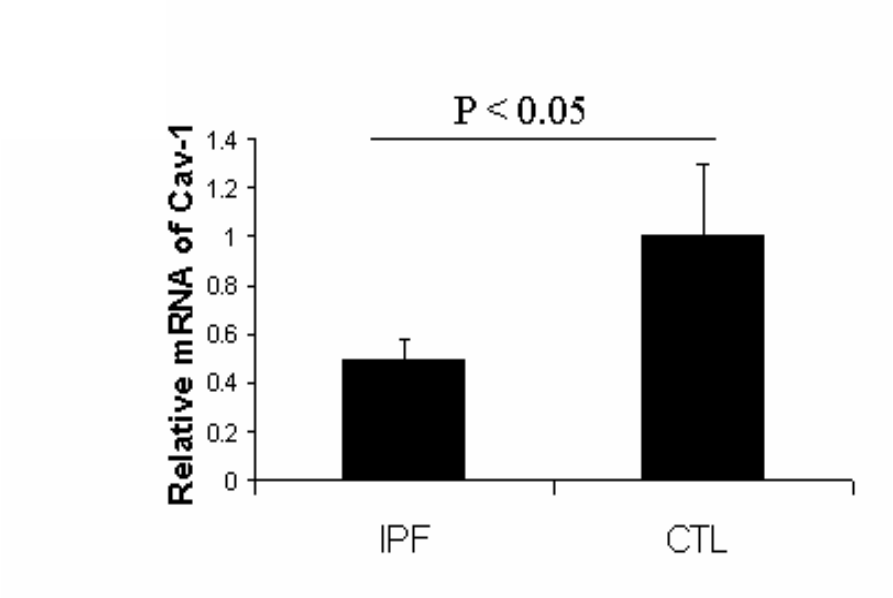

E

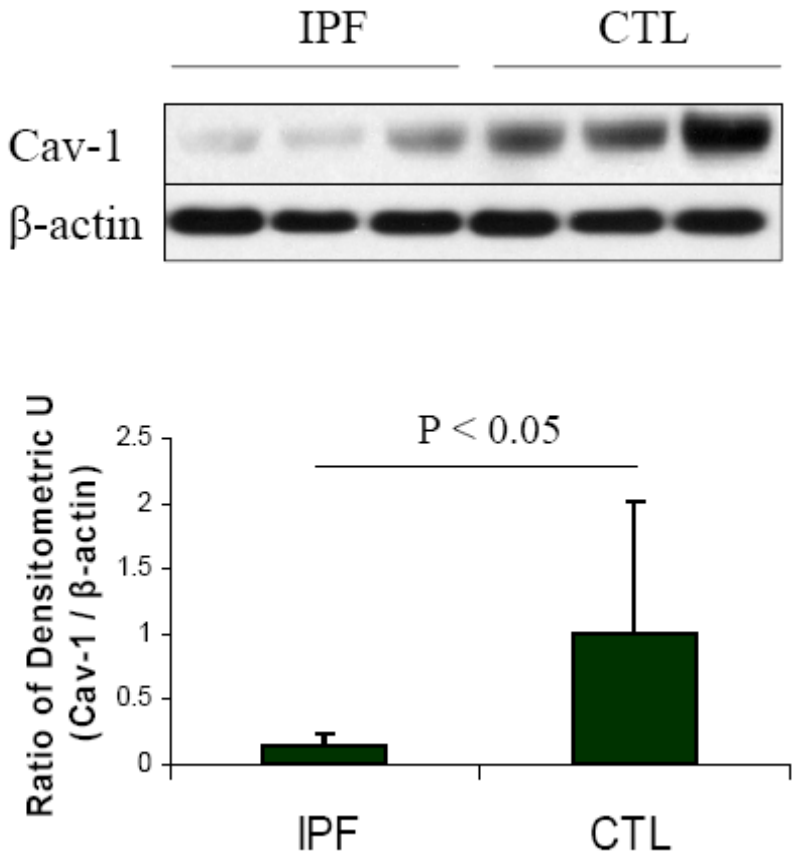

Figure 19 Altered cav-1 expressions in IPF patients. (A) Microarray analysis of Cav-1 mRNA reveals a significant reduction ($p = 0.000087$, fold 0.5) in IPF patients (n=13) compared to controls (n=11). (B) Cav-1 protein expressions as detected by Western blot analysis in lung tissue samples from IPF patients (n = 7) and control subjects (n = 7). 3 representative samples of patient and control were shown. (C) Immunohistochemical analysis of cav-1 expression in lung tissue sections. Green indicates cav-1; blue indicates nucleus; orange indicates α-SMA. A representative example out of seven for patient sample or control subjects was shown. (Original magnification, x20.) (D) Cav-1 mRNA expressions were detected by Taqman PCR in pulmonary fibroblasts derived from IPF patients (n=4) and control subjects (n=5) (E) Cav-1 and β-actin protein expressions were determined by Western blot analysis in pulmonary fibroblasts derived from IPF patients (n=4) and control subjects (n=5). 3 representative samples of patient and control were shown. The differences in mRNA level of cav-1 expression were compared by Student's t-test. The differences in protein level of cav-1 expression were compared by Wilcoxon two-sample test. The differences were considered significant at $p<0.05$.

3.2 TGF-β_1 REGULATES CAV-1 EXPRESSION IN PULMONARY FIBROBLASTS

TGF-β_1 is one of the key cytokines involved in pulmonary fibrosis (102). Its level, contrary to cav-1 expression, increases significantly in active fibrotic areas (102), which leads to the hypothesis that TGF-β_1 might be one of the negative regulators of cav-1 expression. To test this hypothesis, we administered TGF-β_1 to primary human pulmonary fibroblasts and to the human pulmonary fibroblast cell line MRC-5. As detected by Taqman PCR, mRNA of cav-1 decreased in primary fibroblasts ($P = 0.0024$) and in MRC-5 ($P = 0.0002$; Figure 20A) after 1 day of treatment with TGF-β_1. We also observed decreased cav-1 protein expression after TGF-β_1 treatment in a time and dose-dependent manner (Figure 20B,C).

A

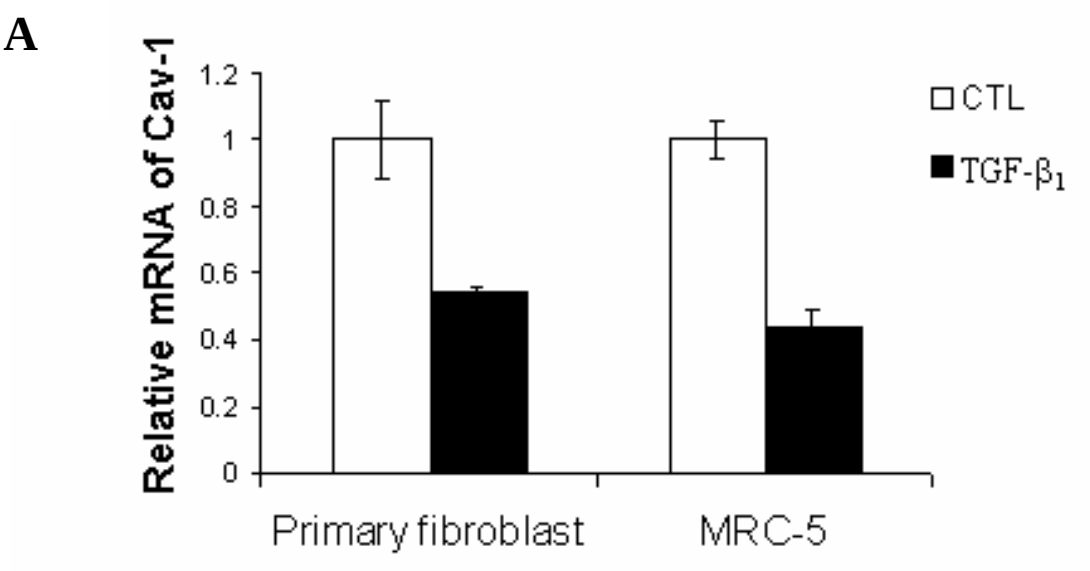

B

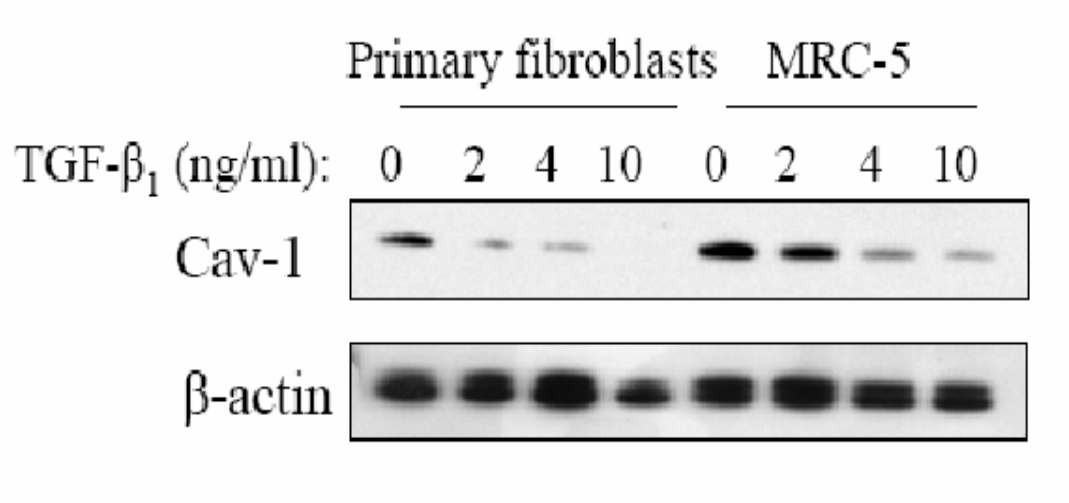

C

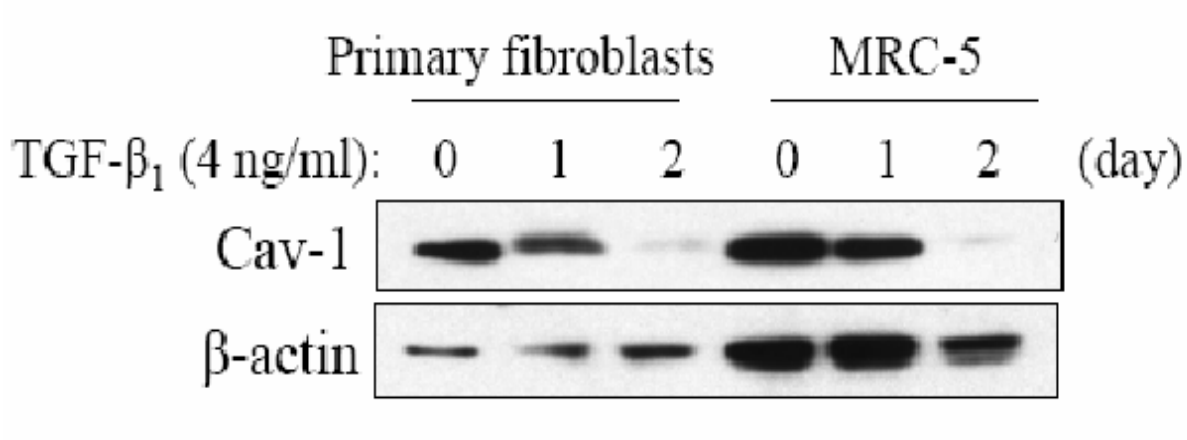

Figure 20 TGF-β_1 regulates cav-1 expression. (A) Human primary pulmonary fibroblasts and MRC-5 cells were treated with 4 ng/ml TGF-β_1 for 24 hours. Cav-1 mRNA levels were determined by Taqman PCR. (B) The same cells were treated with different concentrations of TGF-β_1 for 24 hours; (C) or treated with 4 ng/ml TGF-β_1 for 1 day and 2 days. Cav-1 protein levels were determined by Western blot analysis.

3.3 CAV-1 SUPPRESSES TGF-β_1 INDUCED ECM PRODUCTION IN PULMONARY FIBROBLASTS

In view of our observations that the profibrotic TGF-β_1 can reduce cav-1 expression, we examined the function of cav-1 in response to TGF-β_1. We tested the hypothesis that cav-1 is capable of modifying ECM production. We used both gain of function and loss of function experiments to test our hypothesis. We first performed gain of function experiments; we generated an adenovirus expressing cav-1 gene to upregulate cav-1 expression in MRC-5. Cav-1 expression markedly increased in a dose-dependent manner after Ad-cav-1 infection of MRC-5 (Figure 21A), with optimal cav-1 expression at 2 days post-infection and maintained for 4 days (Figure 21B). Using this adenovirus, we found that overexpressing cav-1 significantly suppressed ECM production including collagen type I and fibronectin, and α-smooth muscle actin (SMA), an indicator for fibroblast activation (Figure 21C). This observation was further confirmed by stable transfection experiments. Likewise, TGF-β_1-stimulated ECM production including collagen type I and fibronectin and α-SMA, were markedly reduced in cav-1 stably transfected MRC-5 compared with the vector transfected control cells (Figure 21D,E). We then performed loss of function experiments. Transfection of siRNA targeting human cav-1 effectively reduced cav-1 expression in MRC-5 (Figure 21F). Down regulation of cav-1 markedly enhanced α-SMA, collagen type I, and fibronectin production (Figure 21G). Taken together, cav-1 appears to be a promising protective molecule in pulmonary fibrosis because of its powerful ability to suppress ECM production and fibroblasts transformation.

A

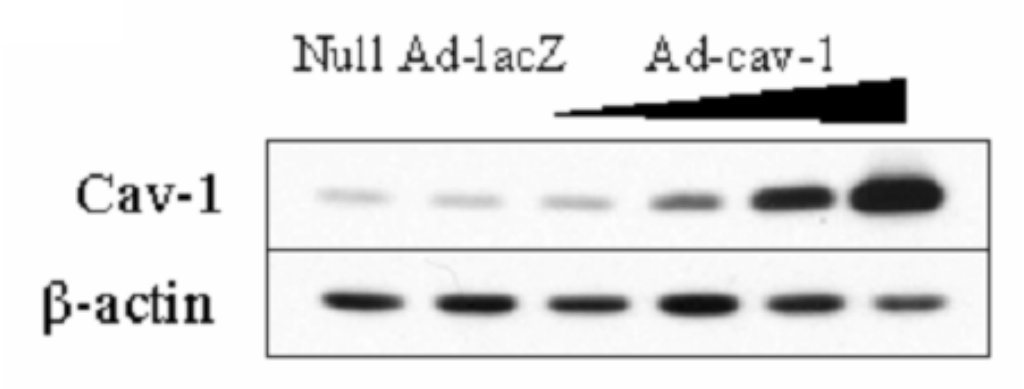

B

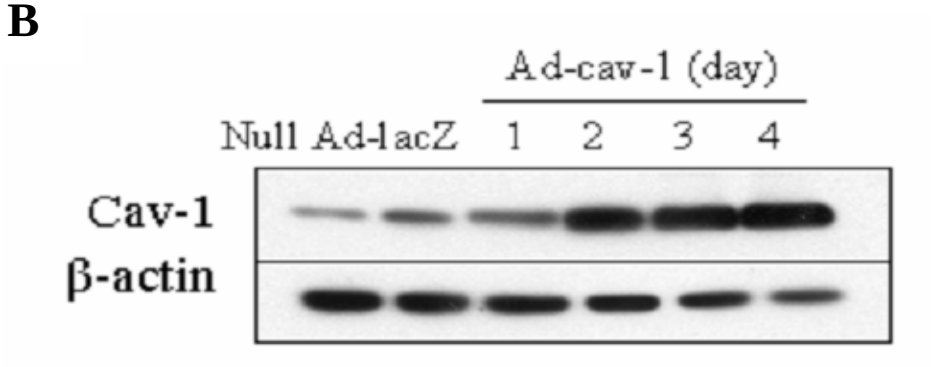
Ad-cav-1 (day)
Null
Ad-lacZ
1
2
3
4
Cav-1
β-actin

C

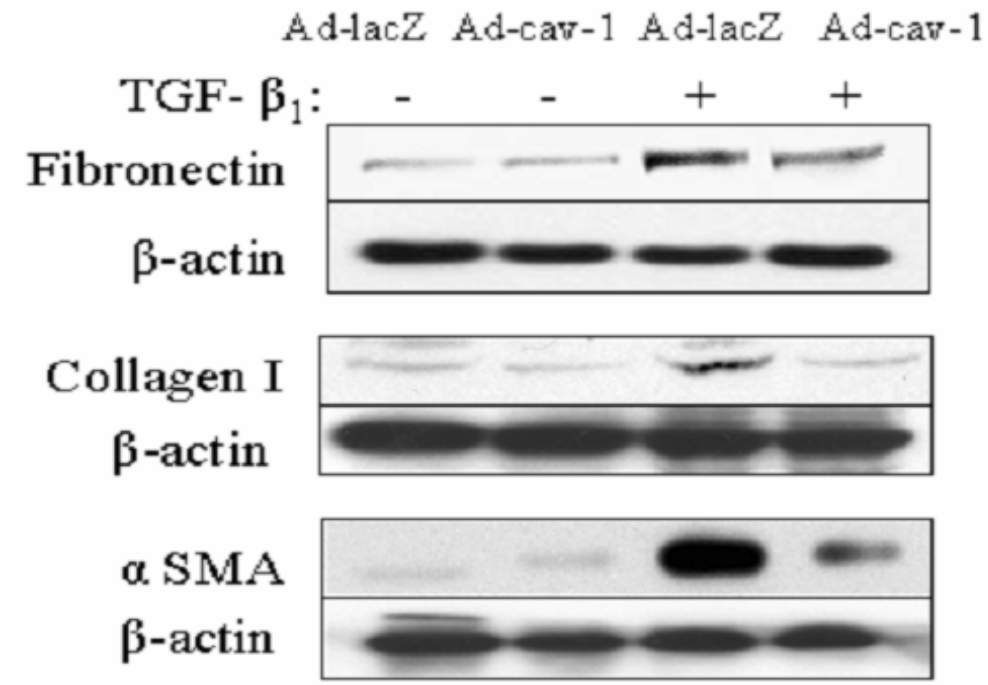
Ad-lacZ
Ad-cav-1
Ad-lacZ
Ad-cav-1
TGF- β1:
-
-
+
+
Fibronectin
β-actin
Collagen I
β-actin
α SMA
β-actin

D

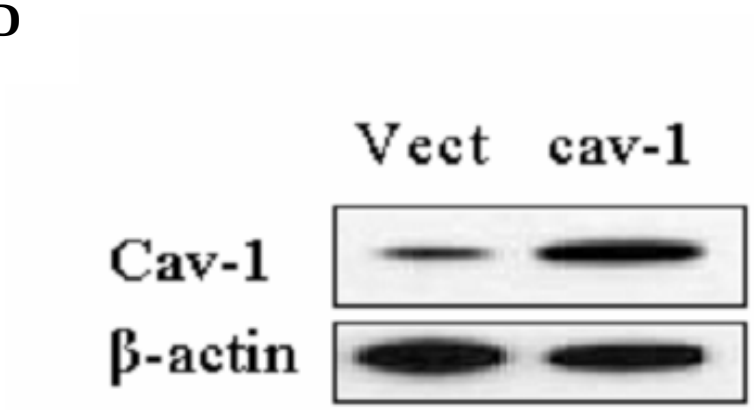
Vect
cav-1
Cav-1
β-actin

E

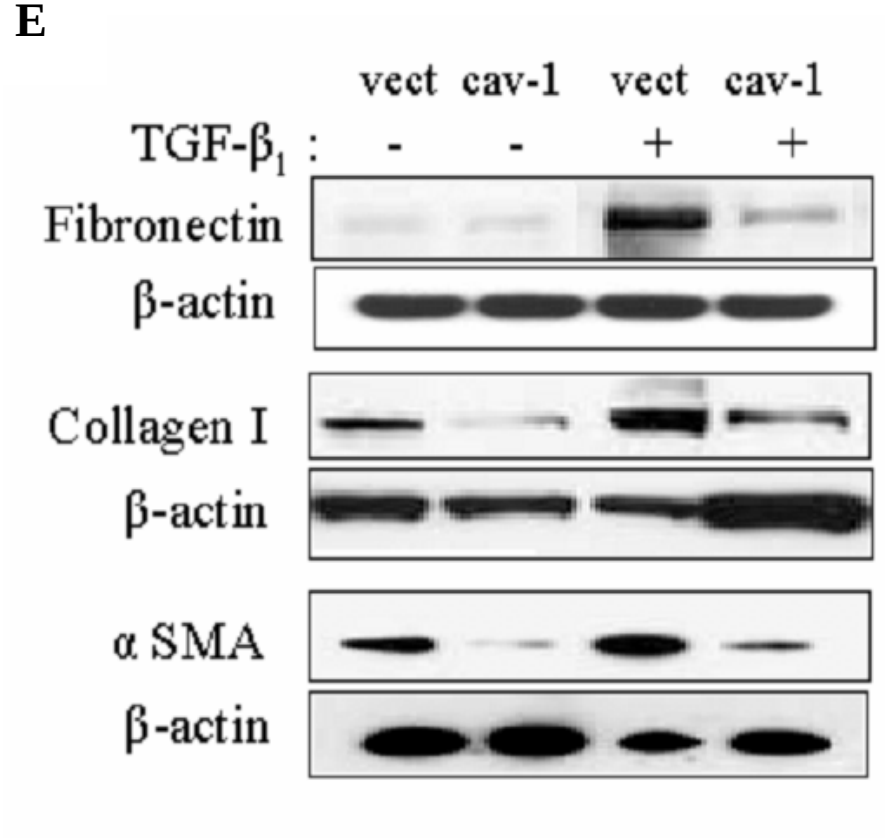
vect
cav-1
vect
cav-1
TGF-β1 :
-
-
+
+
Fibronectin
β-actin
Collagen I
β-actin
α SMA
β-actin

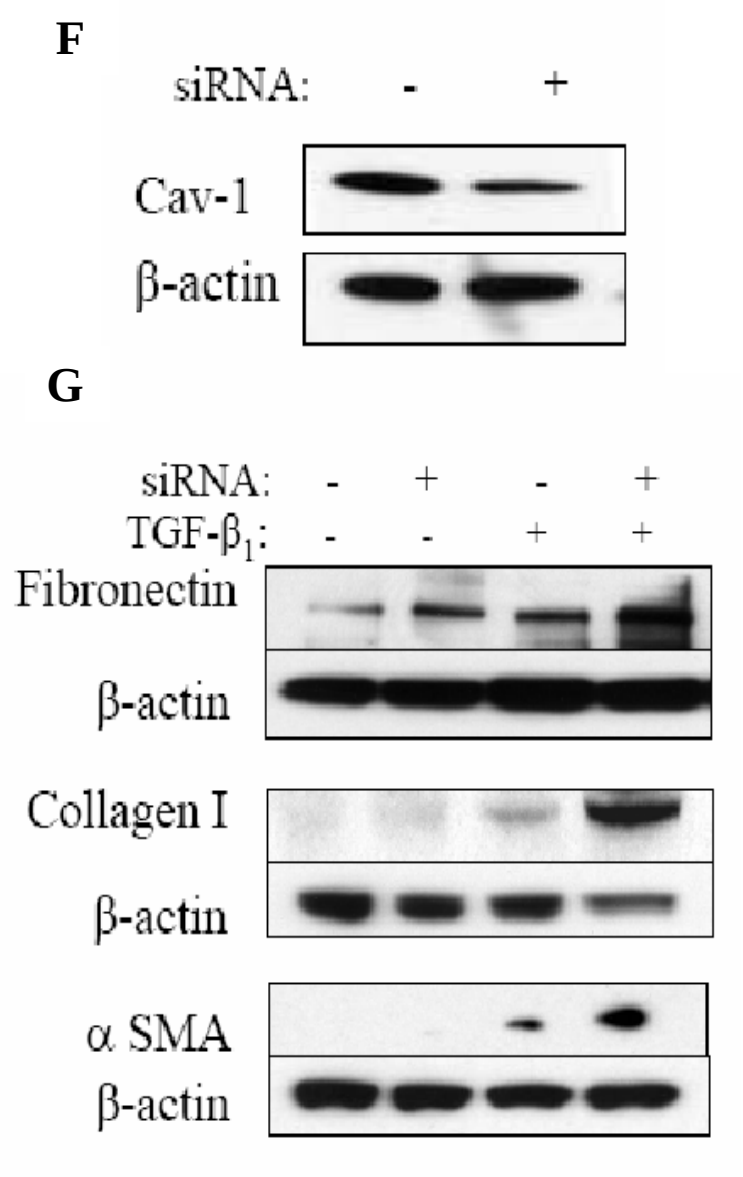

Figure 21 Cav-1 suppresses TGF-β_1 induced ECM production. (A) Western blot analysis of cav-1 expressions in MRC-5 cells infected with different dosage of ad-cav-1 or ad-lacZ virus for 48 hours. (B) infected with 100 pfu/cell cav-1 adenovirus or lacZ virus or not for 1 to 4 days. (C) After adenovirus infection, 4 ng/ml TGF-β_1 was added to MRC-5 for 2 days. ECM productions were determined by Western blot analysis. (D) Western blot analysis of cav-1 expressions in MRC-5 cells stably transfected with cav-1 and vector. (E) ECM productions in cav-1 stable transfected and control MRC-5 cells after 2 days TGF-β_1 treatment of 4 ng/ml. (F) Western blot analysis of cav-1 expressions in MRC-5 cells transfected with siRNA targeting human cav-1 or control siRNA for 24 hours. (G) After siRNA transfection for 24 hours, the MRC-5 cells were serum starved overnight and treated with 4 ng/ml TGF-β_1 for 2 days. ECM productions were determined by Western blot.

3.4 CAV-1 GENE TRANSFER VIA ADENOVIRUS SUPPRESSES BLM-INDUCED PULMONARY FIBROSIS

Based on our *in vitro* observations that cav-1 can attenuate TGF-β_1-induced ECM production, we further tested whether cav-1 can attenuate ECM production using the BLM induced pulmonary fibrosis model *in vivo*. We effectively transferred the cav-1 gene into mouse lung tissue by intratracheal instillation of Ad-cav-1 (Figure 22A,B). Lung histopathological changes were assessed after BLM in saline, Ad-lacZ or cav-1 treated animals (Figure 22C, D).

For groups without BLM treatment, alveolar architecture was preserved (Figure 22C). No significant differences were observed among saline, ad-lacZ and ad-cav-1 groups (Mean fibrosis scores: 0.12 ± 0.12, 0.49 ± 0.43 and 0.56 ± 0.06, respectively, P = 0.162, Figure 22E). Collagen accumulation, an index of lung fibrosis, as determined by the measurement of hydroxyproline content of the left lung, was low and similar (111.58 ±18.9 μg, 133.6 ± 24.2 μg and 144.2 ± 27.7 μg, respectively, P = 0.1987, Figure 22F). Consistently, immunoblots of the homogenized protein of lung tissue demonstrated low ECM production and absence of Smad-2 activation (Figure 22G). TGF-β_1, one of the key cytokines involved in pulmonary fibrosis (177), was found to be low by ELISA (Figure 22H).

In contrast, for groups with BLM treatment, lung tissue sections in either saline or ad-lacZ instilled groups showed extensive patchy areas of regional interstitial fibrosis with marked disruption of the alveolar unit, increased thickening of the interstitium and inflammation. However, in the ad-cav-1 group, the structural integrity of the lung was less severely affected, with less evidence of fibrotic obliteration, destruction of alveolar units and inflammatory cells infiltration (Figure 22 C,D). Mean fibrosis scores were significantly reduced in ad-cav-1 group compared with the lacZ and saline groups (2.83 ± 0.85, 2.18 ± 0.70 and 0.52 ± 0.45 in saline, ad-lacZ and ad-cav1 group respectively, over all P = 0.0056, lacZ and cav-1, P = 0.0009, Figure 22E). The hydroxyproline content was increased after BLM treatment. While ad-cav-1 mice had a markedly reduced hydroxyproline levels compared with lacZ and saline mice (226.1 ± 29.7 μg, 226.8 ± 8.2 μg and 178.4 ± 19.7 μg in saline, ad-lacZ and ad-cav1 group respectively, over all P = 0.0048, lacZ and cav-1, P = 0.001, Figure 22F). Consistently, immunoblot analysis revealed that ad-cav-1 treatment dramatically suppressed fibronectin and collagen deposition compared with the lacZ group (Figure 22G). As we expected, TGF-β_1 was increased along with the

fibrosis development after BLM administration. While it was significantly decreased in ad-cav-1 infection group compared with lacZ group (Figure 22H). The Smad-2 phosphorylation was also markedly diminished by ad-cav-1 infection (Figure 22G).

To further explore the therapeutic potentials of ad-cav-1, we also infected the mice with adenovirus carrying lacZ or cav-1 gene seven days post-BLM instillation. One week later, the whole lung was subjected to hydroxyproline content determination. Ad-cav-1 infection was still capable of suppressing hydroxyproline deposition compared with lacZ mice (400.4 ± 51.1 μg, 208.9 ± 28.4 μg in ad-lacZ and ad-cav1 group respectively, P=0.0048, Figure 22I).

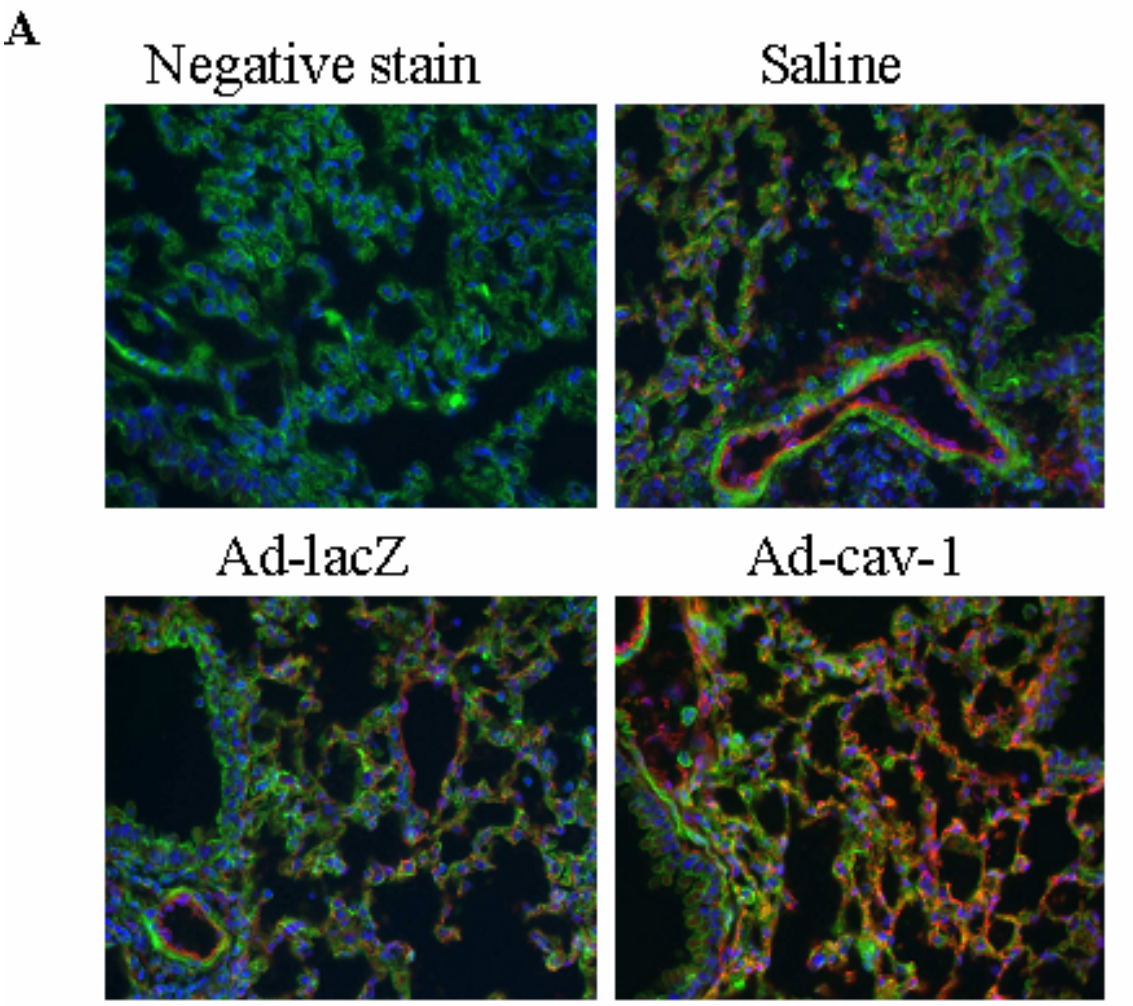

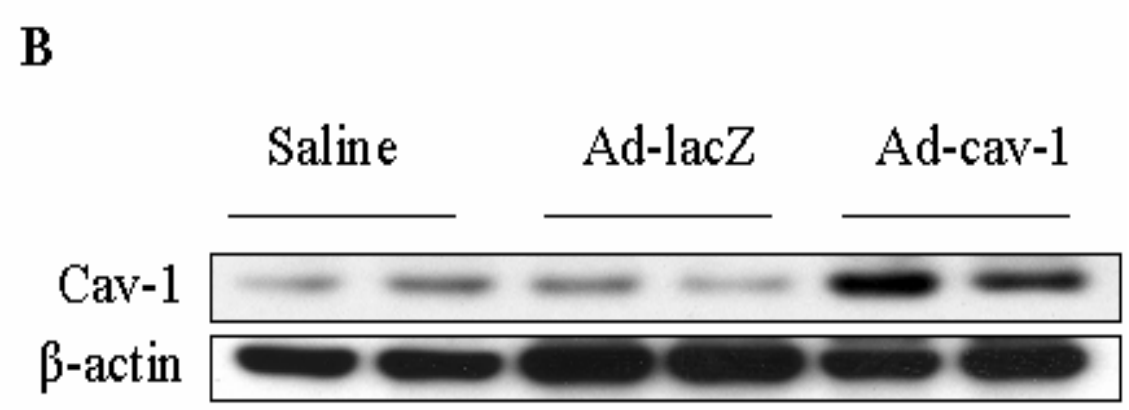
B
Saline
Ad-lacZ
Ad-cav-1
Cav-1
β-actin

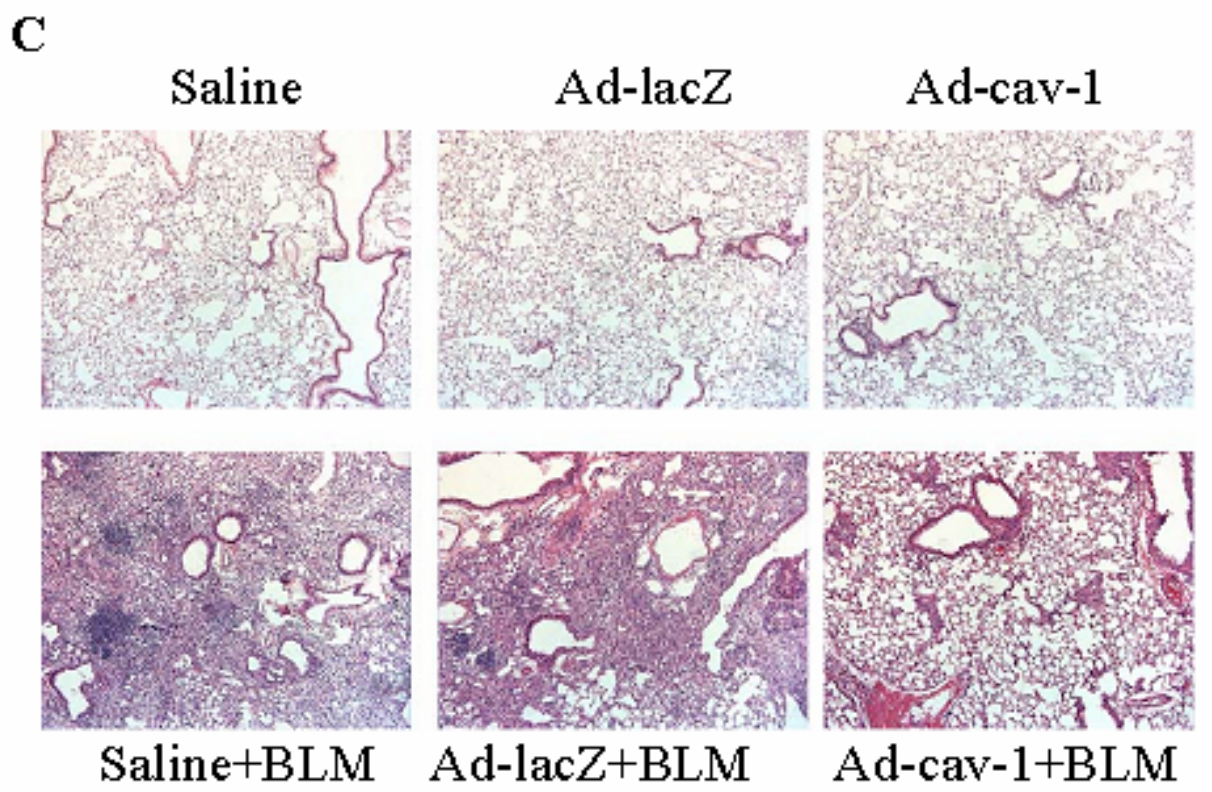
C
Saline
Ad-lacZ
Ad-cav-1
Saline+BLM
Ad-lacZ+BLM
Ad-cav-1+BLM

D

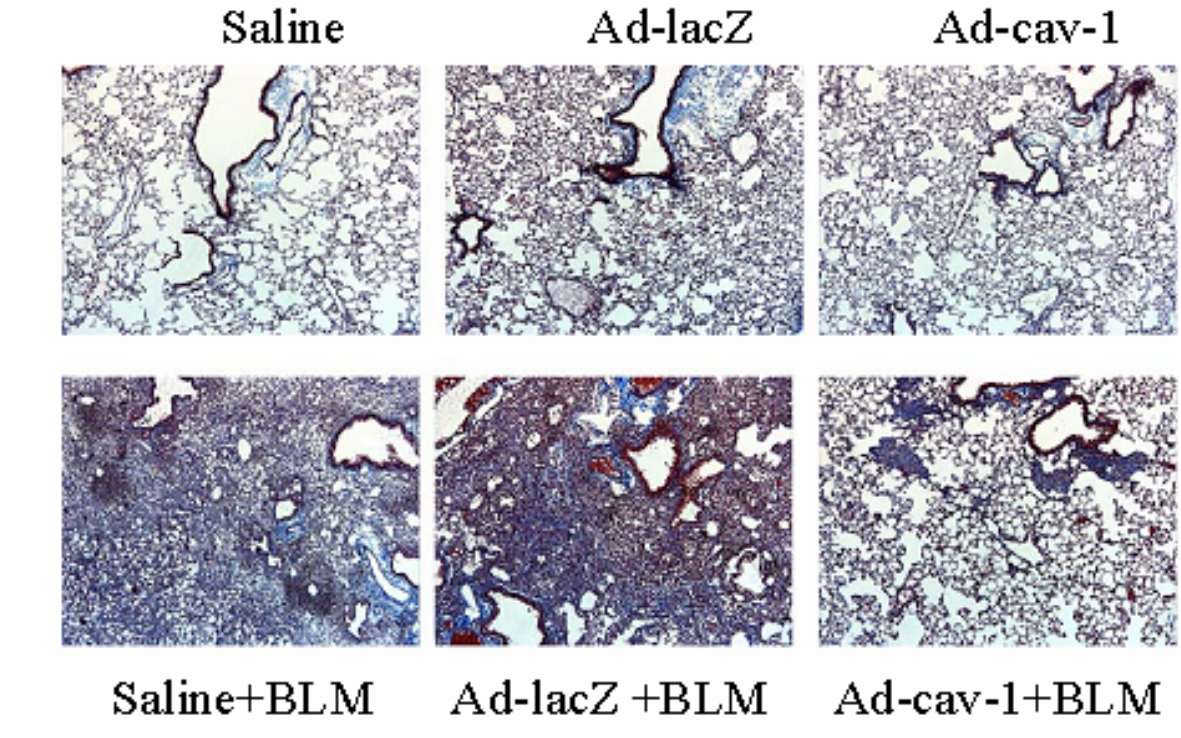
Saline
Ad-lacZ
Ad-cav-1
Saline+BLM
Ad-lacZ +BLM
Ad-cav-1+BLM

E

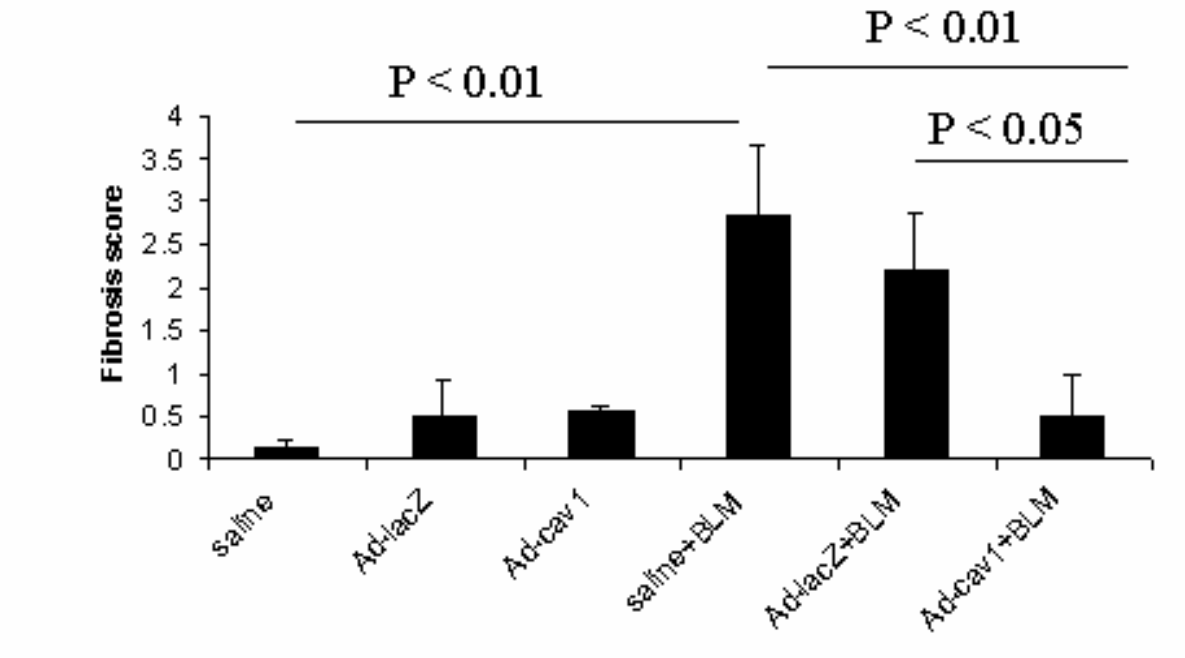
P < 0.01
P < 0.01
P < 0.05
Fibrosis score
0
0.5
1
1.5
2
2.5
3
3.5
4
saline
Ad-lacZ
Ad-cav1
saline+BLM
Ad-lacZ+BLM
Ad-cav1+BLM

F

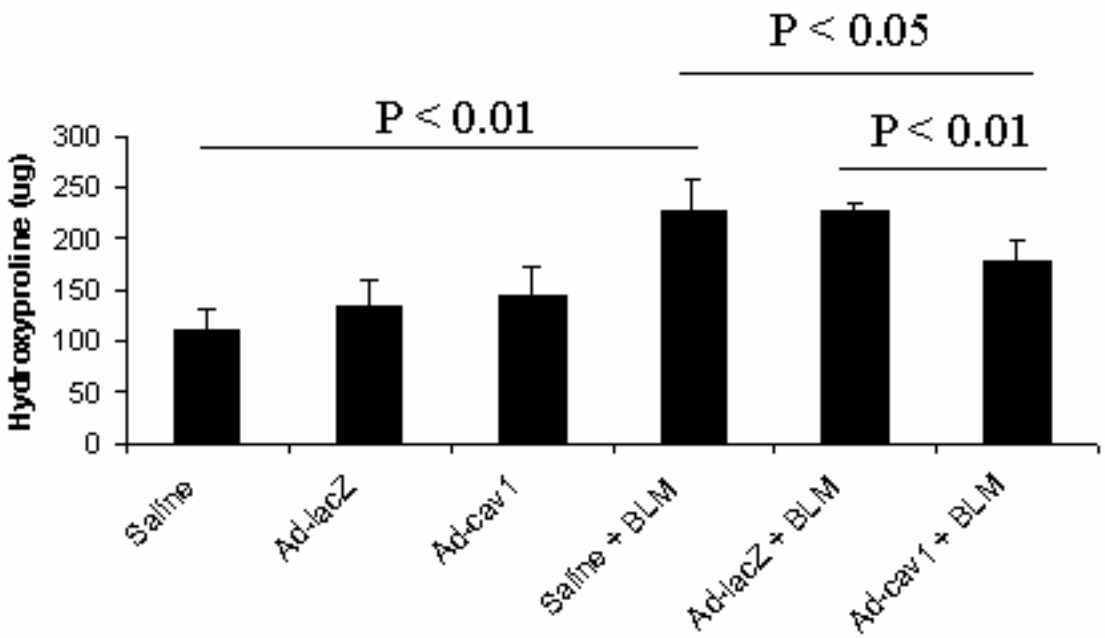
P < 0.05
P < 0.01
P < 0.01
Hydroxyproline (ug)
300
250
200
150
100
50
0
Saline
Ad-lacZ
Ad-cav1
Saline + BLM
Ad-lacZ + BLM
Ad-cav1 + BLM

G

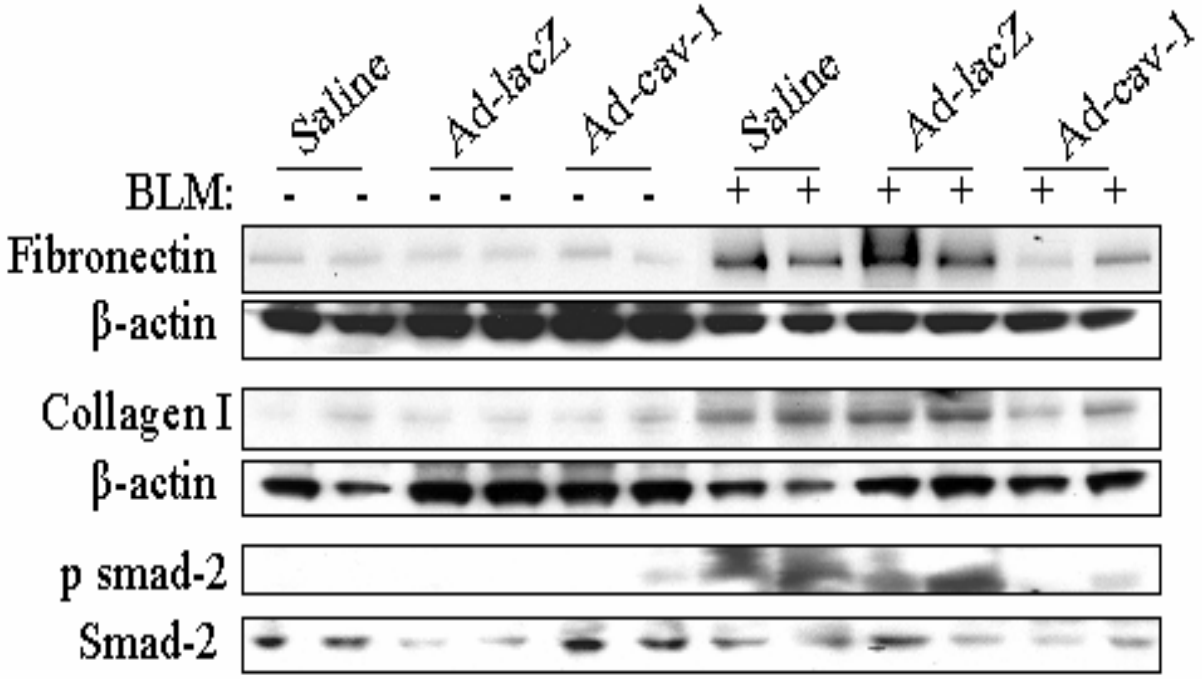
Saline
Ad-lacZ
Ad-cav-1
Saline
Ad-lacZ
Ad-cav-1
BLM: - - - - - - + + + + + +
Fibronectin
β-actin
Collagen I
β-actin
p smad-2
Smad-2

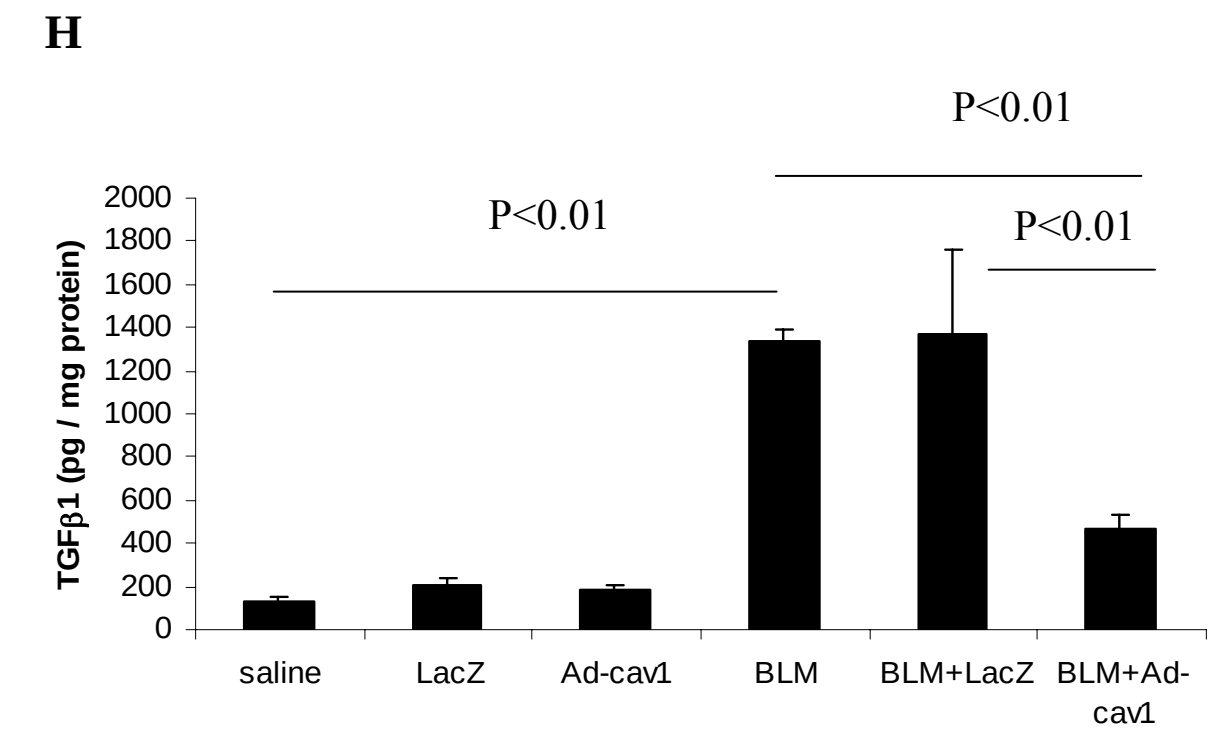

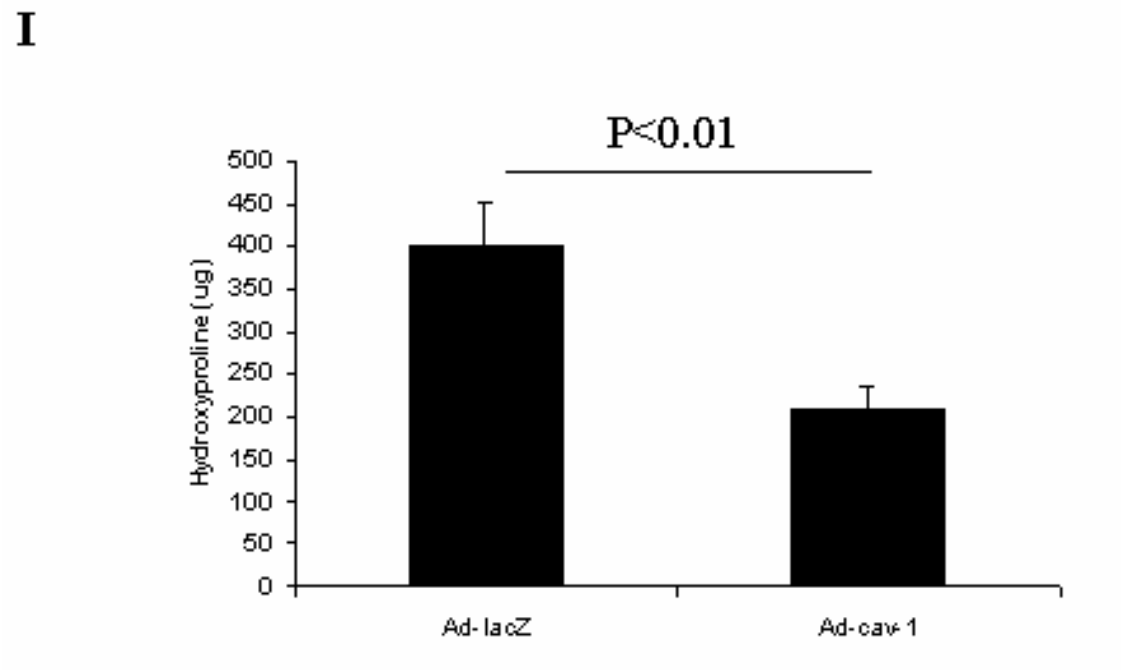

Figure 22 Cav-1 suppresses BLM induced pulmonary fibrosis. (A) Adenovirus vectors containing the cav-1 gene and lacZ gene were administered intratracheally into C57BL/6 mice lung. After 7 days of infection, mice were sacrificed. Cav-1 expression was determined by (A) immunohistochemistry and (B) Western blot. The C57BL/6 mice infected with ad-cav-1 or ad-lacZ or saline were treated with BLM for fourteen days. The lungs were harvested and subjected

to (C) H&E staining and (D) Masson trichrome staining of the right lung tissue. (Original magnification, x10) A representative example of four to five determinations was shown for each group in panel A and B. (E) Histology grade score analysis of the tissue slides. For groups without BLM, n=4; for groups with BLM, n=5. (F) Hydroxyproline content determination of the left lung. For groups without BLM, n=4; for groups with BLM, n=5. (G) ECM deposition and Smad-2 activation in the whole lung as determined by immunoblot analysis. (H) TGF-β_1 content determination by ELISA of the homogenized protein of the whole lung (n=3 for each group). (I) Hydroxyproline content determination of the whole lung seven days after ad-cav-1 infection and fourteen days after BLM instillation (n=3 for each group).

3.5 CAV-1 MODULATES TGF-β_1 INDUCED ECM PRODUCTION VIA MAPK AND SMADS PATHWAY

MAPK pathways are known to regulate TGF-β_1 signaling and TGF-β_1-induced ECM production. Cav-1 has been shown to modulate MAPK activation in mesangial cells. Here, we hypothesized that cav-1 might regulate TGF-β_1 induced ECM production via the MAPK pathway. We first examined whether cav-1 affects MAPK activation in MRC-5. Consistent with previous reports, TGF-β_1 markedly induced ERK and JNK phosphorylation within 10 min of treatment. Overexpressing cav-1 via an adenoviral vector significantly inhibited TGF-β_1 induced ERK and JNK activation (Figure 23A). There was no apparent induction of p38 activation by TGF-β_1 in MRC-5. The involvement of the ERK and JNK pathways was further explored using chemical inhibitors. Overexpressing cav-1 via adenovirus inhibited TGF-β_1-induced ECM production in DMSO treated samples. In contrast, PD 98059 (inhibitor of MEK1) and UO 126 (inhibitor of MEK1/2) administration eliminated the modulation of cav-1 on collagen type I production while having a negligible effect on fibronectin production (Figure 23B). SP 600125 (JNK1/2 inhibitor), on the contrary, eliminated the modulation of cav-1 on fibronectin production while having no effect on collagen type I modulation (Figure 23B). Furthermore, pulmonary fibroblasts isolated from JNK1 null mice did not exhibit differences of TGF-β_1 stimulated fibronectin production between ad-lacZ and ad-cav-1 transfection, compared with the fibroblasts isolated from JNK1 wild type littermates (Figure 23C). These data suggested that cav-

1 modulates TGF-β_1 induced collagen type I production via the ERK1 pathway, while modulating TGF-β_1 induced fibronectin production via the JNK1 pathway.

We determined the regulation of Smads activation by cav-1 in human fibroblasts MRC-5 with both gain of function and loss of function experiments. Similar as in mouse fibroblasts NIH3T3 (14), cav-1 suppressed smad-2 phophorylation and nuclear translocation. Moreover, overexpressing cav-1 effectively attenuated Smad-3 nuclear translocation and seems had no apparent effects on Smad-4 Smad-7 expression and Smad-4 nuclear translocation (Figure 24A). In consistent, down regulating cav-1 by siRNA transfection increased Smad-2 phosphorylation and Smad-2 / Smad-3 nuclear translocation (Figure 24B).

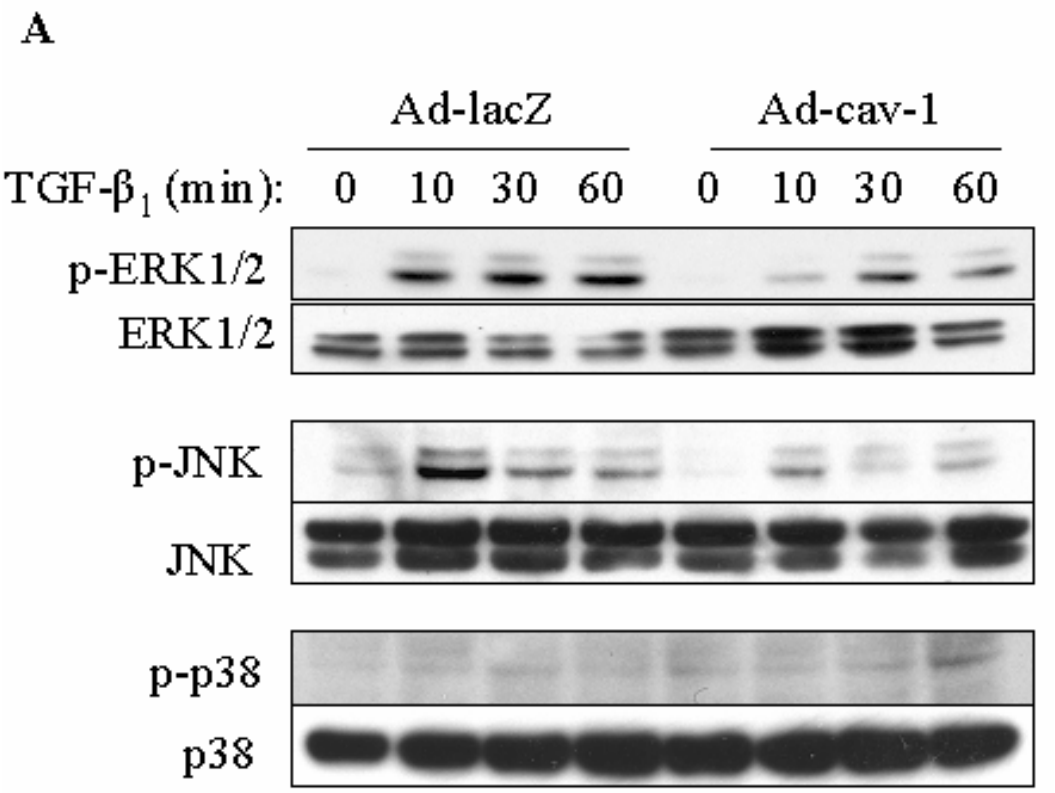

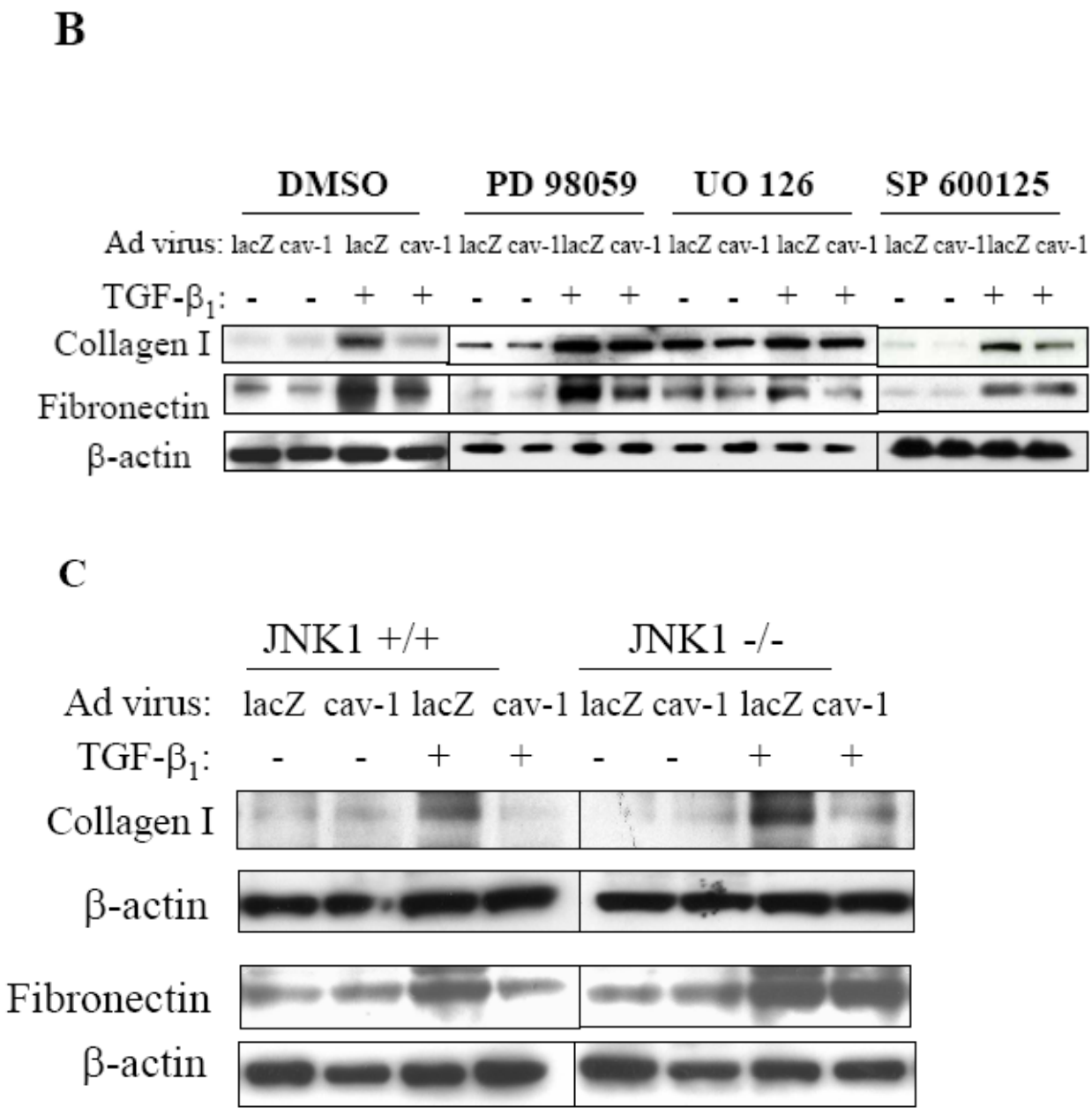

Figure 23 ERK and JNK pathway are involved in ECM regulation of cav-1. (A) Western blot analysis of TGF-β_1 stimulated MAPK activation for 0, 10 min, 30 min and 60 min in MRC-5 cells infected with Ad-cav-1 or Ad-lacZ. (B) Western blot analysis of TGF-β_1 stimulated ECM production in MRC-5 cells infected with Ad-cav-1 or Ad-lacZ. The cells were pre-treated with DMSO or PD 98059, UO 126 or SP 600125 for 1 hour, and then treated with TGF-β_1 for 2 days. (C) Western blot analysis of TGF-β_1 stimulated ECM production in pulmonary fibroblasts isolated from JNK1 (+/+) and (-/-) mice infected with Ad-cav1 or Ad-lacZ. Data are representative of three independent experiments.

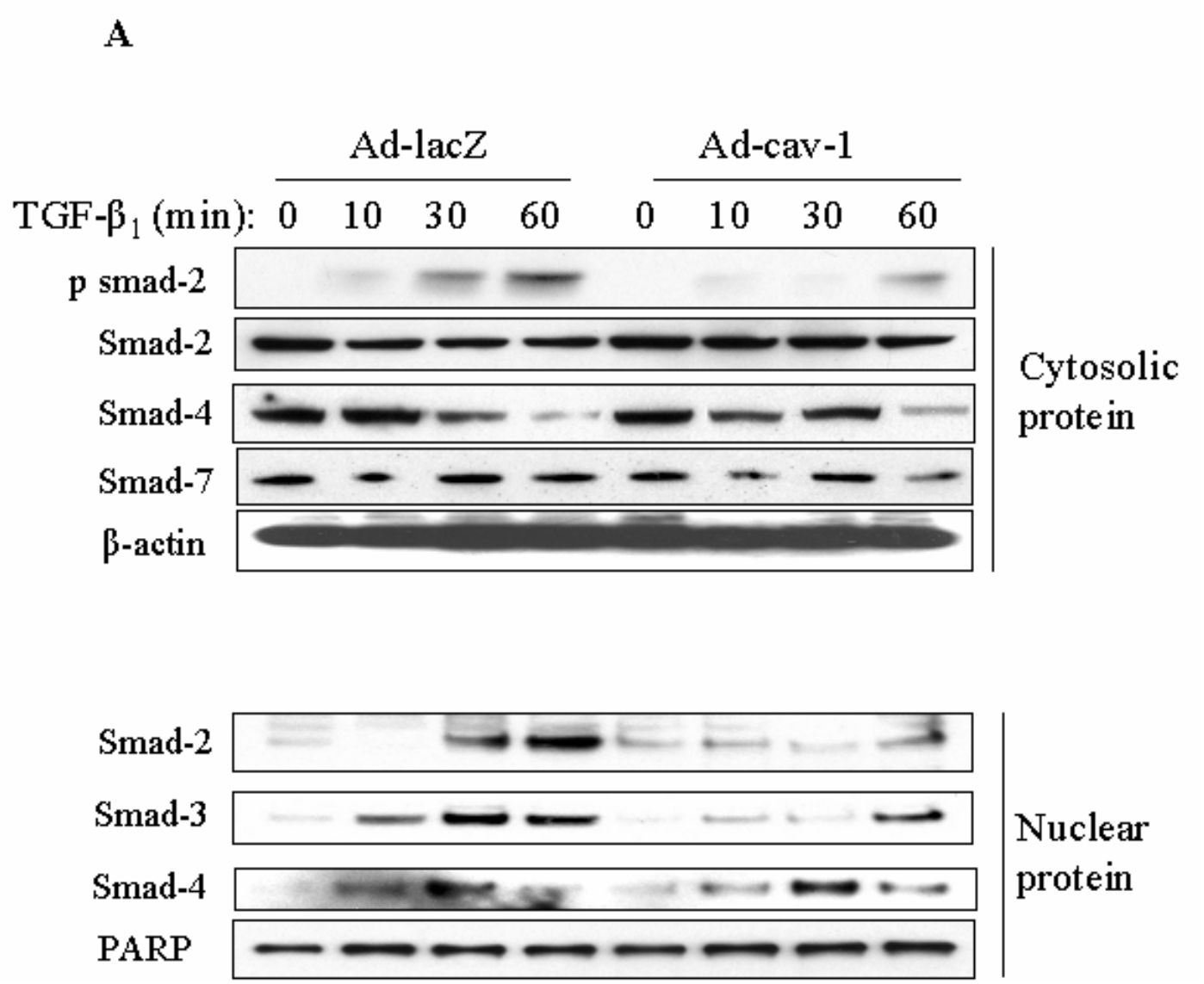
A
Ad-lacZ
Ad-cav-1
TGF-β1 (min): 0 10 30 60 0 10 30 60
p smad-2
Smad-2
Smad-4
Smad-7
β-actin
Cytosolic protein
Smad-2
Smad-3
Smad-4
PARP
Nuclear protein

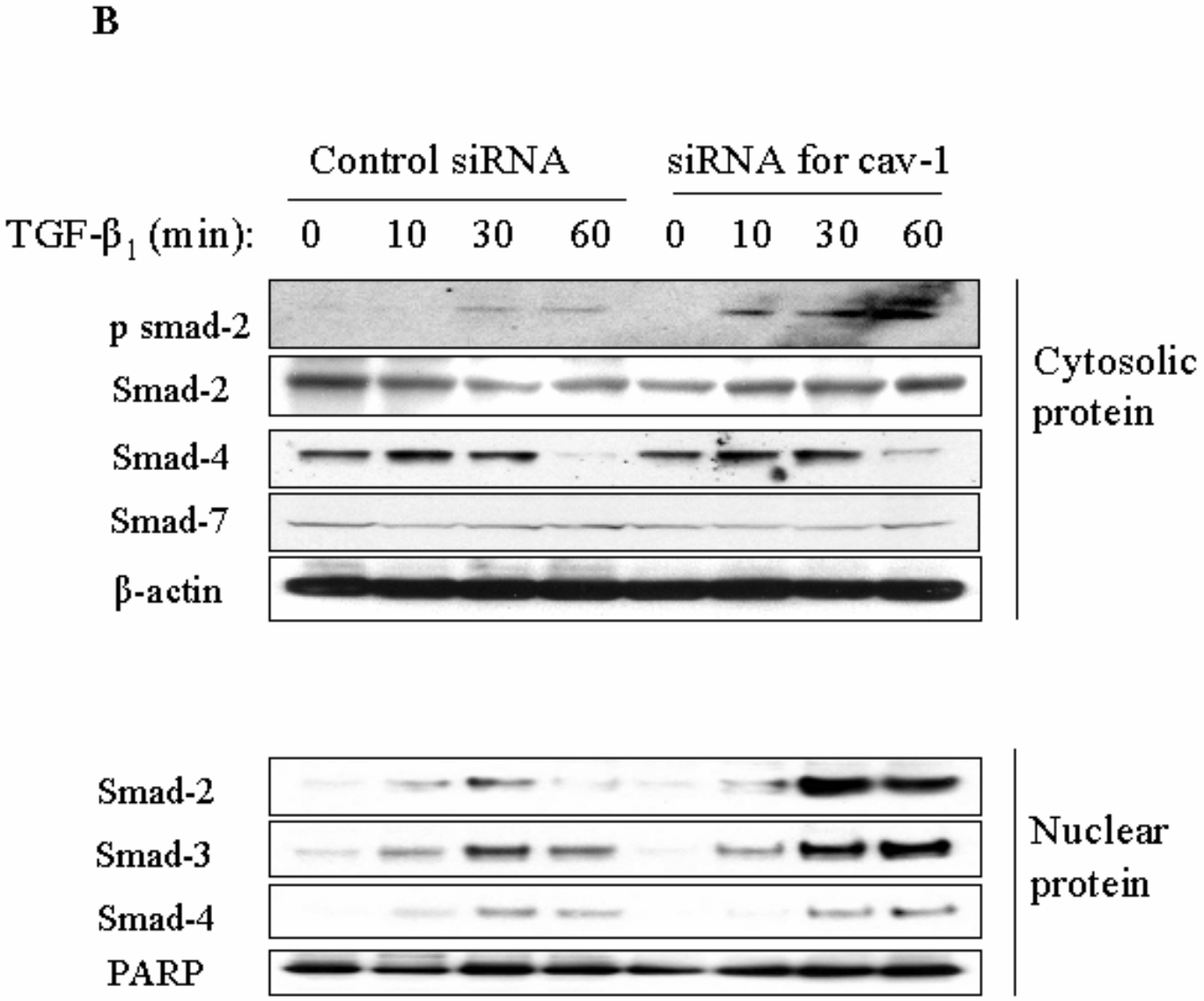

Figure 24 Cav-1 modulates Smads activation. Western blot analysis of Smad-2 activation under different conditions in MRC-5. (A) Cells were infected with Ad-cav1 and Ad-lacZ; (B) transfected with siRNA targeting cav-1 and control for 24 hours. The cells were serum starved overnight and treated with TGF-β_1 for 0, 10 min, 30 min and 60 min. Data are representative of three independent experiments.

We further investigated the involvement of JNK. JNK1 null mouse fibroblasts showed the similar suppressions of Smad-2 and Smad-3 phosporylation and nuclear translocation, mimicking the effects of over expressing cav-1 (Figure 25A), suggesting that cav-1 regulates Smad-2/3 activation via the JNK1 pathway. To clarify this hypothesis, cav-1 was over expressed in JNK1 wild type and null fibroblasts by adenovirus infection. As expected, cav-1 markedly suppressed smad-2 phosphorylation and smad-2/3 nucleus translocation in wild type fibroblasts (Figure 25B). Meanwhile, in JNK 1 null fibroblasts, over expressing cav-1 did not reduce smad-2 phosphorylation and nucleus translocation, while it still suppressed smad-3 nucleus translocation (Figure 25B). To further investigate the role of JNK in vivo, we performed immunochemical analysis with the BLM treated lung fibrosis tissue. As shown in Figure 25C, phosphorylated JNK levels were dramatically high in saline and lacZ mice, while ad-cav-1 infection markedly attenuated phospho-JNK. Moreover, JNK was highly activated in IPF tissues compared with the controls (Figure 25D), indicating its pivotal role in IPF development. These data strongly supported that JNK was involved in the regulation of ECM by cav-1.

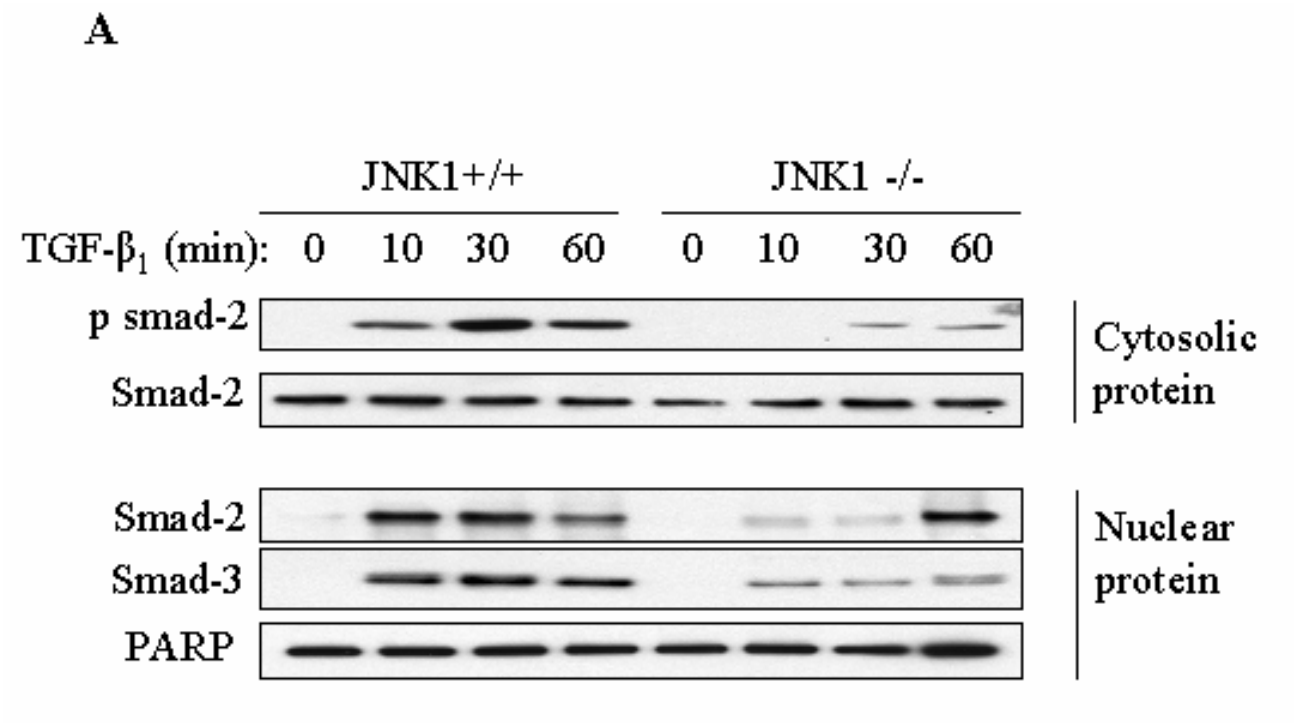

B

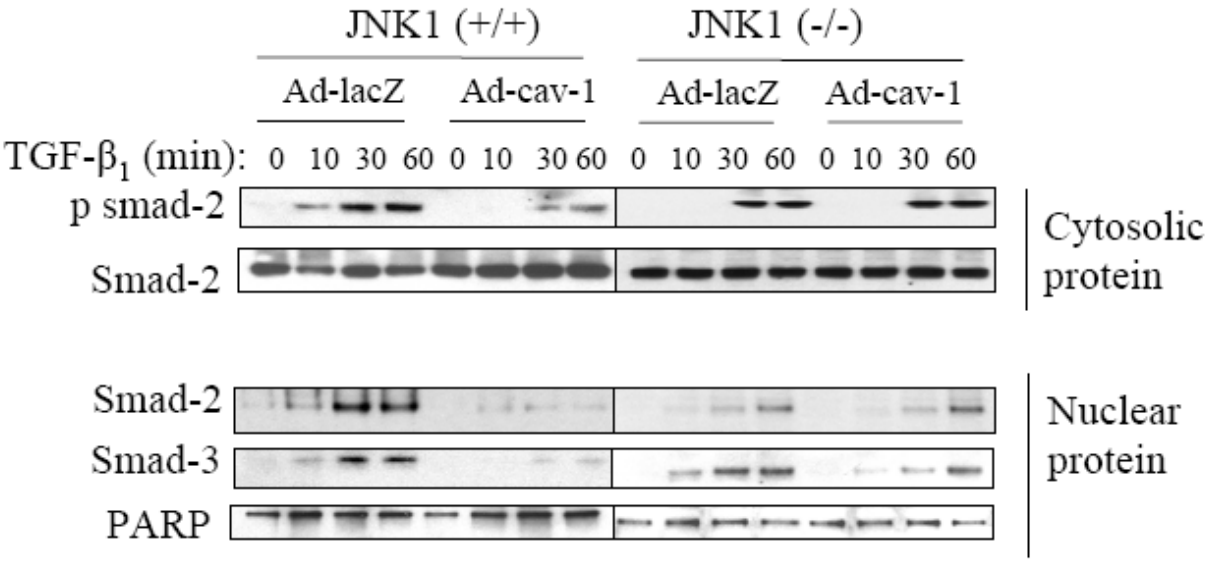

C

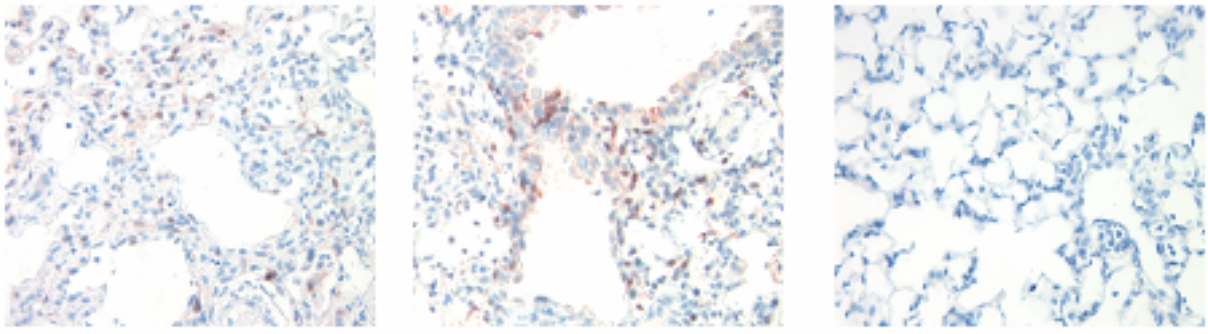

Saline +BLM **Ad-lacZ+BLM** **Ad-cav-1+BLM**

D

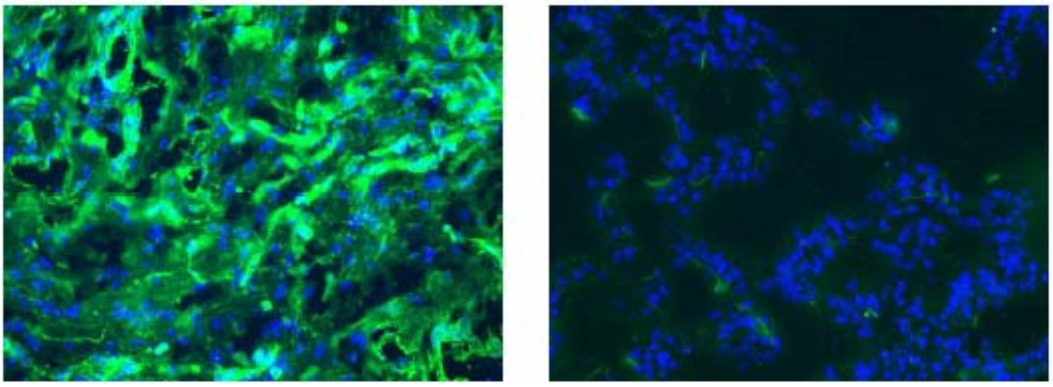

IPF CTL

Figure 25 Role of JNK in pulmonary fibrosis. (A) Immunoblot analysis of Smad-2 phosphorylation in cytosolic extracts and Smad-2/3 levels in nuclear extracts. (B) Immunoblot analysis of smad-2 phosphorylation in cytosolic extracts and smad-2/3 existences in nuclear extracts in JNK1 wild type and null fibroblasts infected with ad-cav-1 or ad-lacZ. Data were representative of three independent experiments for panel A and B. (C) Immunohistochemical analysis of JNK phosphorylation in lung tissue slices treated with BLM and infected with ad-lacZ or cav-1 or instilled with saline. Brown indicated phospho-JNK positive. A representative example out of five was shown. (Original magnification, x40.) (D) Immunohistochemical analysis of JNK phosphorylation in frozen lung tissue slices from IPF patient and control subjects. Green indicates phospho-JNK; blue indicates nucleus. A representative example out of seven samples for patients or control was shown. (Original magnification, x20.)

3.6 SUMARRY

In this charpter, the role of cav-1 in the pathogenesis of IPF was extensively investigated. Cav-1 was first found to be reduced in the IPF tissue and lung fibroblasts. TGF-β_1, the pro-fibrotic cytokine, was demonstrated to decrease cav-1 expression in a dose and time dependent manner. The role of cav-1 on extracellualr matrix production was investigated using several independent methods. Overexpressing cav-1 with adenovirus infection and stable transfection significantly decreased TGF-β_1 induced alpha smooth muscle, collagen type I and fibronectin production. Downregulating cav-1 expression using siRNA targeting cav-1 markedly increased TGF-β_1 induced alpha smooth muscle, collagen type I and fibronectin production. To better understand the potential therapeutic effects of cav-1 in vivo, andenovirus cav-1 was administrated intratrachelly into mouse lung in a bleomycin-induced pulomary fibrosis model. Cav-1 gene was overexpressed by this virus infection. The extent of pulomary fibrosis was markedly suppressed by cav-1 overexpression, as revealed by histological exam, hydroxyproline content determination and western blot of matrix production. TGF-β_1 cytokine production was also shown to be reduced.

The mechanism was further investigated. ERK1/2 and JNK were induced rapidly by TGF-β_1 in MRC-5 cells while p38 seems to have no apparent induction. Up-regulation of cav-1 by adenoviral infection markedly attenuated ERK1/2 and JNK phosporylation. PD 98059 (inhibitor of MEK1) and UO 126 (inhibitor of MEK1/2) selectively block the inhibitory effects of cav-1 on collagen type I production but not fibronectin production. Interestingly, inhibition of the JNK pathway by the chemical inhibitor SP 600125 or genetic knock out selectively blocks the inhibitory effects of cav-1 on fibronectin production but not collagen type I production.Using adenovirus and siRNA transfection, cav-1 was demonstrated to suppress TGF-β_1 induced Smad-2 phosphorylation. Cav-1 was also found to suppress smad-3 nuclear translocation, but had no apparent effects on smad-4 and smad-7 expression. Further investigation using JNK1 null fibroblasts demonstrated same reduced Smad-2 phosphorylation and decreased Smad-2/3 nuclear translocations compared with the wild type fibroblasts. In JNK1 null cells, cav-1 lost the ability to suppress Smad-2 activation, while it was still capable of inhibiting Smad-3 activation. Moreover, phospho-JNK staining was markedly reduced in ad-cav-1 infected BLM-injured mice lung samples compared with lacZ or saline samples. Taken together with the fact that JNK was

highly activated in IPF lung tissues, our data indicates that cav-1 regulates TGF-β_1 induced fibronectin production via JNK pathway, possibly via the modulation of Smad-2 phosphorylation and nuclear translocation.

4.0 DISSCUSION

4.1 CAV-1 AND INFLAMMATION

Cav-1, first identified about one decade ago, was reported to have many functions, including the formation of caveolae, membrane trafficking, regulation of signal transduction pathways, apoptosis, as well as calcium and lipid homeostasis in fibroblasts, adipocytes, and endothelial cells (1). Recently, cav-1 was reported to be expressed in PMs and involved in the pathogenesis of atherosclerosis and inflammation (76). Although Kasper and colleagues found cav-1 staining in rat AMs by immunohistochemistry, they hypothesized that it was the result of phagocytosis of other cell-type debris (106). Thus, studies of cav-1 in AMs are absent, and little is known about the expression and function of cav-1 in AMs. In this study, we used two independent methods to detect cav-1 expression in murine AMs. Using Western blot analysis, we demonstrate that mouse AM expression of cav-1 is similar to that of the PM. Consistent with the notion that cav-1 is primarily a membrane bound protein (34), immunofluorescence staining demonstrated that cav-1 mainly colocalized with Mac-3 on the plasma membrane of primary mouse AMs.

The macrophage is one of the major host immune defensive cells. It plays pivotal roles in phagocytosis, cytokine production, and antigen presentation (178). Many investigators are interested in the function of cav-1 in macrophages (179). Besides lipid metabolism, it is becoming more accepted that cav-1 modulates inflammation. Cav-1 suppresses inflammation via its interaction with and inhibition of eNOS activity (97). Leonard and colleagues reported that filipin and nystatin, drugs that specifically disrupt the caveolae microdomain by cholesterol chelation, impaired the entry of *Chlamydia trachomatis serovar K.* into J774A.1 cells (92). Satizo and colleagues showed that downregulation of cav-1 combined with upregulation of eNOS decreased leukocyte adhesion in pial venules of ovariectomized female rats (97). Bucci

and colleagues used the scaffolding domain of cav-1 to inhibit edema formation and vascular leakage to the same extent as glucocorticoid in rats (91). In our LPS-induced inflammation model, cav-1 has a direct effect on cytokine production in AMs and PMs. We chose siRNA technology to manipulate cav-1 levels in primary macrophages, resulting in a marked suppression of cav-1 expression. Because primary macrophages do not divide, the concentration of siRNA in each cell may remain high for a longer time than in fast-growing cells. Production of the proinflammatory cytokines TNF-α and IL-6 was greatly increased by the treatment of siRNA targeting cav-1, whereas production of the antiinflammatory cytokine IL-10 was markedly attenuated. Consistently, RAW264.7 cells stably transfected with cav-1 demonstrated a markedly attenuated proinflammatory cytokine (TNF-α and IL-6) production and increased antiinflammatory cytokine (IL-10) production.

The MAPK and PI3K pathways are activated by many cellular stresses, including LPS, and are intimately linked with the regulation of cytokine production (97). ERK2 and PI3K were reported to localize in caveolae (1). These findings suggest that the MAPK and PI3K signaling cascades were attractive target candidates for cav-1. We have shown in this study, in a mouse macrophage cell line RAW264.7, that cav-1 selectively augmented p38 phosphorylation but inhibited JNK, ERK1/2, and Akt phosphorylation. The p38 inhibitor (SB203580) blocked the effects of cav-1 on LPS-induced cytokines production. In contrast, inhibition of the ERK1/2 and PI3K/Akt kinase cascades did not affect the modulation of cytokine production by cav-1. The pivotal role of p38 activation was further confirmed by studies on macrophages isolated from MKK3-gene–deleted mice. There are three MKKs that can phosphorylate the p38 MAPKs: MKK3, MKK4, and MKK6 (180, 181). Given that MKK3 is the major activator of p38, we administered LPS to MKK3 null macrophages and found that attenuation of the p38 by MKK3 knockout led to a complete loss of the response. These results indicate that cav-1 affects LPS-induced cytokine production through the activation of MKK3/p38. Using a chemical inhibitor, we also showed that inhibition of the JNK pathway reverses the modulation of proinflammatory cytokine IL-6 production by cav-1, while not affecting TNF-α and IL-10 production. Our data, along with the previous implication of the JNK pathway in the inhibition of macrophage cytokines production by carbon monoxide and heat shock (182), suggest that the JNK pathway is involved in the regulation of inflammatory cytokine IL-6 production. Although the conclusion

drawn from chemical inhibitor experiments alone is not convincing, it is likely that cav-1 has effects via multiple signaling pathways.

It has been previously demonstrated that the effects of LPS on macrophages require recruitment of LPS receptor complex (TLR4 and MD-2) to lipid rafts containing CD14 (183). Walton and colleagues reported that LPS was capable of inducing membrane translocation of TLR4 and MD-2 to caveolar fraction in human aortic endothelial cells with cell fractionation and immunofluorescence analyses (89). Cav-1 has been reported to regulate membrane receptor signaling through direct binding or through the interaction of the downstream signaling molecules (184). TLR4 contains a putative cav-1 binding motif (^{739}FIQSRWCIF^{747}) (6). Our data here demonstrated that cav-1 interacts with TLR4 via the cav-1 binding motif and disrupts downstream adaptor molecules recruitment. The interaction of cav-1 and TLR4 is regulated by CO, which is generated endogenously in caveolae as the byproduct of HO activity. After LPS stimulation, HO-1 translocates to caveolae via the p38 MAPK pathway.

NK-κB and AP-1 are well-known transcription factors that regulate LPS-induced cytokine production (168). We explored the effects of cav-1 on NK-κB and AP-1 activation after LPS treatment. The results demonstrated that cav-1 markedly suppressed the activation of these two transcription factors as measured by EMSA. Given previous reports that p38 regulates NK-κB and AP-1 activation in macrophages (185, 186), we hypothesized that p38 is involved in the suppression of NK-κB and AP-1 activation by cav-1. SB203580, the inhibitor of p38, consistently abolished the suppression of the transcription factors activation by cav-1. The exact mechanisms by which cav-1 and p38 modulate NK-κB and AP-1 will be the subject of ongoing studies.

In summary, we have demonstrated cav-1 expression in mouse AMs. Cav-1 has a protective role for inflammation by suppression of proinflammatory cytokine (TNF-α and IL-6) production and augmentation of antiinflammatory cytokine (IL-10) production in the LPS model. We have also presented evidence that cav-1 interacts with TLR4 and the interaction is regulated by CO and HO-1, which trafficking to caveolae upon LPS stimulation. The effect of cav-1 involves the p38 MAPK signal pathway. We speculate that increased LPS-mediated activation of

p38 and decreased activation of JNK, NK-κB, and AP-1 by cav-1 lead to protection against inflammation. Cav-1 is an important mediator of antiinflammatory effects.

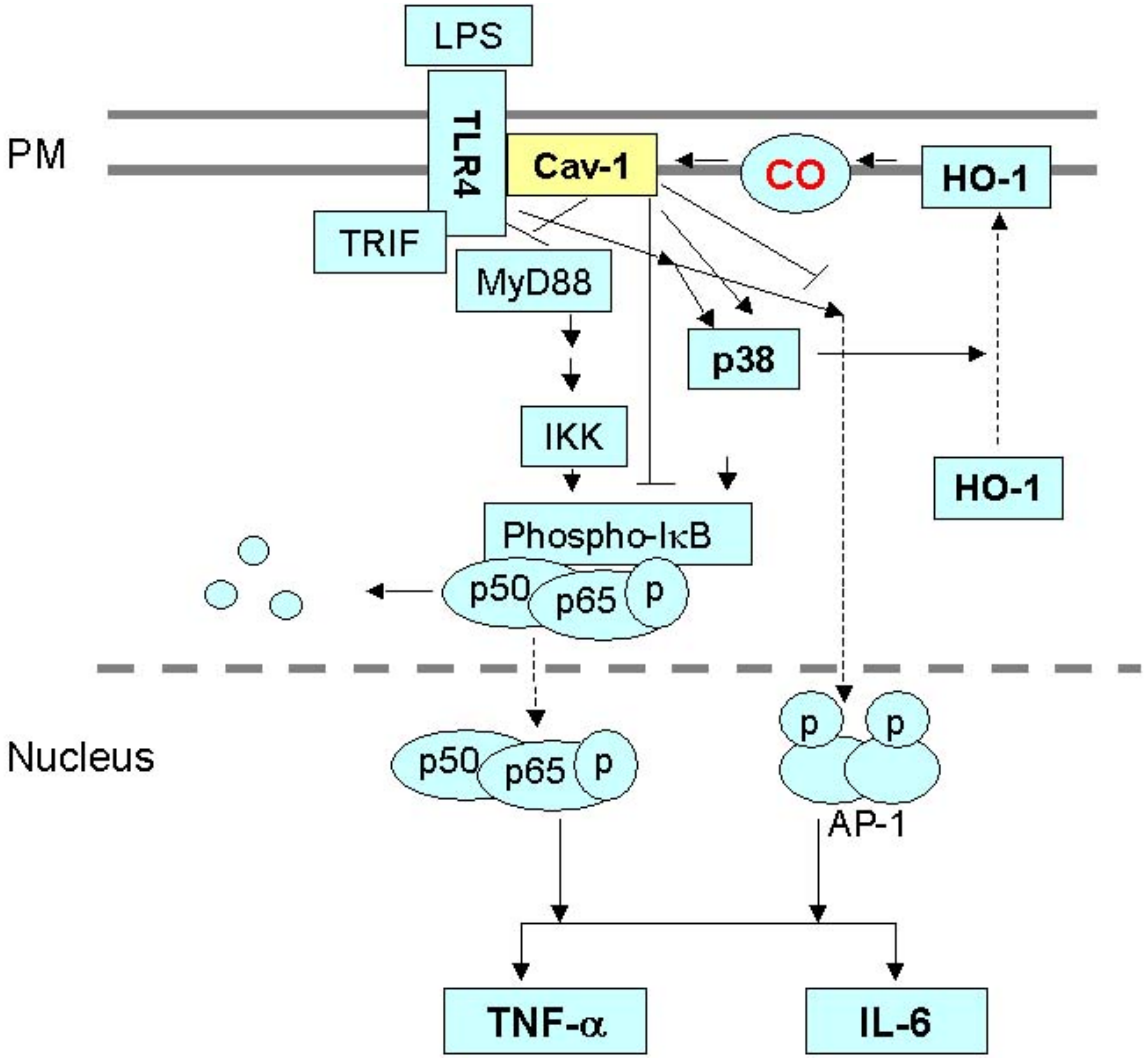

Figure 26 Diagram of cav-1 and inflammation. LPS binds to and activates its receptor TLR4. The activated TLR4 recruits downstream molecules MyD88 and TRIF, which activated the downstream IKK kinase activity. IKK phosphorylates IκB, which promotes IκB degradation. Then p65 will be released and phosphorylated, followed by nuclear translocation. It also activates p38 MAPK pathway and transcription factor AP-1. Cav-1 confers its antiinflammatory effects via several pathways. (1) Cav-1 directly binds to TLR4 and disrupts TLR4 association with MyD88 and TRIF. (2) Cav-1 inhibits IKK activity as well as NF-kB p65 phosphorylation and nuclear translocation. (3) Cav-1 inhibits AP-1 activity. (4) Cav-1 activates p38, which promotes HO-1 caveolar translocation. Carbon monoxide is generated in caveolae due to HO activity there. Carbon monoxide increases cav-1 interaction with TLR4, which further attenuates the TLR4 signal.

4.2 CAV-1 AND FIBROSIS

Although the etiology and pathogenic mechanisms of IPF remain unknown, a complex and poorly understood interaction of genetic and environmental factors appears to be involved (99). In this study we observed that the expression of cav-1 is significantly reduced in lung tissue and fibroblasts derived from IPF patients. Our observations are consistent with previous reports that cav-1 expression is aberrantly regulated in experimental animal models of lung fibrosis (104-106). Our data showing decreased cav-1 expression in lung tissue and fibroblasts might be an important indicator of impaired cellular functions of fibroblasts in the pathogenesis of IPF.

Since IPF shows a distinct histopathology of usual interstitial pneumonia, a commonly held view is that persistent interstitial inflammation leads to and modulates the development of fibrosis (187). This hypothesis is applied in clinic settings in that antiinflammatory therapies combined with immunosuppressive therapy are major strategies used in treating IPF, although the outcome is still poor (188). A new hypothesis has been advanced by Selman et al. that IPF is an epithelial-fibroblastic disease (189). Alveolar epithelial cell injury and activation will release many fibrogenic mediators, which lead to the transformation of fibroblast to myofibroblast and the formation of fibroblasts-myofibroblast foci, characterized by fibroblast-myofibroblast migration and proliferation, decreased apoptosis and enhanced release of fibrogenic growth factors. TGF-β_1 is one of those major pivotal fibrogenic factors (176). It promotes myofibroblast transformation, which is responsible for secreting large amounts of ECM, and presents only in fibrotic lung tissue but not in normal lung tissue (176). It suppresses ECM degradation through the regulation of metalloproteases and their inhibitors (190). TGF-β_1 caused minor inflammation but marked progressive fibrosis in the lung. It has many diverse functions including chemoattractant and mitogenic activities, and the regulation of lung inflammation and functions of epithelial cells which might have further impact on the fibrotic process through autocrine or paracrine mechanisms (102). Transferring of the TGF-β_1 gene into rat lungs via an adenoviral vector can induce a severe and progressive lung fibrosis (191). Blocking TGF-β_1 can effectively reduce fibrosis in different animal models (102).

While TGF-β_1 can promote the fibrotic progress, it decreased cav-1 expression in a dose and time dependent manner in both human primary pulmonary fibroblasts and MRC cells. The

modulation in mRNA was in accordance with protein levels and suggested that cav-1 was regulated both transcriptionally and translationally. TGF-β_1 was demonstrated to be produced at the sites of active fibrosis and its level in the lung was reported to be proportionate to the degree of fibrosis generated (102). The increased levels of TGF-β_1 might contribute to the attenuated cav-1 expression in IPF patients. Consistently, myofibroblasts were reported to be lacking of caveolae as revealed by electron microscopy (192).

Inhibition of TGF-β_1 signaling was capable of slowing the progression of IPF when administered to patients (193). Here we showed that cav-1 can modulate TGF-β_1 induced ECM production in vitro. Gain of function experiments demonstrated that exogenous cav-1 either by adenoviral infection or stable transfection in MRC fibroblasts markedly decreased TGF-β_1 induced α-smooth muscle actin gene expression, and ECM production including collagen type I and fibronectin. Consistently, loss of function experiments using siRNA showed that down-regulating cav-1 expression in MRC fibroblasts increase α-smooth muscle actin gene expression, and ECM production in response to TGF-β_1 stimulation. Cav-1 has recently been reported to regulate collagen type I expression through the ERK pathway in normal pulmonary fibroblasts (104). However, the current studies using several independent and complementary approaches are the first to extensively demonstrate that cav-1 can directly affect α-smooth muscle actin gene expression, and ECM production in a TGF-β_1 stimulated fibrosis model, which is more similar to the pathogenesis of pulmonary fibrosis *in vivo*.

The therapeutic effects of cav-1 on pulmonary fibrosis were further confirmed *in vivo* using a BLM-induced pulmonary fibrosis model. Overexpression of cav-1 by adenoviral gene transfer significantly decreased lung fibrosis scores ($P < 0.01$, Figure 22E) and lung hydroxyproline content ($P < 0.05$, Figure 22F) compared with lacZ virus, accomplished by attenuated collagen deposition as revealed by Masson trichrome staining (Figure 22D) and reduced fibronectin production (Figure 22G) as demonstrated by Western blot. As we noticed, the reduction of hydroxyproline content is not as impressive as histology examination scores. This may due to the low sensitivity of the assay or uneven distribution of virus and BLM in the left and right lung when the reagent is administered intratracheally through the mouth because of the asymmetric lung anatomy structure of mice. The improvement in BLM-induced lung fibrosis resulting from

treatment with the cav-1 adenovirus further supports the beneficial effects of cav-1 during pulmonary fibrosis.

The anti-fibrotic effects of cav-1 are obvious and significant, which made the investigation of the molecular mechanism more interesting and important. Here, we examined the role of the MAPK signaling cascades in mediating the effect of TGF-β_1 in collagen and fibronectin synthesis. The family of MAPKs consists of three known subfamilies including the ERK1/2, JNK1/2 and p38. All these kinases are reported to be involved in the regulation of TGF-β_1 induced ECM production and pulmonary fibrosis (194, 195). However, the effects and the pathways varied greatly depending on the cell types and conditions. In the present studies, ERK1/2 and JNK were induced rapidly by TGF-β_1 even after 10 min treatment in MRC-5 cells while p38 seems to have no apparent induction. Up-regulation of cav-1 by adenoviral infection markedly attenuated ERK1/2 and JNK phosporylation. Cav-1 has been demonstrated to regulate ERK1/2 activation in a variety of cells including pulmonary fibroblasts, mesangial cells, bovine parathyroid cells, cancer cells and endothelial cells etc. It has also been shown that ERK localizes in caveolae and interacts with cav-1 directly (184). With respect to ECM regulation, we find that PD 98059 (inhibitor of MEK1) and UO 126 (inhibitor of MEK1/2) selectively block the inhibitory effects of cav-1 on collagen type I production but not fibronectin production. Previously, ERK1/2 has been shown to regulate collagen expression in pulmonary and dermal fibroblasts (157, 196). Interestingly, inhibition of the JNK pathway by the chemical inhibitor SP 600125 or genetic knock out selectively blocks the inhibitory effects of cav-1 on fibronectin production but not collagen type I production. In a human fibrosarcoma cell line, similar findings were reported that JNK activation was essential for TGF-β_1 stimulate fibronectin production, as stable transfection of dominant negative mutant of JNK1 markedly suppressed TGF-β_1 stimulated fibronectin mRNA and protein expression (197).

Given the previous report that cav-1 interacted with TGF-βRI and transfection of a HA-tag cav-1 inhibited smad-2 phosphorylation in NIH3T3 cells (104), we postulated that cav-1 might modulates Smads activity. The effect of cav-1 on Smad-3, Smad-4 and Smad-7 has not, to our knowledge, previously been examined. Using adenovirus and siRNA transfection, cav-1 was demonstrated to suppress TGF-β_1 induced Smad-2 phosphorylation, similar with the studies

before (104). Cav-1 was also found to suppress smad-3 nuclear translocation, but had no apparent effects on smad-4 and smad-7 expression.

Further investigation using JNK1 null fibroblasts demonstrated same reduced Smad-2 phosphorylation and decreased Smad-2/3 nuclear translocations compared with the wild type fibroblasts. In JNK1 null cells, cav-1 lost the ability to suppress Smad-2 activation, while it was still capable of inhibiting Smad-3 activation. Moreover, phospho-JNK staining was markedly reduced in ad-cav-1 infected BLM-injured mice lung samples compared with lacZ or saline samples. Taken together with the fact that JNK was highly activated in IPF lung tissues, our data indicates that cav-1 regulates TGF-β_1 induced fibronectin production via JNK pathway, possibly via the modulation of Smad-2 phosphorylation and nuclear translocation.

In summary, we have demonstrated that cav-1 is capable of inhibiting the production of matrix molecules by fibroblasts, and exogenous transfer of cav-1 can inhibit the pulmonary fibrotic response in a BLM rodent model. We have also shown that cav-1 inhibited TGF-β_1 induced collagen type I production via the ERK pathway, and fibronectin production via JNK pathway. We found that cav-1 mRNA and protein expression were low in lung tissues and fibroblasts of IPF patients. We postulate that one of the mechanisms for the phenomenon is through TGF-β_1, which was shown to be an effective regulator of cav-1 expression in pulmonary fibroblasts. We delineated that the inhibition of Smad-2 activation by cav-1 regulated JNK pathway. Our study strongly supports a pivotal role for cav-1 in ECM regulation and suggests a novel therapeutic target for patients with pulmonary fibrosis.

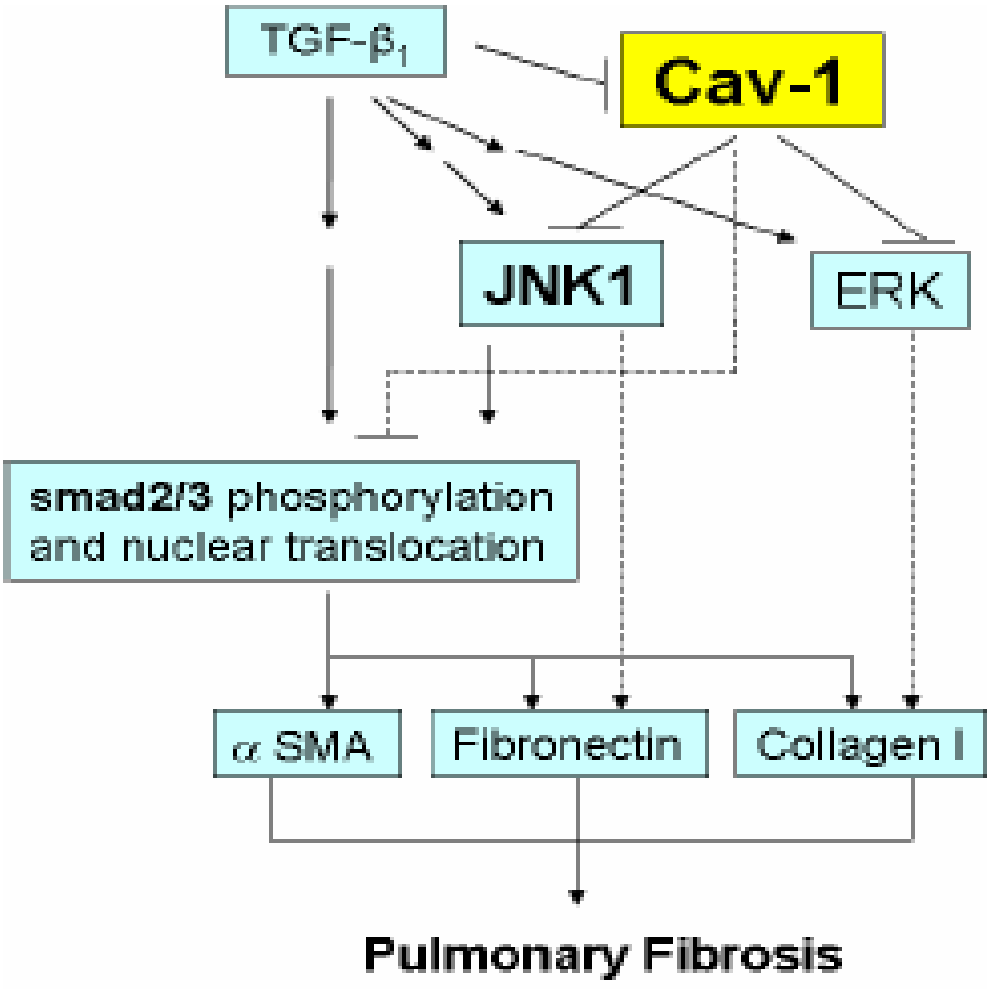

Figure 27 Diagram of cav-1 and fibrosis. TGF-β_1 activates downstream kinases activity. Smad 2/3 are phosphorylated and translocates into nucleus. JNK and ERK pathways are activated. These will result in a-SMA, fibronectin and collagen I productions. Cav-1 performs its anti-fibrotic effects via several pathways. (1) Cav-1 inhibits JNK and ERK activation. (2) Cav-1 inhibits Smad 2 phosphorylation and Smad 2/3 nuclear translocation. (3) Cav-1 inhibits fibronectin production via JNK1 pathway. (4) Cav-1 inhibits collagen I production via ERK pathway.

4.3 THE RELATIONSHIP OF INFLAMMATION AND FIBROSIS

Fibrosis is usually regarded as the terminal stage of inflammation. Inflammation relates to fibrosis in various diseases and organs.

For instance, pulmonary fibrosis is a common response to various injuries of the lung including pneumonia (99). The pathogenesis of pulmonary fibrosis includes endothelial and epithelial cell injury, production of inflammatory cells and their mediators, and fibroblast activation (99, 189). The terminal stages of fibrosis are characterized by proliferation and progressive accumulation of connective tissue replacing normal functional parenchyma, despite the different initiating factors (99). Although antiinflammatory therapies combined with immunosuppressive therapy are ineffective in preventing progression of the disease, these strategies remain the major and conventional therapy in treating fibrosis (100). Further understanding of the molecular mechanisms of inflammatory reaction, fibroblast proliferation, endothelial and epithelial cell apoptosis, collagen deposition should lead to the development of effective treatments against pulmonary fibrosis (100).

IPF is a chronic inflammatory disease. Inflammatory processes injure the lung parenchyma, modulate the proliferation of mesenchymal cells and result in the fibrotic change (101). Numerous cell types' interactions and activations are following after the lung injury (101). Lung injuries including exposure to inorganic dusts or viral infection may trigger activation of inflammatory cells, such as macrophages (101). The oxidants and/or proteases produced by macrophages and neutrophils lead to further injury to the alveolar epithelium and capillary endothelial cells and result in the derangement of the lung parenchyma (101, 189). Subsequent change of pulmonary interstitium is characterized by the accumulation of mesenchymal cells such as fibroblasts and deposition of connective tissue production in the alveolar walls (101).

Inflammatory cells have been extensively suggested to play pivotal roles in the pathogenesis of pulmonary fibrosis (101, 188). Macrophages at first may release oxidants and/or proteases. It recruits and stimulates fibroblasts (198, 199). Later macrophages lead to the production of prostaglandins, which lead to suppression of macrophage, neutrophil, and lymphocyte responses (200, 201). This leads to attenuating tissue injury and the development of fibrosis (202). Macrophages are also considered to play a major role by secreting large amount of growth factors and cytokines (102). Neutrophils may initially damage parenchyma via releasing

toxic metabolites and enzymes (203). However, they may later attenuate fibrosis, perhaps through collagenase secretion (204, 205). Lymphocytes may initially participate in a number of damaging ways by secreting chemotactic factors and participating in destructive autoimmune processes (206). However, certain subpopulations of T cells may markedly shift during the process of fibrosis, leading to attenuation of the development (207-210). Granulocytes, eosinophils and mast cells are also involved during the development of pulmonary fibrosis (211-217). More recently novel mechanisms have been proposed: bone marrow-derived stem cells may play a crucial role in the fibroproliferative response and epithelial regeneration (218-220).

A variety of biological substances can modulate the development of pulmonary fibrosis, including cytokines, chemotactic factors, and adhesion molecules (102). These cytokines include TGF-β, TNF-α, PDGF, TGF-alpha, IL-1, IL-6, monocyte chemoattractant protein (MCP)-1 and macrophage inflammatory protein (MIP)-1 α, etc (102). These cytokines secreted by activated inflammatory cells, such as macrophages and eosinophils, as well as noinflammatory cells, such as myofibroblasts and epithelial cells, exists at the sites of active fibrosis (102). Studies have revealed a variety of potential roles of the cyokines, including chemoattractant, mitogenic activities for fibroblasts, stimulation of extracellular matrix and alpha-smooth muscle actin production, alteration of the contractile phenotype of fibroblasts and regulation of diverse functions of lung inflammatory and epithelial cells (102). Besides TGF-β, a complex network of cytokines is responsible for the fibrotic process rather than any single cytokine. It is the balance of profibrogenic and antifibrogenic forces generated from interaction among the various cytokines in the network, which finally determines the outcome of lung injury (102). TNF-α promotes fibroblast proliferation and chemotaxia, which appears to be profibrogenic. It also has antifibrotic property, such as inhibition of collagen production (221-224). Studies in vivo demonstrated that neutralization of TNF decreased inflammatory cell accumulation and pulmonary fibrosis in BLM-induced injury (224, 225). TNF-α transgenic mice, which overexpress TNF-α in the lungs, develop interstitial pneumonitis (152). This indicates that overall TNF-α is a pro-fibrotic cytokine. IL-6 is a major cytokines released by activated macrophages (226). It is secreted in BAL fluid in BLM-induced lung injury model (227). IL-6 modulates neutrophil and B cell activation (228, 229). Neutralization of IL-6 and/or TNF in vivo markedly attenuates MIP-1α expression (230), which is an important anti-fibrotic cytokine, as neutralization of it dramatically suppresses pulmonary fibrosis in mice (231).

The present study demonstrated cav-1 serves to inhibit inflammatory cytokines production including TNF-α and IL-6 in alveolar macrophages. It also suppresses myofibroblasts transformation and production of ECM in pulmonary fibroblasts. Taken together with the reports that cav-1 has anti-proliferation effect in epithelial cells and fibroblasts, our study suggests that cav-1 will become a promising target molecule for therapy of lung injury.

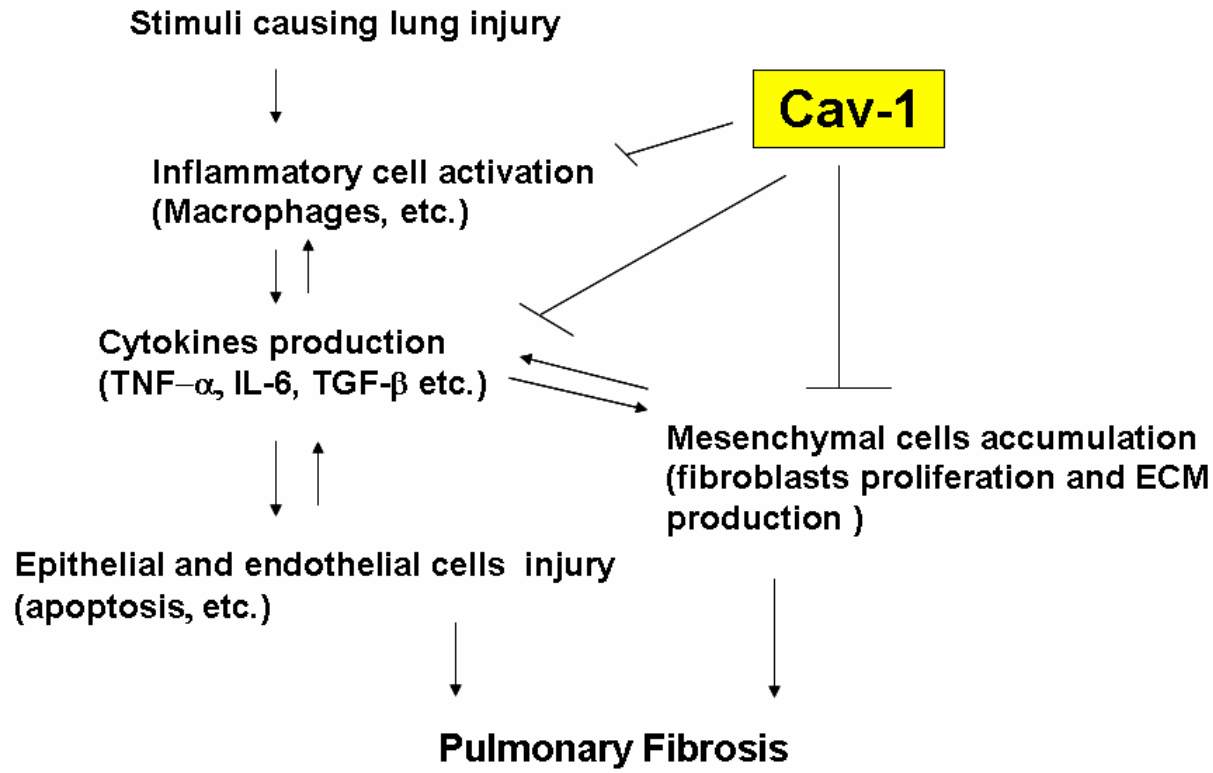

Figure 28 Diagram of cav-1 effects in lung injury.

APPENDIX A

[MATERIALS AND METHODS]

Cell Culture, Animals and Reagents. Primary peritoneal and alveolar macrophages were maintained in 10% fetal bovine serum (FBS) Dulbecoo's modified Eagle's medium (DMEM). RAW264.7 cells were grown in 5% FBS DMEM (Gibco-BR). Cav-1 stably transfected RAW264.7 cells and vector control cells were generated and maintained as described previously (232). Cultures were maintained at 37º C in a humidified atmosphere of 5% CO_2 and 95% air. The cells were serum starved before 100 ng/ml LPS stimulation. C57BL/6 mice were purchased from Jackson Laboratory (Bar Harbor, ME) and acclimated 1 week before experiments. All animals were housed in accordance with guidelines from the American Association for Laboratory Animal Care and Research Protocols and were approved by the Animal Care and Use Committee of University of Pittsburgh School of Medicine. PD 98059 (10 μM), UO 126 (10 μM), and SP 600125 (10 μM) (Calbiochem, Darmstadt, Germany) were dissolved in DMSO. All reagents were added to the culture medium 1 hour before other treatments. MKK3 (-/-) mice were generated as described before. Wortmannin (100 nM), SB203580 (10 μM), SP600125 (10 μM) and UO126 (10 μM) (Calbiochem, Darmstadt) were dissolved in DMSO. All reagents were added to the culture medium 1 hour before other treatments.

Human Tissues, Samples and Cells. This study was approved by the Institutional Review Board for Human Subject Research at the University of Pittsburgh. Human lung tissues were obtained from the tissue bank of the Department of Pathology at the University of Pittsburgh. Diagnosis of IPF was supported by history, physical examination, pulmonary function studies, chest high-resolution computed tomography (HRCT), bronchoalveolar lavage findings, and corroborated by open lung biopsy. The morphologic diagnosis of IPF was based on typical

microscopic findings consistent with usual interstitial pneumonia. The patients fulfilled the criteria of the American Thoracic Society and European Respiratory Society (233). Age, race, and sex matched control samples, included normal histology lung samples from patients with lung cancer or healthy subjects died from traffic accident, were obtained from the Pittsburgh Tissue Bank. Fibroblasts were derived from lung tissue obtained at autopsy from IPF and controls were maintained in 10 % fetal bovine serum (FBS) Dulbecco's modified Eagle's medium (DMEM) with 50 μg/ml gentamicin. Primary lung fibroblasts were isolated from JNK1 (-/-) mice and wild type littermates as described before (234). Human fetal lung fibroblasts (MRC-5) (purchased from the American Type Culture Collection, Rockville, MD) were maintained in 10 % FBS DMEM. MRC-5 cells were cotransfected (1:10) with pcDNA3.0 containing the neomycin selection marker, the expression vector pCAGGS containing cav-1 cDNA in the sense orientation, or with the pCAGGS control vector. Transfected cells were grown in DMEM, 10% FBS containing G418 (200 μg/ml). Cultures were maintained at 37 ºC in a humidified atmosphere of 5 % CO2 and 95 % air. Cell culture reagents were purchased from Gibco-BR. The cells were serum starved before TGF-β1 (R&D Systems, Minneapolis, MN) stimulation. TGF-β1 was reconstituted in sterile 4 mM HCl containing 0.1% bovine serum albumin (BSA).

Isolation of peritoneal macrophages and alveolar macrophages. The experimental protocols were performed in accordance with the guidelines of institutional animal care & use committee (IACUC) of University of Pittsburgh. Briefly, after the mice were anesthetized with isoflurane, peritoneal macrophages were isolated by peritoneal lavage with 2 ml PBS each time for 3 times. For alveolar macrophages isolation, mice were tracheotomized after transection of the abdomen. A blunt 21-gauge needle was secured into the trachea. Bronchoalveolar lavage (BAL) was performed 5 times with 0.3 ml phosphate buffered saline (PBS). Cell pellets were collected after centrifuging at 1000 g for 10 min at 4º C. The supernatant was discarded and the cells were resuspended in 10% FBS DMEM. Unattached cells were washed off twice with PBS after 3 hours culture, and the remaining macrophages were incubated overnight in DMEM supplemented with 10% FBS. On the following day, cells were washed twice again before treated as indicated.

Synthesis and Transfection of Small Interfering RNA (siRNA). siRNA sequences targeting mouse cav-1 gene were designed using software (Dharmacon, Inc). Among the five siRNAs synthesized, two sequences with better effects (AAAGAUGUGAUUGCAGAACCA;

AAUCAGCCGCGUCUACUCCAU) were used. The sequence (AACGCGCACACCAAGGAGAUU) with no apparent effects was used as a negative control. SiRNA sequence targeting human cav-1 gene (AA CCA GAA GGG ACA CAC AGT T) was synthesized (Dharmacon, Inc. Lafayette, CO). The sequence (AA CGC GCA CAC CAA GGA GAT T) targeting the mice cav-1 gene with no apparent effects in human cells was used as a negative control. For transfection, cells were plated on 6-well plates or 24-well plates. Transfections were performed with TransIT-TKO reagent (Mirus Corp) as directed by the manufacturer. For 6-well plates, each well received 10 nM siRNA in a volume of 1ml in triplicate. For 24-well plates, each well received 2 nM siRNA in a volume of 200 µl in triplicate. For macrophages study, cells were plated on 24-well plates. LPS was added after 24 hours of transfection. For fibroblasts study, cells were plated on 6-well plates. Other treatment was added after 24 hour of transfection.

Cytokine Analysis. The level of cytokines (TNF-α, IL-6, and IL-10) released by LPS stimulated macrophages into the culture supernatant were measured by enzyme-linked immunosorbent assay (ELISA) kits (R&D Systems), following the manufacturer's instructions.

Western blot analysis. Cells were rinsed with ice-cold PBS and homogenized in lyses buffer (1% NP-40, 20 mM Tris pH 8.0, 137.5 mM NaCl, 1 mM Na_3VO_4, and 1 mM PMSF) with complete protease inhibitor mixture (Roche Diagnostics). The supernatant was collected after centrifugation for 20 min at 14,000 g at 4° C. The protein concentrations were determined by Coomassie (Bradford) protein assay kit (Pierce Biotechnology Inc.) with bovine serum albumin as a standard. A total of 50 to 100 µg proteins in each sample were subjected to electrophoresis through a 4-12% SDS-polyacrylamide gel (Novex). The proteins were electro transferred onto polyvinylidene difluoride membrane (Immobilon-P). Membranes were blocked in TTBS buffer (Tris-buffered saline with 0.1% Tween 20) containing 5% low fat milk for one hour and incubated overnight at 4 °C with the corresponding primary antibody. After washing with TTBS, membranes were incubated for 2 hours at room temperature with the corresponding secondary antibody. Membranes were washed again and developed with ECL reagent (Amersham Biosciences). Anti-cav-1 polyclonal antibody was purchased form Santa Cruz (Santa Cruz Biotechnology Inc). Anti-mouse ß-actin monoclonal antibody was purchased from Sigma (Sigma Chemical Co). Total and phosphorylated forms of MAPK were from Cell Signaling Technology.

Immunofluorescence Microscopy. BAL cells were seeded on cover slips at a density of 5×10^4/well (24-well). Cells were rinsed 3 times with PBS and then fixed in 2% paraformaldehyde. The cover slips were then sequentially incubated at room temperature in PBS containing 4% goat serum for 60 min, and immunostained with polyclonal rabbit cav-1 and Mac-3 antibodies in 0.5% bovine serum albumin/PBS for 60 min. Bound primary antibodies were visualized with Cy-3 and Alexa 488-conjugated secondary antibodies (Jackson ImmunoResearch Laboratories). Cells were viewed with an Olympus Fluoview BX 61 confocal microscope and images were collected using a DC-330S cooled CCD camera (DAGE-MTI Inc.).

Electrophoretic Mobility Shift Assay (EMSA). Nuclear protein extracts were made as described previously (136). Double-stranded oligonucleotides containing the transcription factor-binding site for AP-1 (5'-CGCTTGATGAGTCAGCCGGAA-3') and NF-κB (5'-AGTTGAGGGGACTTTCCCAGGC-3') (Promega, Madison) were labeled with ^{32}P-ATP using T4 polynucleotide kinase (Promega, Madison) as described. Four micrograms of nuclear proteins were incubated with the probe in binding buffer (Promega, Madison) for 20 min at 37º C. The reaction mixture then was subjected to electrophoresis through 5% native polyacrylamide gels. The gels were dried and exposed.

Purification of RNA and Quantitative RT-PCR. Total RNA was isolated from lung fibroblasts or cell lines with TRIzol reagent using the manufacturer's protocol (Invitrogen, Carlsbad, CA) and cleared with Rneasy Mini kit (Qiagen, Hilden, Germany). The reverse transcription (RT) was performed with reagents from Invitrogen. Isolated RNA was first incubated with random hexamer at 65°C for 5 min for annealing. The optimal RT reaction was then carried out in 20 µl volumes consisting of 1x RT buffer, 1 µl of SuperScript II reverse transcriptase, 1 µl of RNaseOUT, 5 mM $MgCl_2$, 0.5 mM each dNTP, 0.01 mM DTT, 5 µmol/L random hexamers, and 500 ng total RNA. Reactions were incubated at 25°C for 10 minutes, 48°C for 30 minutes, and 95°C for 5 minutes. "No RT " controls were carried out in all samples using the same RT reaction mix but substituting DEPC-H_2O for SuperScript II reverse transcriptase. PCR primers, fluorogenic probe (Taqman) and all other reagents were purchased from Applied Biosystems (Applied Biosystems, Foster City, CA) (human cav-1: Hs00184697_m1; human beta-glucuronidase: Hs99999908_m1) and used following the manufacturer's protocol. Quantitative RT-PCR was performed in triplicate in 40 µl reaction volumes consisting of 1x PCR buffer A,

3.5 mM $MgCl_2$, 0.3 mM dNTP, 0.025 U/µl AmpliTaq Gold, and 4 µl of the RT reaction. Two-step PCR cycling was carried out as follows: 95°C 12 minutes x 1 cycle, 95°C 15 seconds, 60°C 1 minute x 40 cycles. At the end of the PCR, baseline and threshold values were set in the ABI 7700 Prism software and the relative cav-1 expression were calculated as described before (235).

Cav-1 Adenovirus construction and Infection. Cav-1 cDNA were inserted into a pAdlox plasmid. Cav-1 and LacZ adenovirus productions were performed by the Vector Core Facility in University of Pittsburgh. For cell infection, 2×10^5 MRC cells were cultured in 6-well plates and exposed to 2×10^7 plaque-forming units of each virus in 1 ml of serum-free medium for 4 hours. The cells were then washed and incubated in serum-containing media for 36 hours. The cells were then subjected to other treatment as indicated. For animal infection, 1×10^{11} plaque-forming units of each virus in 50 µl of PBS were administrated intratracheally per mice. After 7 days of infection, mice were sacrificed. Cav-1 expression was determined by immunoblot and immunohistochemistry.

Immunohistochemistry. Briefly, lung tissues were fixed in 2 % paraformaldehyde for 2 h and in 30% sucrose overnight. The tissues were frozen in liquid nitrogen and subjected to immunohistochemistry. The 6-µm tissue sections were washed three times in 0.5% BSA (Sigma-Aldrich), and blocked for 1 h in 2% BSA. After three washing of the samples in 0.5% BSA, tissue sections were incubated with the cav-1 antibody at a dilution of 1 to 5000 (Santa Cruz Biotechnology) for 1 hour. The samples were then washed 5 times in BSA and incubated with Cy3-conjugated goat anti-rabbit Fab fragment (Jackson ImmunoResearch Laboratories, West Grove, PA) for 1 hour. After 5 washing in BSA, the sections were incubated with the Alexa fluor 647 phalloidin (Invitrogen) for 1 hour. Samples were washed 5 times in BSA and PBS. Hoechst dye (Sigma-Aldrich) was added for 30 seconds, and samples were washed in PBS and then mounted. Tissue sections were viewed with an Olympus BX51 fluorescent microscope (Olympus America, Melville, NY).

Bleomycin Administration. After 2 days adenovirus infection, the mice were lightly sedated with isofluorane. Bleomycin (BLM) (Bristol-Myers Squibb, Princeton, NJ) at a dose of 0.075 U/mouse in 50 µl of sterile saline was administered intratracheally by canulation of the trachea via the mouth with a 20-gauge feeding needle.

Hyproxyproline Assay. After fourteen days of bleomycin administration, the left lungs were harvested and dried at 110°C until a constant weight was obtained. The dried lung was hydrolyzed under vacuum in a glass vial containing 1 ml of 6N HCl at 110°C overnight. The samples were lyophilized and assayed for hydroxyproline content using a chloramine-T method as previously described (236).

Histopathology. The right lungs were fixed in 10% formaldehyde for 24 hours and then processed for paraffin embedding. Sections of lung were stained with routine hematoxylin and eosin or with a Masson trichrome stain to assess the degree of fibrosis. The extent of lung fibrosis was graded by a pathologist in a blinded manner on a scale of 0 for normal lung to 8 as previously described (236). The major criteria examined included interstitial thickening of alveolar or bronchiolar walls, collagen deposition, and inflammatory cell infiltration. Scores were then averaged per treatment group and compared to control using ANOVA analysis.

Statistic Analysis. The differences in cytokine expression were compared by unpaired Student's t test, since the cytokines production follows a normal distribution as tested by Anderson-Darling goodness-of-fit test. The variances are equal across groups as verified by the Bartlett test. All analyses were performed with SPSS 12.0.1 for Windows, and were considered significant at $p < 0.05$. The differences in mRNA level of cav-1 expression determined by quantitative RT-PCR were compared by Student's t-test. The differences in protein level of cav-1 expression determined by immunoblot analysis were compared by Wilcoxon two-sample test. For animal experiments, differences in measured variables between experimental and control group were analyzed using ANOVA. Groups containing multiple comparisons were assessed by analysis of variance, and Bonferroni's correction was used in determining P values. All analyses were performed with SPSS 12.0.1 for Windows, and were considered significant at $p \leq 0.05$. For promoter polymorphism studies, each case-control comparison we computed standard χ^2 tests of independence between genotype distribution, allele frequency, haplotypes and phenotype. *P*-value ≤ 0.05 consider significant. Haplotypes were estimated using the resulting genotypes by disease status using the Genetic software of SAS. Allele and genotype specific odd ratios were estimated. Hardy-Weinberg equilibrium test and all statistical analysis were performed using the Genetic software of SAS.

APPENDIX B

[ABBREVIATES]

Active protein-1 (AP-1)

Alveolar macrophages (AM)

Bleomycin (BLM)

Bronchoalveolar lavage (BAL)

cAMP-activated protein kinase (PKA)

Carbon monoxide (CO)

Caveolin-1 (cav-1)

Chest high-resolution computed tomography (HRCT)

c-Jun N-terminal kinase (JNK)

Dulbecco's modified Eagle's medium (DMEM)

Electrophoretic Mobility Shift Assay (EMSA)

Endoplasmic reticulum (ER)

Endothelial nitric oxide synthase (eNOS)

Epidermal growth factor receptor (EGF-R)

Extracellular matrix (ECM)

Extracellular signal regulated kinase (ERK)

Fetal bovine serum (FBS)

Harvey rat sarcoma viral oncogene (H-Ras)

Heme oxygenase-1 (HO-1)

High density lipid (HDL)

Hydrogen peroxide (H_2O_2)

Idiopathic pulmonary fibrosis (IPF)

Interferon-γ (IFN-γ)

Interleukine-1 (IL-1)

Interleukin-5 (IL-5)

Interleukin-6 (IL-6)

Interleukin-10 (IL-10)

Lipopolysaccharide (LPS)

Macrophage inflammatory protein (MIP)

Mitogen-activated protein kinase (MAPK)

Monocyte chemoattractant protein (MCP)

Nitric oxide (NO)

Nuclear factor-κB (NF-κB)

Peritoneal macrophages (PM)

Phosphoinositide kinase-3 (PI3K)

Platelet-derived growth factor receptor (PDGF-R)

Reactive oxygen species (ROS)

Small Interfering RNA (siRNA)

Sodium m-arsenite ($NaAsO_2$)

TGF-β receptor I (TGF-βRI)

Toll like receptor 4 (TLR4)

Transforming growth factor β_1 (TGF-β_1)

Tumor necrosis factor-alpha (TNF-α)

BIBLIOGRAPHY

1. Anderson, R. G. 1993. Caveolae: where incoming and outgoing messengers meet. *Proc Natl Acad Sci U S A* 90(23):10909-13.
2. Harder, T., and K. Simons. 1997. Caveolae, DIGs, and the dynamics of sphingolipid-cholesterol microdomains. *Curr Opin Cell Biol* 9(4):534-42.
3. Michel, C. C. 1998. Capillaries, caveolae, calcium and cyclic nucleotides: a new look at microvascular permeability. *J Mol Cell Cardiol* 30(12):2541-6.
4. Liu, J., and J. E. Schnitzer. 1999. Analysis of lipids in caveolae. *Methods Mol Biol* 116:61-72.
5. Hnasko, R., and M. P. Lisanti. 2003. The biology of caveolae: lessons from caveolin knockout mice and implications for human disease. *Mol Interv* 3(8):445-64.
6. Schlegel, A., D. Volonte, J. A. Engelman, F. Galbiati, P. Mehta, X. L. Zhang, P. E. Scherer, and M. P. Lisanti. 1998. Crowded little caves: structure and function of caveolae. *Cell Signal* 10(7):457-63.
7. Kurzchalia, T. V., and R. G. Parton. 1996. And still they are moving.... dynamic properties of caveolae. *FEBS Lett* 389(1):52-4.
8. Fujimoto, T., H. Hagiwara, T. Aoki, H. Kogo, and R. Nomura. 1998. Caveolae: from a morphological point of view. *J Electron Microsc (Tokyo)* 47(5):451-60.
9. Stan, R. V. 2005. Structure of caveolae. *Biochim Biophys Acta* 1746(3):334-48.
10. Halayko, A. J., and G. L. Stelmack. 2005. The association of caveolae, actin, and the dystrophin-glycoprotein complex: a role in smooth muscle phenotype and function? *Can J Physiol Pharmacol* 83(10):877-91.
11. Parton, R. G. 1996. Caveolae and caveolins. *Curr Opin Cell Biol* 8(4):542-8.
12. Gumbleton, M., A. G. Abulrob, and L. Campbell. 2000. Caveolae: an alternative membrane transport compartment. *Pharm Res* 17(9):1035-48.

13. Silva, W., H. Maldonado, G. Chompre, and N. Mayol. 1998. Caveolae a new subcellular transport organelle. *Bol Asoc Med P R* 90(1-3):30-3.

14. Zuwala-Jagiello, J. 2004. [Role of endothelial caveolae in the endocytosis of advanced glycation endproducts]. *Postepy Biochem* 50(3):272-81.

15. Frank, P. G., and M. P. Lisanti. 2004. Caveolin-1 and caveolae in atherosclerosis: differential roles in fatty streak formation and neointimal hyperplasia. *Curr Opin Lipidol* 15(5):523-9.

16. Brazer, S. C., B. B. Singh, X. Liu, W. Swaim, and I. S. Ambudkar. 2003. Caveolin-1 contributes to assembly of store-operated Ca2+ influx channels by regulating plasma membrane localization of TRPC1. *J Biol Chem* 278(29):27208-15.

17. Kasahara, K., and Y. Sanai. 1998. [Glycosphingolipid microdomains/caveolae and signal transduction]. *Tanpakushitsu Kakusan Koso* 43(16 Suppl):2522-30.

18. Kirkham, M., and R. G. Parton. 2005. Clathrin-independent endocytosis: new insights into caveolae and non-caveolar lipid raft carriers. *Biochim Biophys Acta* 1746(3):349-63.

19. Pelkmans, L. 2005. Secrets of caveolae- and lipid raft-mediated endocytosis revealed by mammalian viruses. *Biochim Biophys Acta* 1746(3):295-304.

20. Insel, P. A., B. P. Head, R. S. Ostrom, H. H. Patel, J. S. Swaney, C. M. Tang, and D. M. Roth. 2005. Caveolae and lipid rafts: G protein-coupled receptor signaling microdomains in cardiac myocytes. *Ann N Y Acad Sci* 1047:166-72.

21. Barnett-Norris, J., D. Lynch, and P. H. Reggio. 2005. Lipids, lipid rafts and caveolae: their importance for GPCR signaling and their centrality to the endocannabinoid system. *Life Sci* 77(14):1625-39.

22. Pike, L. J. 2005. Growth factor receptors, lipid rafts and caveolae: an evolving story. *Biochim Biophys Acta* 1746(3):260-73.

23. Navarro, A., B. Anand-Apte, and M. O. Parat. 2004. A role for caveolae in cell migration. *Faseb J* 18(15):1801-11.

24. Massimino, M. L., C. Griffoni, E. Spisni, M. Toni, and V. Tomasi. 2002. Involvement of caveolae and caveolae-like domains in signalling, cell survival and angiogenesis. *Cell Signal* 14(2):93-8.

25. Engelman, J. A., X. L. Zhang, and M. P. Lisanti. 1998. Genes encoding human caveolin-1 and -2 are co-localized to the D7S522 locus (7q31.1), a known fragile site (FRA7G) that is frequently deleted in human cancers. *FEBS Lett* 436(3):403-10.

26. Engelman, J. A., X. L. Zhang, and M. P. Lisanti. 1999. Sequence and detailed organization of the human caveolin-1 and -2 genes located near the D7S522 locus (7q31.1). Methylation of a CpG island in the 5' promoter region of the caveolin-1 gene in human breast cancer cell lines. *FEBS Lett* 448(2-3):221-30.

27. Fra, A. M., N. Mastroianni, M. Mancini, E. Pasqualetto, and R. Sitia. 1999. Human caveolin-1 and caveolin-2 are closely linked genes colocalized with WI-5336 in a region of 7q31 frequently deleted in tumors. *Genomics* 56(3):355-6.

28. Song, K. S., P. E. Scherer, Z. Tang, T. Okamoto, S. Li, M. Chafel, C. Chu, D. S. Kohtz, and M. P. Lisanti. 1996. Expression of caveolin-3 in skeletal, cardiac, and smooth muscle cells. Caveolin-3 is a component of the sarcolemma and co-fractionates with dystrophin and dystrophin-associated glycoproteins. *J Biol Chem* 271(25):15160-5.

29. Sotgia, F., C. Minetti, and M. P. Lisanti. 1999. Localization of the human caveolin-3 gene to the D3S18/D3S4163/D3S4539 locus (3p25), in close proximity to the human oxytocin receptor gene. Identification of the caveolin-3 gene as a candidate for deletion in 3p-syndrome. *FEBS Lett* 452(3):177-80.

30. Fujimoto, T., H. Kogo, R. Nomura, and T. Une. 2000. Isoforms of caveolin-1 and caveolar structure. *J Cell Sci* 113 Pt 19:3509-17.

31. Nohe, A., E. Keating, C. Loh, M. T. Underhill, and N. O. Petersen. 2004. Caveolin-1 isoform reorganization studied by image correlation spectroscopy. *Faraday Discuss* 126:185-95; discussion 245-54.

32. Byrne, S., A. Cheent, J. Dimond, G. Fisher, and C. D. Ockleford. 2001. Immunocytochemical localization of a caveolin-1 isoform in human term extra-embryonic membranes using confocal laser scanning microscopy: implications for the complexity of the materno-fetal junction. *Placenta* 22(6):499-510.

33. Kogo, H., and T. Fujimoto. 2000. Caveolin-1 isoforms are encoded by distinct mRNAs. Identification Of mouse caveolin-1 mRNA variants caused by alternative transcription initiation and splicing. *FEBS Lett* 465(2-3):119-23.

34. Rothberg, K. G., J. E. Heuser, W. C. Donzell, Y. S. Ying, J. R. Glenney, and R. G. Anderson. 1992. Caveolin, a protein component of caveolae membrane coats. *Cell* 68(4):673-82.

35. Schlegel, A., R. B. Schwab, P. E. Scherer, and M. P. Lisanti. 1999. A role for the caveolin scaffolding domain in mediating the membrane attachment of caveolin-1. The caveolin scaffolding domain is both necessary and sufficient for membrane binding in vitro. *J Biol Chem* 274(32):22660-7.

36. Schlegel, A., and M. P. Lisanti. 2000. A molecular dissection of caveolin-1 membrane attachment and oligomerization. Two separate regions of the caveolin-1 C-terminal domain mediate membrane binding and oligomer/oligomer interactions in vivo. *J Biol Chem* 275(28):21605-17.

37. Woodman, S. E., A. Schlegel, A. W. Cohen, and M. P. Lisanti. 2002. Mutational analysis identifies a short atypical membrane attachment sequence (KYWFYR) within caveolin-1. *Biochemistry* 41(11):3790-5.

38. Galbiati, F., D. Volonte, D. Meani, G. Milligan, D. M. Lublin, M. P. Lisanti, and M. Parenti. 1999. The dually acylated NH2-terminal domain of gi1alpha is sufficient to target a green fluorescent protein reporter to caveolin-enriched plasma membrane domains. Palmitoylation of caveolin-1 is required for the recognition of dually acylated g-protein alpha subunits in vivo. *J Biol Chem* 274(9):5843-50.

39. Song, K. S., Z. Tang, S. Li, and M. P. Lisanti. 1997. Mutational analysis of the properties of caveolin-1. A novel role for the C-terminal domain in mediating homo-typic caveolin-caveolin interactions. *J Biol Chem* 272(7):4398-403.

40. Li, S., F. Galbiati, D. Volonte, M. Sargiacomo, J. A. Engelman, K. Das, P. E. Scherer, and M. P. Lisanti. 1998. Mutational analysis of caveolin-induced vesicle formation. Expression of caveolin-1 recruits caveolin-2 to caveolae membranes. *FEBS Lett* 434(1-2):127-34.

41. Vogel, U., K. Sandvig, and B. van Deurs. 1998. Expression of caveolin-1 and polarized formation of invaginated caveolae in Caco-2 and MDCK II cells. *J Cell Sci* 111 (Pt 6):825-32.

42. Razani, B., X. B. Wang, J. A. Engelman, M. Battista, G. Lagaud, X. L. Zhang, B. Kneitz, H. Hou, Jr., G. J. Christ, W. Edelmann, and M. P. Lisanti. 2002. Caveolin-2-deficient mice show evidence of severe pulmonary dysfunction without disruption of caveolae. *Mol Cell Biol* 22(7):2329-44.

43. Tang, Z. L., P. E. Scherer, and M. P. Lisanti. 1994. The primary sequence of murine caveolin reveals a conserved consensus site for phosphorylation by protein kinase C. *Gene* 147(2):299-300.

44. Lee, H., S. E. Woodman, J. A. Engelman, D. Volonte, F. Galbiati, H. L. Kaufman, D. M. Lublin, and M. P. Lisanti. 2001. Palmitoylation of caveolin-1 at a single site (Cys-156) controls its coupling to the c-Src tyrosine kinase: targeting of dually acylated molecules (GPI-linked, transmembrane, or cytoplasmic) to caveolae effectively uncouples c-Src and caveolin-1 (TYR-14). *J Biol Chem* 276(37):35150-8.

45. Cao, H., W. E. Courchesne, and C. C. Mastick. 2002. A phosphotyrosine-dependent protein interaction screen reveals a role for phosphorylation of caveolin-1 on tyrosine 14: recruitment of C-terminal Src kinase. *J Biol Chem* 277(11):8771-4.

46. Uittenbogaard, A., and E. J. Smart. 2000. Palmitoylation of caveolin-1 is required for cholesterol binding, chaperone complex formation, and rapid transport of cholesterol to caveolae. *J Biol Chem* 275(33):25595-9.

47. Razani, B., and M. P. Lisanti. 2001. Two distinct caveolin-1 domains mediate the functional interaction of caveolin-1 with protein kinase A. *Am J Physiol Cell Physiol* 281(4):C1241-50.

48. Abulrob, A., S. Giuseppin, M. F. Andrade, A. McDermid, M. Moreno, and D. Stanimirovic. 2004. Interactions of EGFR and caveolin-1 in human glioblastoma cells: evidence that tyrosine phosphorylation regulates EGFR association with caveolae. *Oncogene* 23(41):6967-79.

49. Lu, Z., S. Ghosh, Z. Wang, and T. Hunter. 2003. Downregulation of caveolin-1 function by EGF leads to the loss of E-cadherin, increased transcriptional activity of beta-catenin, and enhanced tumor cell invasion. *Cancer Cell* 4(6):499-515.

50. Lee, H., D. Volonte, F. Galbiati, P. Iyengar, D. M. Lublin, D. B. Bregman, M. T. Wilson, R. Campos-Gonzalez, B. Bouzahzah, R. G. Pestell, P. E. Scherer, and M. P. Lisanti. 2000. Constitutive and growth factor-regulated phosphorylation of caveolin-1 occurs at the same site (Tyr-14) in vivo: identification of a c-Src/Cav-1/Grb7 signaling cassette. *Mol Endocrinol* 14(11):1750-75.

51. Kim, Y. N., G. J. Wiepz, A. G. Guadarrama, and P. J. Bertics. 2000. Epidermal growth factor-stimulated tyrosine phosphorylation of caveolin-1. Enhanced caveolin-1 tyrosine

phosphorylation following aberrant epidermal growth factor receptor status. *J Biol Chem* 275(11):7481-91.

52. Peterson, T. E., M. E. Guicciardi, R. Gulati, L. S. Kleppe, C. S. Mueske, M. Mookadam, G. Sowa, G. J. Gores, W. C. Sessa, and R. D. Simari. 2003. Caveolin-1 can regulate vascular smooth muscle cell fate by switching platelet-derived growth factor signaling from a proliferative to an apoptotic pathway. *Arterioscler Thromb Vasc Biol* 23(9):1521-7.

53. Wary, K. K., A. Mariotti, C. Zurzolo, and F. G. Giancotti. 1998. A requirement for caveolin-1 and associated kinase Fyn in integrin signaling and anchorage-dependent cell growth. *Cell* 94(5):625-34.

54. Sedding, D. G., J. Hermsen, U. Seay, O. Eickelberg, W. Kummer, C. Schwencke, R. H. Strasser, H. Tillmanns, and R. C. Braun-Dullaeus. 2005. Caveolin-1 facilitates mechanosensitive protein kinase B (Akt) signaling in vitro and in vivo. *Circ Res* 96(6):635-42.

55. Li, S., J. Couet, and M. P. Lisanti. 1996. Src tyrosine kinases, Galpha subunits, and H-Ras share a common membrane-anchored scaffolding protein, caveolin. Caveolin binding negatively regulates the auto-activation of Src tyrosine kinases. *J Biol Chem* 271(46):29182-90.

56. Razani, B., X. L. Zhang, M. Bitzer, G. von Gersdorff, E. P. Bottinger, and M. P. Lisanti. 2001. Caveolin-1 regulates transforming growth factor (TGF)-beta/SMAD signaling through an interaction with the TGF-beta type I receptor. *J Biol Chem* 276(9):6727-38.

57. Fujita, Y., S. Maruyama, H. Kogo, S. Matsuo, and T. Fujimoto. 2004. Caveolin-1 in mesangial cells suppresses MAP kinase activation and cell proliferation induced by bFGF and PDGF. *Kidney Int* 66(5):1794-804.

58. Lin, D., J. Zhou, P. S. Zelenka, and D. J. Takemoto. 2003. Protein kinase Cgamma regulation of gap junction activity through caveolin-1-containing lipid rafts. *Invest Ophthalmol Vis Sci* 44(12):5259-68.

59. Toya, Y., C. Schwencke, J. Couet, M. P. Lisanti, and Y. Ishikawa. 1998. Inhibition of adenylyl cyclase by caveolin peptides. *Endocrinology* 139(4):2025-31.

60. Huang, C., J. R. Hepler, L. T. Chen, A. G. Gilman, R. G. Anderson, and S. M. Mumby. 1997. Organization of G proteins and adenylyl cyclase at the plasma membrane. *Mol Biol Cell* 8(12):2365-78.

61. Schwencke, C., M. Yamamoto, S. Okumura, Y. Toya, S. J. Kim, and Y. Ishikawa. 1999. Compartmentation of cyclic adenosine 3',5'-monophosphate signaling in caveolae. *Mol Endocrinol* 13(7):1061-70.

62. Ostrom, R. S., X. Liu, B. P. Head, C. Gregorian, T. M. Seasholtz, and P. A. Insel. 2002. Localization of adenylyl cyclase isoforms and G protein-coupled receptors in vascular smooth muscle cells: expression in caveolin-rich and noncaveolin domains. *Mol Pharmacol* 62(5):983-92.

63. Lu, M. L., M. C. Schneider, Y. Zheng, X. Zhang, and J. P. Richie. 2001. Caveolin-1 interacts with androgen receptor. A positive modulator of androgen receptor mediated transactivation. *J Biol Chem* 276(16):13442-51.

64. Chambliss, K. L., I. S. Yuhanna, C. Mineo, P. Liu, Z. German, T. S. Sherman, M. E. Mendelsohn, R. G. Anderson, and P. W. Shaul. 2000. Estrogen receptor alpha and endothelial nitric oxide synthase are organized into a functional signaling module in caveolae. *Circ Res* 87(11):E44-52.

65. Schlegel, A., C. Wang, B. S. Katzenellenbogen, R. G. Pestell, and M. P. Lisanti. 1999. Caveolin-1 potentiates estrogen receptor alpha (ERalpha) signaling. caveolin-1 drives ligand-independent nuclear translocation and activation of ERalpha. *J Biol Chem* 274(47):33551-6.

66. Ghosh, S., R. Gachhui, C. Crooks, C. Wu, M. P. Lisanti, and D. J. Stuehr. 1998. Interaction between caveolin-1 and the reductase domain of endothelial nitric-oxide synthase. Consequences for catalysis. *J Biol Chem* 273(35):22267-71.

67. Ju, H., R. Zou, V. J. Venema, and R. C. Venema. 1997. Direct interaction of endothelial nitric-oxide synthase and caveolin-1 inhibits synthase activity. *J Biol Chem* 272(30):18522-5.

68. Venema, V. J., R. Zou, H. Ju, M. B. Marrero, and R. C. Venema. 1997. Caveolin-1 detergent solubility and association with endothelial nitric oxide synthase is modulated by tyrosine phosphorylation. *Biochem Biophys Res Commun* 236(1):155-61.

69. Kiss, A. L., A. Turi, N. Mullner, and J. Timar. 2000. Caveolin isoforms in resident and elicited rat peritoneal macrophages. *Eur J Cell Biol* 79(5):343-9.

70. Malerod, L., K. Juvet, T. Gjoen, and T. Berg. 2002. The expression of scavenger receptor class B, type I (SR-BI) and caveolin-1 in parenchymal and nonparenchymal liver cells. *Cell Tissue Res* 307(2):173-80.

71. MG, L., and M. DC. 2000. - Differential expression of caveolin-1 in lipopolysaccharide-activated. *Infect Immun* 68(9):5084-9.

72. Harris, J., D. Werling, M. Koss, P. Monaghan, G. Taylor, and C. J. Howard. 2002. Expression of caveolin by bovine lymphocytes and antigen-presenting cells. *Immunology* 105(2):190-5.

73. Shin, J. S., Z. Gao, and S. N. Abraham. 2000. Involvement of cellular caveolae in bacterial entry into mast cells. *Science* 289(5480):785-8.

74. Gargalovic, P., and L. Dory. 2001. Caveolin-1 and caveolin-2 expression in mouse macrophages. High density lipoprotein 3-stimulated secretion and a lack of significant subcellular co-localization. *J Biol Chem* 276(28):26164-70.

75. Lei, M. G., and D. C. Morrison. 2000. Differential expression of caveolin-1 in lipopolysaccharide-activated murine macrophages. *Infect Immun* 68(9):5084-9.

76. Gargalovic, P., and L. Dory. 2003. Caveolins and macrophage lipid metabolism. *J Lipid Res* 44(1):11-21.

77. Kiss, A. L., A. Turi, N. Muller, O. Kantor, and E. Botos. 2002. Caveolae and caveolin isoforms in rat peritoneal macrophages. *Micron* 33(1):75-93.

78. Matveev, S., D. R. van der Westhuyzen, and E. J. Smart. 1999. Co-expression of scavenger receptor-BI and caveolin-1 is associated with enhanced selective cholesteryl ester uptake in THP-1 macrophages. *J Lipid Res* 40(9):1647-54.

79. Dougherty, G. J., and W. H. McBride. 1984. Macrophage heterogeneity. *J Clin Lab Immunol* 14(1):1-11.

80. Bowden, D. H. 1984. The alveolar macrophage. *Environ Health Perspect* 55:327-41.

81. Perez-Arellano, J. L., M. C. Alcazar-Montero, and A. Jimenez-Lopez. 1990. Alveolar macrophage: origin, kinetics and relationship with cells of the alveolo-interstitial region. *Allergol Immunopathol (Madr)* 18(3):175-83.

82. Kasper, M., K. Sakai, R. Koslowski, K. W. Wenzel, G. Haroske, D. Schuh, and M. Muller. 1994. Localization of surfactant protein A (SP-A) in alveolar macrophage subpopulations of normal and fibrotic rat lung. *Histochemistry* 102(5):345-52.

83. Gargalovic, P., and L. Dory. 2003. Cellular apoptosis is associated with increased caveolin-1 expression in macrophages. *J Lipid Res* 44(9):1622-32.

84. Navakauskiene, R., G. Treigyte, A. Gineitis, and K. E. Magnusson. 2004. Identification of apoptotic tyrosine-phosphorylated proteins after etoposide or retinoic acid treatment. *Proteomics* 4(4):1029-41.

85. Frank, P. G., M. W. Cheung, S. Pavlides, G. Llaverias, D. S. Park, and M. P. Lisanti. 2006. Caveolin-1 and regulation of cellular cholesterol homeostasis. *Am J Physiol Heart Circ Physiol* 291(2):H677-86.

86. Murata, M., J. Peranen, R. Schreiner, F. Wieland, T. V. Kurzchalia, and K. Simons. 1995. VIP21/caveolin is a cholesterol-binding protein. *Proc Natl Acad Sci U S A* 92(22):10339-43.

87. Matveev, S., A. Uittenbogaard, D. van Der Westhuyzen, and E. J. Smart. 2001. Caveolin-1 negatively regulates SR-BI mediated selective uptake of high-density lipoprotein-derived cholesteryl ester. *Eur J Biochem* 268(21):5609-16.

88. Mulcahy, J. V., D. R. Riddell, and J. S. Owen. 2004. Human scavenger receptor class B type II (SR-BII) and cellular cholesterol efflux. *Biochem J* 377(Pt 3):741-7.

89. Walton, K. A., A. L. Cole, M. Yeh, G. Subbanagounder, S. R. Krutzik, R. L. Modlin, R. M. Lucas, J. Nakai, E. J. Smart, D. K. Vora, and J. A. Berliner. 2003. Specific phospholipid oxidation products inhibit ligand activation of toll-like receptors 4 and 2. *Arterioscler Thromb Vasc Biol* 23(7):1197-203.

90. Mulvey, M. A., and S. J. Hultgren. 2000. Cell biology. Bacterial spelunkers. *Science* 289(5480):732-3.

91. Bucci, M., J. P. Gratton, R. D. Rudic, L. Acevedo, F. Roviezzo, G. Cirino, and W. C. Sessa. 2000. In vivo delivery of the caveolin-1 scaffolding domain inhibits nitric oxide synthesis and reduces inflammation. *Nat Med* 6(12):1362-7.

92. Norkin, L. C., S. A. Wolfrom, and E. S. Stuart. 2001. Association of caveolin with Chlamydia trachomatis inclusions at early and late stages of infection. *Exp Cell Res* 266(2):229-38.

93. Rohde, M., E. Muller, G. S. Chhatwal, and S. R. Talay. 2003. Host cell caveolae act as an entry-port for group A streptococci. *Cell Microbiol* 5(5):323-42.

94. Tsuda, K., A. Amano, K. Umebayashi, H. Inaba, I. Nakagawa, Y. Nakanishi, and T. Yoshimori. 2005. Molecular dissection of internalization of Porphyromonas gingivalis by cells using fluorescent beads coated with bacterial membrane vesicle. *Cell Struct Funct* 30(2):81-91.

95. Kiss, A. L., and H. J. Geuze. 1997. Caveolae can be alternative endocytotic structures in elicited macrophages. *Eur J Cell Biol* 73(1):19-27.
96. Stuart, E. S., W. C. Webley, and L. C. Norkin. 2003. Lipid rafts, caveolae, caveolin-1, and entry by Chlamydiae into host cells. *Exp Cell Res* 287(1):67-78.
97. Santizo, R. A., H. L. Xu, E. Galea, S. Muyskens, V. L. Baughman, and D. A. Pelligrino. 2002. Combined endothelial nitric oxide synthase upregulation and caveolin-1 downregulation decrease leukocyte adhesion in pial venules of ovariectomized female rats. *Stroke* 33(2):613-6.
98. Panos, R. J., R. L. Mortenson, S. A. Niccoli, and T. E. King, Jr. 1990. Clinical deterioration in patients with idiopathic pulmonary fibrosis: causes and assessment. *Am J Med* 88(4):396-404.
99. van den Blink, B., H. M. Jansen, and M. P. Peppelenbosch. 2000. Idiopathic pulmonary fibrosis: molecular mechanisms and possible therapeutic strategies. *Arch Immunol Ther Exp (Warsz)* 48(6):539-45.
100. Panos, R. J. 1994. Therapy and management of idiopathic pulmonary fibrosis. *Compr Ther* 20(5):289-93.
101. Reiser, K. M., and J. A. Last. 1986. Early cellular events in pulmonary fibrosis. *Exp Lung Res* 10(4):331-55.
102. Lasky, J. A., and A. R. Brody. 2000. Interstitial fibrosis and growth factors. *Environ Health Perspect* 108 Suppl 4:751-62.
103. Schwartz, E. A., E. Reaven, J. N. Topper, and P. S. Tsao. 2005. Transforming growth factor-beta receptors localize to caveolae and regulate endothelial nitric oxide synthase in normal human endothelial cells. *Biochem J* 390(Pt 1):199-206.
104. Tourkina, E., P. Gooz, J. Pannu, M. Bonner, D. Scholz, S. Hacker, R. M. Silver, M. Trojanowska, and S. Hoffman. 2005. Opposing effects of protein kinase Calpha and protein kinase Cepsilon on collagen expression by human lung fibroblasts are mediated via MEK/ERK and caveolin-1 signaling. *J Biol Chem* 280(14):13879-87.
105. Kasper, M., T. Reimann, U. Hempel, K. W. Wenzel, A. Bierhaus, D. Schuh, V. Dimmer, G. Haroske, and M. Muller. 1998. Loss of caveolin expression in type I pneumocytes as an indicator of subcellular alterations during lung fibrogenesis. *Histochem Cell Biol* 109(1):41-8.

106. Kasper, M., D. Seidel, L. Knels, N. Morishima, A. Neisser, S. Bramke, and R. Koslowski. 2004. Early signs of lung fibrosis after in vitro treatment of rat lung slices with CdCl2 and TGF-beta1. *Histochem Cell Biol* 121(2):131-40.

107. Drab, M., P. Verkade, M. Elger, M. Kasper, M. Lohn, B. Lauterbach, J. Menne, C. Lindschau, F. Mende, F. C. Luft, A. Schedl, H. Haller, and T. V. Kurzchalia. 2001. Loss of caveolae, vascular dysfunction, and pulmonary defects in caveolin-1 gene-disrupted mice. *Science* 293(5539):2449-52.

108. Choi, A. M., and J. Alam. 1996. Heme oxygenase-1: function, regulation, and implication of a novel stress-inducible protein in oxidant-induced lung injury. *Am J Respir Cell Mol Biol* 15(1):9-19.

109. Rodgers, P. A., and D. K. Stevenson. 1990. Developmental biology of heme oxygenase. *Clin Perinatol* 17(2):275-91.

110. Yoshida, T. 1987. [Heme degradation by heme oxygenase system]. *Tanpakushitsu Kakusan Koso* 32(6):822-9.

111. Wagener, F. A., J. L. da Silva, T. Farley, T. de Witte, A. Kappas, and N. G. Abraham. 1999. Differential effects of heme oxygenase isoforms on heme mediation of endothelial intracellular adhesion molecule 1 expression. *J Pharmacol Exp Ther* 291(1):416-23.

112. Kutty, R. K., G. Kutty, I. R. Rodriguez, G. J. Chader, and B. Wiggert. 1994. Chromosomal localization of the human heme oxygenase genes: heme oxygenase-1 (HMOX1) maps to chromosome 22q12 and heme oxygenase-2 (HMOX2) maps to chromosome 16p13.3. *Genomics* 20(3):513-6.

113. Ryter, S. W., J. Alam, and A. M. Choi. 2006. Heme oxygenase-1/carbon monoxide: from basic science to therapeutic applications. *Physiol Rev* 86(2):583-650.

114. Ishikawa, K., M. Sato, and T. Yoshida. 1991. Expression of rat heme oxygenase in Escherichia coli as a catalytically active, full-length form that binds to bacterial membranes. *Eur J Biochem* 202(1):161-5.

115. Shibahara, S., R. Muller, H. Taguchi, and T. Yoshida. 1985. Cloning and expression of cDNA for rat heme oxygenase. *Proc Natl Acad Sci U S A* 82(23):7865-9.

116. Kim, H. P., X. Wang, F. Galbiati, S. W. Ryter, and A. M. Choi. 2004. Caveolae compartmentalization of heme oxygenase-1 in endothelial cells. *Faseb J* 18(10):1080-9.

117. Li Volti, G., R. Ientile, N. G. Abraham, A. Vanella, G. Cannavo, F. Mazza, M. Curro, G. Raciti, R. Avola, and A. Campisi. 2004. Immunocytochemical localization and expression of heme oxygenase-1 in primary astroglial cell cultures during differentiation: effect of glutamate. *Biochem Biophys Res Commun* 315(2):517-24.

118. Morse, D., and A. M. Choi. 2002. Heme oxygenase-1: the "emerging molecule" has arrived. *Am J Respir Cell Mol Biol* 27(1):8-16.

119. Camhi, S. L., J. Alam, L. Otterbein, S. L. Sylvester, and A. M. Choi. 1995. Induction of heme oxygenase-1 gene expression by lipopolysaccharide is mediated by AP-1 activation. *Am J Respir Cell Mol Biol* 13(4):387-98.

120. Lee, P. J., S. L. Camhi, B. Y. Chin, J. Alam, and A. M. Choi. 2000. AP-1 and STAT mediate hyperoxia-induced gene transcription of heme oxygenase-1. *Am J Physiol Lung Cell Mol Physiol* 279(1):L175-82.

121. Rensing, H., H. Jaeschke, I. Bauer, C. Patau, V. Datene, B. H. Pannen, and M. Bauer. 2001. Differential activation pattern of redox-sensitive transcription factors and stress-inducible dilator systems heme oxygenase-1 and inducible nitric oxide synthase in hemorrhagic and endotoxic shock. *Crit Care Med* 29(10):1962-71.

122. Lee, P. J., B. H. Jiang, B. Y. Chin, N. V. Iyer, J. Alam, G. L. Semenza, and A. M. Choi. 1997. Hypoxia-inducible factor-1 mediates transcriptional activation of the heme oxygenase-1 gene in response to hypoxia. *J Biol Chem* 272(9):5375-81.

123. Yuan, J., U. M. Wegenka, C. Lutticken, J. Buschmann, T. Decker, C. Schindler, P. C. Heinrich, and F. Horn. 1994. The signalling pathways of interleukin-6 and gamma interferon converge by the activation of different transcription factors which bind to common responsive DNA elements. *Mol Cell Biol* 14(3):1657-68.

124. Petrache, I., L. E. Otterbein, J. Alam, G. W. Wiegand, and A. M. Choi. 2000. Heme oxygenase-1 inhibits TNF-alpha-induced apoptosis in cultured fibroblasts. *Am J Physiol Lung Cell Mol Physiol* 278(2):L312-9.

125. Sarady-Andrews, J. K., F. Liu, D. Gallo, A. Nakao, M. Overhaus, R. Ollinger, A. M. Choi, and L. E. Otterbein. 2005. Biliverdin administration protects against endotoxin-induced acute lung injury in rats. *Am J Physiol Lung Cell Mol Physiol* 289(6):L1131-7.

126. Sassa, S. 2004. Why heme needs to be degraded to iron, biliverdin IXalpha, and carbon monoxide? *Antioxid Redox Signal* 6(5):819-24.

127. Taylor, J. L., M. S. Carraway, and C. A. Piantadosi. 1998. Lung-specific induction of heme oxygenase-1 and hyperoxic lung injury. *Am J Physiol* 274(4 Pt 1):L582-90.
128. Yachie, A., Y. Niida, T. Wada, N. Igarashi, H. Kaneda, T. Toma, K. Ohta, Y. Kasahara, and S. Koizumi. 1999. Oxidative stress causes enhanced endothelial cell injury in human heme oxygenase-1 deficiency. *J Clin Invest* 103(1):129-35.
129. Minamino, T., H. Christou, C. M. Hsieh, Y. Liu, V. Dhawan, N. G. Abraham, M. A. Perrella, S. A. Mitsialis, and S. Kourembanas. 2001. Targeted expression of heme oxygenase-1 prevents the pulmonary inflammatory and vascular responses to hypoxia. *Proc Natl Acad Sci U S A* 98(15):8798-803.
130. Otterbein, L. E., J. K. Kolls, L. L. Mantell, J. L. Cook, J. Alam, and A. M. Choi. 1999. Exogenous administration of heme oxygenase-1 by gene transfer provides protection against hyperoxia-induced lung injury. *J Clin Invest* 103(7):1047-54.
131. Kaizu, T., T. Tamaki, M. Tanaka, Y. Uchida, S. Tsuchihashi, A. Kawamura, and A. Kakita. 2003. Preconditioning with tin-protoporphyrin IX attenuates ischemia/reperfusion injury in the rat kidney. *Kidney Int* 63(4):1393-403.
132. Inoue, S., M. Suzuki, Y. Nagashima, S. Suzuki, T. Hashiba, T. Tsuburai, K. Ikehara, T. Matsuse, and Y. Ishigatsubo. 2001. Transfer of heme oxygenase 1 cDNA by a replication-deficient adenovirus enhances interleukin 10 production from alveolar macrophages that attenuates lipopolysaccharide-induced acute lung injury in mice. *Hum Gene Ther* 12(8):967-79.
133. Chen, Y. H., S. F. Yet, and M. A. Perrella. 2003. Role of heme oxygenase-1 in the regulation of blood pressure and cardiac function. *Exp Biol Med (Maywood)* 228(5):447-53.
134. Otterbein, L. E., M. P. Soares, K. Yamashita, and F. H. Bach. 2003. Heme oxygenase-1: unleashing the protective properties of heme. *Trends Immunol* 24(8):449-55.
135. Alcaraz, M. J., P. Fernandez, and M. I. Guillen. 2003. Anti-inflammatory actions of the heme oxygenase-1 pathway. *Curr Pharm Des* 9(30):2541-51.
136. Sarady, J. K., S. L. Otterbein, F. Liu, L. E. Otterbein, and A. M. Choi. 2002. Carbon monoxide modulates endotoxin-induced production of granulocyte macrophage colony-stimulating factor in macrophages. *Am J Respir Cell Mol Biol* 27(6):739-45.
137. Bach, F. H. 2006. Carbon monoxide: from the origin of life to molecular medicine. *Trends Mol Med*.

138. Stocker, R., Y. Yamamoto, A. F. McDonagh, A. N. Glazer, and B. N. Ames. 1987. Bilirubin is an antioxidant of possible physiological importance. *Science* 235(4792):1043-6.
139. Clark, J. E., R. Foresti, P. Sarathchandra, H. Kaur, C. J. Green, and R. Motterlini. 2000. Heme oxygenase-1-derived bilirubin ameliorates postischemic myocardial dysfunction. *Am J Physiol Heart Circ Physiol* 278(2):H643-51.
140. Balla, G., H. S. Jacob, J. Balla, M. Rosenberg, K. Nath, F. Apple, J. W. Eaton, and G. M. Vercellotti. 1992. Ferritin: a cytoprotective antioxidant strategem of endothelium. *J Biol Chem* 267(25):18148-53.
141. Otterbein, L., B. Y. Chin, S. L. Otterbein, V. C. Lowe, H. E. Fessler, and A. M. Choi. 1997. Mechanism of hemoglobin-induced protection against endotoxemia in rats: a ferritin-independent pathway. *Am J Physiol* 272(2 Pt 1):L268-75.
142. Kirkby, K. A., and C. A. Adin. 2006. Products of heme oxygenase and their potential therapeutic applications. *Am J Physiol Renal Physiol* 290(3):F563-71.
143. Schober, P., A. Koch, K. Zacharowski, and S. A. Loer. 2006. [Carbon monoxide: toxic molecule with antiinflammatory and cytoprotective properties]. *Anasthesiol Intensivmed Notfallmed Schmerzther* 41(3):140-9.
144. Ryter, S. W., and L. E. Otterbein. 2004. Carbon monoxide in biology and medicine. *Bioessays* 26(3):270-80.
145. Ryter, S. W., L. E. Otterbein, D. Morse, and A. M. Choi. 2002. Heme oxygenase/carbon monoxide signaling pathways: regulation and functional significance. *Mol Cell Biochem* 234-235(1-2):249-63.
146. Gibbons, S. J., and G. Farrugia. 2004. The role of carbon monoxide in the gastrointestinal tract. *J Physiol* 556(Pt 2):325-36.
147. Brouard, S., L. E. Otterbein, J. Anrather, E. Tobiasch, F. H. Bach, A. M. Choi, and M. P. Soares. 2000. Carbon monoxide generated by heme oxygenase 1 suppresses endothelial cell apoptosis. *J Exp Med* 192(7):1015-26.
148. Brouard, S., P. O. Berberat, E. Tobiasch, M. P. Seldon, F. H. Bach, and M. P. Soares. 2002. Heme oxygenase-1-derived carbon monoxide requires the activation of transcription factor NF-kappa B to protect endothelial cells from tumor necrosis factor-alpha-mediated apoptosis. *J Biol Chem* 277(20):17950-61.

149. Morita, T., and S. Kourembanas. 1995. Endothelial cell expression of vasoconstrictors and growth factors is regulated by smooth muscle cell-derived carbon monoxide. *J Clin Invest* 96(6):2676-82.

150. Jozkowicz, A., I. Huk, A. Nigisch, G. Weigel, W. Dietrich, R. Motterlini, and J. Dulak. 2003. Heme oxygenase and angiogenic activity of endothelial cells: stimulation by carbon monoxide and inhibition by tin protoporphyrin-IX. *Antioxid Redox Signal* 5(2):155-62.

151. Chapman, J. T., L. E. Otterbein, J. A. Elias, and A. M. Choi. 2001. Carbon monoxide attenuates aeroallergen-induced inflammation in mice. *Am J Physiol Lung Cell Mol Physiol* 281(1):L209-16.

152. Sueoka, N., E. Sueoka, Y. Miyazaki, S. Okabe, M. Kurosumi, S. Takayama, and H. Fujiki. 1998. Molecular pathogenesis of interstitial pneumonitis with TNF-alpha transgenic mice. *Cytokine* 10(2):124-31.

153. Uasuf, C. G., A. Jatakanon, A. James, S. A. Kharitonov, N. M. Wilson, and P. J. Barnes. 1999. Exhaled carbon monoxide in childhood asthma. *J Pediatr* 135(5):569-74.

154. Antuni, J. D., S. A. Kharitonov, D. Hughes, M. E. Hodson, and P. J. Barnes. 2000. Increase in exhaled carbon monoxide during exacerbations of cystic fibrosis. *Thorax* 55(2):138-42.

155. Biernacki, W. A., S. A. Kharitonov, and P. J. Barnes. 2001. Exhaled carbon monoxide in patients with lower respiratory tract infection. *Respir Med* 95(12):1003-5.

156. Chauveau, C., D. Bouchet, J. C. Roussel, P. Mathieu, C. Braudeau, K. Renaudin, L. Tesson, J. P. Soulillou, S. Iyer, R. Buelow, and I. Anegon. 2002. Gene transfer of heme oxygenase-1 and carbon monoxide delivery inhibit chronic rejection. *Am J Transplant* 2(7):581-92.

157. Sato, M., D. Shegogue, A. Hatamochi, S. Yamazaki, and M. Trojanowska. 2004. Lysophosphatidic acid inhibits TGF-beta-mediated stimulation of type I collagen mRNA stability via an ERK-dependent pathway in dermal fibroblasts. *Matrix Biol* 23(6):353-61.

158. Kwak, H. J., J. S. Song, Z. S. No, J. H. Song, S. D. Yang, and H. G. Cheon. 2005. The inhibitory effects of roflumilast on lipopolysaccharide-induced nitric oxide production in RAW264.7 cells are mediated by heme oxygenase-1 and its product carbon monoxide. *Inflamm Res* 54(12):508-13.

159. Botros, F. T., and L. G. Navar. 2006. Interaction between endogenously-produced carbon monoxide and nitric oxide in regulation of renal afferent arterioles. *Am J Physiol Heart Circ Physiol*.

160. Thorup, C., C. L. Jones, S. S. Gross, L. C. Moore, and M. S. Goligorsky. 1999. Carbon monoxide induces vasodilation and nitric oxide release but suppresses endothelial NOS. *Am J Physiol* 277(6 Pt 2):F882-9.

161. Ott, M. C., J. R. Scott, A. Bihari, A. Badhwar, L. E. Otterbein, D. K. Gray, K. A. Harris, and R. F. Potter. 2005. Inhalation of carbon monoxide prevents liver injury and inflammation following hind limb ischemia/reperfusion. *Faseb J* 19(1):106-8.

162. Goligorsky, M. S., H. Li, S. Brodsky, and J. Chen. 2002. Relationships between caveolae and eNOS: everything in proximity and the proximity of everything. *Am J Physiol Renal Physiol* 283(1):F1-10.

163. Dioum, E. M., J. Rutter, J. R. Tuckerman, G. Gonzalez, M. A. Gilles-Gonzalez, and S. L. McKnight. 2002. NPAS2: a gas-responsive transcription factor. *Science* 298(5602):2385-7.

164. Coceani, F., L. Kelsey, and E. Seidlitz. 1996. Carbon monoxide-induced relaxation of the ductus arteriosus in the lamb: evidence against the prime role of guanylyl cyclase. *Br J Pharmacol* 118(7):1689-96.

165. Shibata, Y., Z. Zsengeller, K. Otake, N. Palaniyar, and B. C. Trapnell. 2001. Alveolar macrophage deficiency in osteopetrotic mice deficient in macrophage colony-stimulating factor is spontaneously corrected with age and associated with matrix metalloproteinase expression and emphysema. *Blood* 98(9):2845-52.

166. Dai, Q., J. Zhang, and S. B. Pruett. 2005. Ethanol alters cellular activation and CD14 partitioning in lipid rafts. *Biochem Biophys Res Commun* 332(1):37-42.

167. Walton, K. A., B. G. Gugiu, M. Thomas, R. J. Basseri, D. R. Eliav, R. G. Salomon, and J. A. Berliner. 2006. A role for neutral sphingomyelinase activation in the inhibition of LPS action by phospholipid. *J Lipid Res*.

168. Takeda, K., T. Kaisho, and S. Akira. 2003. Toll-like receptors. *Annu Rev Immunol* 21:335-76.

169. Li, L., C. H. Ren, S. A. Tahir, C. Ren, and T. C. Thompson. 2003. Caveolin-1 maintains activated Akt in prostate cancer cells through scaffolding domain binding site interactions with

and inhibition of serine/threonine protein phosphatases PP1 and PP2A. *Mol Cell Biol* 23(24):9389-404.

170. Kifor, O., I. Kifor, F. D. Moore, Jr., R. R. Butters, Jr., T. Cantor, P. Gao, and E. M. Brown. 2003. Decreased expression of caveolin-1 and altered regulation of mitogen-activated protein kinase in cultured bovine parathyroid cells and human parathyroid adenomas. *J Clin Endocrinol Metab* 88(9):4455-64.

171. Lisanti, M. P., M. Sargiacomo, and P. E. Scherer. 1999. Purification of caveolae-derived membrane microdomains containing lipid-anchored signaling molecules, such as GPI-anchored proteins, H-Ras, Src-family tyrosine kinases, eNOS, and G-protein alpha-, beta-, and gamma-subunits. *Methods Mol Biol* 116:51-60.

172. Su, T. T., B. Guo, Y. Kawakami, K. Sommer, K. Chae, L. A. Humphries, R. M. Kato, S. Kang, L. Patrone, R. Wall, M. Teitell, M. Leitges, T. Kawakami, and D. J. Rawlings. 2002. PKC-beta controls I kappa B kinase lipid raft recruitment and activation in response to BCR signaling. *Nat Immunol* 3(8):780-6.

173. E, T., G. P, P. J, B. M, S. D, H. S, S. RM, T. M, and H. S. 2005. Opposing effects of protein kinase Calpha and protein kinase Cepsilon on collagen expression by human lung fibroblasts are mediated via MEK/ERK and caveolin-1 signaling. *J Biol Chem* 280(14):13879-87.

174. M, K., S. D, K. L, M. N, N. A, B. S, and K. R. 2004. Early signs of lung fibrosis after in vitro treatment of rat lung slices. *Histochem Cell Biol* 121(2):131-40.

175. M, K., R. T, H. U, W. KW, B. A, S. D, D. V, H. G, and M. M. 1998. Loss of caveolin expression in type I pneumocytes as an indicator of subcellular alterations during lung fibrogenesis. *Histochem Cell Biol* 109(1):41 8.

176. Allen, J. T., and M. A. Spiteri. 2002. Growth factors in idiopathic pulmonary fibrosis: relative roles. *Respir Res* 3:13.

177. JA, L., and B. AR. 2000. Interstitial fibrosis and growth factors. *Environ Health Perspect* 108(Suppl 4):751-62.

178. van Furth, R., Z. A. Cohn, J. G. Hirsch, J. H. Humphrey, W. G. Spector, and H. L. Langevoort. 1972. The mononuclear phagocyte system: a new classification of macrophages, monocytes, and their precursor cells. *Bull World Health Organ* 46(6):845-52.

179. Harris, J., D. Werling, J. C. Hope, G. Taylor, and C. J. Howard. 2002. Caveolae and caveolin in immune cells: distribution and functions. *Trends Immunol* 23(3):158-64.

180. Derijard, B., J. Raingeaud, T. Barrett, I. H. Wu, J. Han, R. J. Ulevitch, and R. J. Davis. 1995. Independent human MAP-kinase signal transduction pathways defined by MEK and MKK isoforms. *Science* 267(5198):682-5.

181. Raingeaud, J., A. J. Whitmarsh, T. Barrett, B. Derijard, and R. J. Davis. 1996. MKK3- and MKK6-regulated gene expression is mediated by the p38 mitogen-activated protein kinase signal transduction pathway. *Mol Cell Biol* 16(3):1247-55.

182. Morse, D., S. E. Pischke, Z. Zhou, R. J. Davis, R. A. Flavell, T. Loop, S. L. Otterbein, L. E. Otterbein, and A. M. Choi. 2003. Suppression of inflammatory cytokine production by carbon monoxide involves the JNK pathway and AP-1. *J Biol Chem* 278(39):36993-8.

183. Triantafilou, M., K. Miyake, D. T. Golenbock, and K. Triantafilou. 2002. Mediators of innate immune recognition of bacteria concentrate in lipid rafts and facilitate lipopolysaccharide-induced cell activation. *J Cell Sci* 115(Pt 12):2603-11.

184. Mineo, C., G. L. James, E. J. Smart, and R. G. Anderson. 1996. Localization of epidermal growth factor-stimulated Ras/Raf-1 interaction to caveolae membrane. *J Biol Chem* 271(20):11930-5.

185. Woo, C. H., J. H. Lim, and J. H. Kim. 2004. Lipopolysaccharide induces matrix metalloproteinase-9 expression via a mitochondrial reactive oxygen species-p38 kinase-activator protein-1 pathway in Raw 264.7 cells. *J Immunol* 173(11):6973-80.

186. Matsuyama, W., L. Wang, W. L. Farrar, M. Faure, and T. Yoshimura. 2004. Activation of discoidin domain receptor 1 isoform b with collagen up-regulates chemokine production in human macrophages: role of p38 mitogen-activated protein kinase and NF-kappa B. *J Immunol* 172(4):2332-40.

187. Katzenstein, A. L., and J. L. Myers. 1998. Idiopathic pulmonary fibrosis: clinical relevance of pathologic classification. *Am J Respir Crit Care Med* 157(4 Pt 1):1301-15.

188. Selman, M., V. J. Thannickal, A. Pardo, D. A. Zisman, F. J. Martinez, and J. P. Lynch, 3rd. 2004. Idiopathic pulmonary fibrosis: pathogenesis and therapeutic approaches. *Drugs* 64(4):405-30.

189. Selman, M., and A. Pardo. 2002. Idiopathic pulmonary fibrosis: an epithelial/fibroblastic cross-talk disorder. *Respir Res* 3:3.

190. Schiller, M., D. Javelaud, and A. Mauviel. 2004. TGF-beta-induced SMAD signaling and gene regulation: consequences for extracellular matrix remodeling and wound healing. *J Dermatol Sci* 35(2):83-92.

191. Sime, P. J., Z. Xing, F. L. Graham, K. G. Csaky, and J. Gauldie. 1997. Adenovector-mediated gene transfer of active transforming growth factor-beta1 induces prolonged severe fibrosis in rat lung. *J Clin Invest* 100(4):768-76.

192. Yamamoto, Y., T. Kubota, Y. Atoji, and Y. Suzuki. 1996. Structure of the perilobular sheath of the deep proventricular gland of the chicken: presence and possible role of myofibroblasts. *Cell Tissue Res* 285(1):109-17.

193. Raghu, G., W. C. Johnson, D. Lockhart, and Y. Mageto. 1999. Treatment of idiopathic pulmonary fibrosis with a new antifibrotic agent, pirfenidone: results of a prospective, open-label Phase II study. *Am J Respir Crit Care Med* 159(4 Pt 1):1061-9.

194. Pardo, A., K. Gibson, J. Cisneros, T. J. Richards, Y. Yang, C. Becerril, S. Yousem, I. Herrera, V. Ruiz, M. Selman, and N. Kaminski. 2005. Up-regulation and profibrotic role of osteopontin in human idiopathic pulmonary fibrosis. *PLoS Med* 2(9):e251.

195. Selman, M., A. Pardo, L. Barrera, A. Estrada, S. R. Watson, K. Wilson, N. Aziz, N. Kaminski, and A. Zlotnik. 2006. Gene expression profiles distinguish idiopathic pulmonary fibrosis from hypersensitivity pneumonitis. *Am J Respir Crit Care Med* 173(2):188-98.

196. Atamas, S. P., I. G. Luzina, J. Choi, N. Tsymbalyuk, N. H. Carbonetti, I. S. Singh, M. Trojanowska, S. A. Jimenez, and B. White. 2003. Pulmonary and activation-regulated chemokine stimulates collagen production in lung fibroblasts. *Am J Respir Cell Mol Biol* 29(6):743-9.

197. Hocevar, B. A., T. L. Brown, and P. H. Howe. 1999. TGF-beta induces fibronectin synthesis through a c-Jun N-terminal kinase-dependent, Smad4-independent pathway. *Embo J* 18(5):1345-56.

198. Bitterman, P. B., M. D. Wewers, S. I. Rennard, S. Adelberg, and R. G. Crystal. 1986. Modulation of alveolar macrophage-driven fibroblast proliferation by alternative macrophage mediators. *J Clin Invest* 77(3):700-8.

199. Clark, J. G., and J. Greenberg. 1987. Modulation of the effects of alveolar macrophages on lung fibroblast collagen production rate. *Am Rev Respir Dis* 135(1):52-6.

200. Clark, J. G., K. M. Kostal, and B. A. Marino. 1983. Bleomycin-induced pulmonary fibrosis in hamsters. An alveolar macrophage product increases fibroblast prostaglandin E2 and cyclic adenosine monophosphate and suppresses fibroblast proliferation and collagen production. *J Clin Invest* 72(6):2082-91.

201. Elias, J. A., T. J. Ferro, M. D. Rossman, J. A. Greenberg, R. P. Daniele, A. D. Schreiber, and B. Freundlich. 1987. Differential prostaglandin production by unfractionated and density-fractionated human monocytes and alveolar macrophages. *J Leukoc Biol* 42(2):114-21.

202. Smith, J. B., N. F. Hassan, S. D. Douglas, and R. A. Polin. 1991. Effects of indomethacin and prostaglandin E1 on the production of fibronectin and lysozyme by monocyte-derived macrophages in vitro. *J Clin Lab Immunol* 35(4):147-55.

203. Kolodkina, L. A., T. P. Ses, I. V. Pokhodzei, and G. P. Orlova. 1999. [Role of neutrophilic leukocytes in pathogenesis of idiopathic fibrosing pulmonary alveolitis]. *Probl Tuberk*(4):35-7.

204. Gadek, J. E., G. A. Fells, R. L. Zimmerman, B. A. Keogh, and R. G. Crystal. 1983. Role of proteolytic and oxidative products of the neutrophil in determining the specificity of the pulmonary lesion in fibrotic and destructive lung disease. *Chest* 83(5 Suppl):59S.

205. de Cremoux, H., and J. Bignon. 1988. [Collagenase and diffuse interstitial pneumopathy]. *Pathol Biol (Paris)* 36(9):1119-23.

206. Arras, M., J. Louahed, V. Simoen, V. Barbarin, P. Misson, S. van den Brule, M. Delos, L. Knoops, J. C. Renauld, D. Lison, and F. Huaux. 2006. B lymphocytes are critical for lung fibrosis control and prostaglandin E2 regulation in IL-9 transgenic mice. *Am J Respir Cell Mol Biol* 34(5):573-80.

207. Daniil, Z., P. Kitsanta, G. Kapotsis, M. Mathioudaki, A. Kollintza, M. Karatza, J. Milic-Emili, C. Roussos, and S. A. Papiris. 2005. CD8+ T lymphocytes in lung tissue from patients with idiopathic pulmonary fibrosis. *Respir Res* 6:81.

208. Gruber, R., A. Pforte, B. Beer, and G. Riethmuller. 1996. Determination of gamma/delta and other T-lymphocyte subsets in bronchoalveolar lavage fluid and peripheral blood from patients with sarcoidosis and idiopathic fibrosis of the lung. *Apmis* 104(3):199-205.

209. Fireman, E., N. Vardinon, M. Burke, S. Spizer, S. Levin, A. Endler, D. Stav, M. Topilsky, A. Mann, Y. Schwarz, S. Kivity, and J. Greif. 1998. Predictive value of response to

treatment of T-lymphocyte subpopulations in idiopathic pulmonary fibrosis. *Eur Respir J* 11(3):706-11.

210. Papiris, S. A., A. Kollintza, P. Kitsanta, G. Kapotsis, M. Karatza, J. Milic-Emili, C. Roussos, and Z. Daniil. 2005. Relationship of BAL and lung tissue CD4+ and CD8+ T lymphocytes, and their ratio in idiopathic pulmonary fibrosis. *Chest* 128(4):2971-7.

211. Shindoh, Y., Y. Tanno, S. Ida, and T. Takishima. 1987. Morphological characterization of basophilic cells in bronchoalveolar lavage fluids from patients with bronchial asthma and idiopathic pulmonary fibrosis. *Tohoku J Exp Med* 152(1):101-2.

212. Pohl, W. R., E. Schenk, H. Umek, M. Micksche, F. Kummer, and H. Kohn. 1993. [Diagnostic value of secretory products of eosinophils and neutrophils in bronchoalveolar lavage in patients with idiopathic lung fibrosis]. *Wien Klin Wochenschr* 105(14):387-92.

213. Boomars, K. A., R. C. Schweizer, P. Zanen, J. M. van den Bosch, J. W. Lammers, and L. Koenderman. 1998. Eosinophil chemotactic activity in bronchoalveolar lavage from idiopathic pulmonary fibrosis is dependent on cytokine priming of eosinophils. *Eur Respir J* 11(5):1009-14.

214. Fujimoto, K., K. Kubo, S. Yamaguchi, T. Honda, and Y. Matsuzawa. 1995. Eosinophil activation in patients with pulmonary fibrosis. *Chest* 108(1):48-54.

215. Hunt, L. W., T. V. Colby, D. A. Weiler, S. Sur, and J. H. Butterfield. 1992. Immunofluorescent staining for mast cells in idiopathic pulmonary fibrosis: quantification and evidence for extracellular release of mast cell tryptase. *Mayo Clin Proc* 67(10):941-8.

216. Fortoul, T. I., and R. Barrios. 1990. Mast cells and idiopathic lung fibrosis. *Arch Invest Med (Mex)* 21(1):5-10.

217. Schildge, J., B. Klar, and M. Hardung-Backes. 2003. [Mast cells in bronchoalveolar lavage fluid of patients with interstitial lung diseases]. *Pneumologie* 57(4):202-7.

218. Lama, V. N., and S. H. Phan. 2006. The extrapulmonary origin of fibroblasts: stem/progenitor cells and beyond. *Proc Am Thorac Soc* 3(4):373-6.

219. Rojas, M., J. Xu, C. R. Woods, A. L. Mora, W. Spears, J. Roman, and K. L. Brigham. 2005. Bone marrow-derived mesenchymal stem cells in repair of the injured lung. *Am J Respir Cell Mol Biol* 33(2):145-52.

220. Hashimoto, N., H. Jin, T. Liu, S. W. Chensue, and S. H. Phan. 2004. Bone marrow-derived progenitor cells in pulmonary fibrosis. *J Clin Invest* 113(2):243-52.

221. Zhang, K., and S. H. Phan. 1996. Cytokines and pulmonary fibrosis. *Biol Signals* 5(4):232-9.

222. Vaillant, P., O. Menard, J. M. Vignaud, N. Martinet, and Y. Martinet. 1996. The role of cytokines in human lung fibrosis. *Monaldi Arch Chest Dis* 51(2):145-52.

223. Martinet, Y., O. Menard, P. Vaillant, J. M. Vignaud, and N. Martinet. 1996. Cytokines in human lung fibrosis. *Arch Toxicol Suppl* 18:127-39.

224. Zhang, K., M. Gharaee-Kermani, B. McGarry, D. Remick, and S. H. Phan. 1997. TNF-alpha-mediated lung cytokine networking and eosinophil recruitment in pulmonary fibrosis. *J Immunol* 158(2):954-9.

225. Piguet, P. F., M. A. Collart, G. E. Grau, Y. Kapanci, and P. Vassalli. 1989. Tumor necrosis factor/cachectin plays a key role in bleomycin-induced pneumopathy and fibrosis. *J Exp Med* 170(3):655-63.

226. Micallef, M., M. Hosokawa, Y. Togashi, and H. Kobayashi. 1992. Rat macrophage activation after treatment with the bleomycin group of antitumour antibiotics in vivo. *Cancer Immunol Immunother* 35(2):106-12.

227. Giri, S. N., D. M. Hyde, and J. M. Nakashima. 1986. Analysis of bronchoalveolar lavage fluid from bleomycin-induced pulmonary fibrosis in hamsters. *Toxicol Pathol* 14(2):149-57.

228. Biffl, W. L., E. E. Moore, F. A. Moore, and C. C. Barnett, Jr. 1996. Interleukin-6 delays neutrophil apoptosis via a mechanism involving platelet-activating factor. *J Trauma* 40(4):575-8; discussion 578-9.

229. Burdin, N., C. Van Kooten, L. Galibert, J. S. Abrams, J. Wijdenes, J. Banchereau, and F. Rousset. 1995. Endogenous IL-6 and IL-10 contribute to the differentiation of CD40-activated human B lymphocytes. *J Immunol* 154(6):2533-44.

230. Smith, R. E., R. M. Strieter, S. H. Phan, N. Lukacs, and S. L. Kunkel. 1998. TNF and IL-6 mediate MIP-1alpha expression in bleomycin-induced lung injury. *J Leukoc Biol* 64(4):528-36.

231. Smith, R. E., R. M. Strieter, S. H. Phan, N. W. Lukacs, G. B. Huffnagle, C. A. Wilke, M. D. Burdick, P. Lincoln, H. Evanoff, and S. L. Kunkel. 1994. Production and function of murine macrophage inflammatory protein-1 alpha in bleomycin-induced lung injury. *J Immunol* 153(10):4704-12.

232. Wang, X. M., H. P. Kim, R. Song, and A. M. Choi. 2006. Caveolin-1 confers antiinflammatory effects in murine macrophages via the MKK3/p38 MAPK pathway. *Am J Respir Cell Mol Biol* 34(4):434-42.

233. 2002. American Thoracic Society/European Respiratory Society International Multidisciplinary Consensus Classification of the Idiopathic Interstitial Pneumonias. This joint statement of the American Thoracic Society (ATS), and the European Respiratory Society (ERS) was adopted by the ATS board of directors, June 2001 and by the ERS Executive Committee, June 2001. *Am J Respir Crit Care Med* 165(2):277-304.

234. Kuan, C. Y., D. D. Yang, D. R. Samanta Roy, R. J. Davis, P. Rakic, and R. A. Flavell. 1999. The Jnk1 and Jnk2 protein kinases are required for regional specific apoptosis during early brain development. *Neuron* 22(4):667-76.

235. Godfrey, T. E., S. H. Kim, M. Chavira, D. W. Ruff, R. S. Warren, J. W. Gray, and R. H. Jensen. 2000. Quantitative mRNA expression analysis from formalin-fixed, paraffin-embedded tissues using 5' nuclease quantitative reverse transcription-polymerase chain reaction. *J Mol Diagn* 2(2):84-91.

236. Fattman, C. L., L. Y. Chang, T. A. Termin, L. Petersen, J. J. Enghild, and T. D. Oury. 2003. Enhanced bleomycin-induced pulmonary damage in mice lacking extracellular superoxide dismutase. *Free Radic Biol Med* 35(7):763-71.